Functional Analysis of *ACD* Mutations in Dyskeratosis Congenita

by

Hande Koçak

A dissertation submitted in partial fulfillment
of the requirements for the degree of
Doctor of Philosophy
(Human Genetics)
in The University of Michigan
2014

Doctoral Committee:

Associate Professor Catherine E. H. Keegan, Chair
Professor Sally A. Camper
Professor Thomas W. Glover
Assistant Professor Jayakrishnan Nandakumar
Associate Professor JoAnn M. Sekiguchi

To

My wonderful parents, Hatice and Basri Yücel Koçak

and

My wonderful sister, Emine Koçak

We made it.

ACKNOWLEDGEMENTS

Foremost, I would like to express my appreciation and thanks to my PhD advisor, Catherine Keegan, for her encouragement, support, and patience. I am sincerely thankful for her research insight and guidance throughout my graduate studies.

I am very grateful that Jayakrishnan Nandakumar agreed to become involved in my project and let me spend time in his lab. It is difficult for me to list all that I have learned from him and to express how thankful I am for his help.

I cannot find words to express my gratitude to Jayakrishnan Nandakumar, JoAnn Sekiguchi, Thomas Glover and Sally Camper for serving on my thesis committee. They have always been very helpful and supportive. Their advices have kept me focused and goal-oriented during my studies. I have been very lucky to have them in my thesis committee. My special thanks go to JoAnn Sekiguchi for sparing time for me week after week to discuss my data and even just to chat about my concerns.

I would like to thank all the former and current members of Keegan Lab. Special thanks to Gail Osawa, Andrea Krause, Ceren Sucularli and Christopher Vlangos for their friendship, help and support.

I consider myself really lucky to get the chance to work in Nandakumar Lab. I would like to thank Valerie Tesmer, Sherilyn Grill, Eric Smith and Andrew Polzin for their friendship and support. I would like to express my special thanks to Kamlesh Bisht for his friendship, support and for his patience to my endless questions. This research would not have been possible without his technical help and support.

I would like to thank my friends who have been a family for me in Ann Arbor. Special thanks to my roommate Ayşe Büyüktür and her mom, Güniz Büyüktür for being there for me while I was writing my dissertation.

Finally, I would like to express my deepest love and appreciation to my family; my mother Hatice Koçak, my father Basri Yücel Koçak and my sister Emine Koçak. I am

very grateful for their unconditional love and support. They have been the biggest inspiration for me all along and I would not find my way in life without their guidance.

TABLE OF CONTENTS

LIST OF FIGURES

LIST OF TABLES

ABSTRACT

Eukaryotic linear chromosomes face two problems that pose threats to genome integrity: (i) the end-protection problem, in which chromosome ends are recognized as double-stranded breaks by DNA damage responses, and (ii) the end-replication problem, in which loss of the chromosome extreme ends occurs in each cell division due to failure of DNA polymerases to replicate these termini. The shelterin complex solves both the end-protection problem and regulates access of telomerase to solve the end-replication problem.

Decreased telomerase activity in stem cells causes dyskeratosis congenita (DC), an inherited bone marrow failure syndrome characterized by telomere lengths <1st percentile. Accordingly, germline mutations in telomerase subunit genes (*TERC* and *TERT*) or telomerase biogenesis genes (*DKC1*, *NOP10*, *NHP2*, and *WRAP53*) are commonly associated with DC. Mutations in telomere biology genes (*TINF2*, *CTC1*, and *RTEL1*) are also observed in DC. However, in ~30 % of DC cases, the underlying genetic cause is unknown.

TPP1, encoded by the *ACD* gene, is a component of the shelterin complex. Like other shelterin proteins, TPP1 protects the ends of chromosomes from illicit fusion events. In addition, TPP1 is uniquely responsible for recruiting telomerase to telomeres. A group of amino acids on the surface of TPP1, termed the TEL patch, is critical for telomerase recruitment and telomerase processivity. These functions of TPP1 make it an excellent candidate for harboring causative mutations of DC.

Here, I report the identification of a single-amino acid deletion in the TEL patch and a missense mutation in the TIN2-binding domain of TPP1 in a patient suffering from a severe variant of DC, Hoyeraal-Hreidarsson syndrome. I further showed that the deletion abrogates both telomerase recruitment and enzymatic processivity, whereas the missense mutation does not have a significant effect on these functions. The missense mutation, on the other hand, inhibits the interaction between TPP1 and TIN2,

another shelterin component responsible for recruitment of TPP1 to telomeres. Therefore, inhibition of this interaction may exert an indirect effect on the recruitment of telomerase to telomeres due to reduced TPP1. Thus, I propose that both the single-amino acid deletion and the missense mutation contribute to the severe phenotype of the proband.

In this study, I report the first instance of DC caused by a germline mutation in *ACD,* adding to the list of DC genes. This study demonstrates for the first time that telomerase recruitment and processivity defect, caused by dysfunction of the TEL patch of TPP1 , results in secondary telomerase deficiency in DC. Thus, it reveals the critical role of TPP1 in telomerase recruitment and processivity in stem cells. Future animal models engineered to carry patient and TEL patch mutations will reveal the full extent of the contribution of the TEL patch to proper functioning of stem cells.

CHAPTER1: INTRODUCTION

A. TELOMERES

Eukaryotic chromosomes are linear. Although their linear structure confers certain advantages during evolution, chromosome ends have the potential to be mistakenly recognized as double-stranded breaks by the DNA repair machinery in cells. Thus, there must be a mechanism to protect natural chromosome ends from being recognized as DNA breaks. Well before the discovery of the double-helix structure of DNA, Hermann Muller (1938) and Barbara McClintock (1939) observed that the natural ends of linear chromosomes are protected from rearrangements and fusion events that often occur at internal regions in the chromosomes of fruit flies and of maize, respectively. Muller named these protected ends of chromosomes “telomeres”, which originates from the Greek word “telos” meaning end and “meros” meaning component.

In the following decades, it has become clear that chromosome ends have special properties and structures, including species-specific telomeric DNA repeats, telomere-associated proteins and specific terminal DNA end structures for telomere maintenance and end-protection. Our current-day definition of telomeres is that they are nucleoprotein complexes found at the end of all eukaryotic chromosomes. They are composed of telomeric DNA consisting of tandem GT-rich repeats and bound protein complexes.

A.1. Telomeric DNA

The telomeric DNA of most eukaryotes is composed of double-stranded short tandem DNA repeats followed by a G-rich 3’-overhang [4]. The sequence of these tandem repeats is dictated by telomerase, the ribonucleprotein complex responsible for telomeric repeat synthesis at telomeres. Telomerase is composed of a reverse transcriptase subunit (TERT) catalyzing telomeric DNA synthesis and an RNA subunit (TERC) serving as a template for DNA synthesis. Mammalian telomeres are comprised

of 5'- TTAGGG- 3' with variable repeat numbers in different mammals [5],[6]. Laboratory mice have long, hypervariable telomere lengths, ranging from 30kb to 150 kb, whereas telomere length in humans is 10-15kb at birth [7-9].

Telomeric DNA has been proposed to form a higher order structure, called a t-loop, in which the telomere end folds back on itself and the 3'-overhang invades into the double-stranded DNA, forming a D-loop [10]. Recently, t-loop structures have been visualized at telomeres using super-resolution fluorescence imaging (STORM) in mouse splenocytes or in mouse embryonic fibroblasts (MEFs) [11]. Although the exact role of t-loops in end protection is not known, the t-loop structure is thought to be involved in telomere protection of 3' overhang via sequestration [12]. In addition to t-loop structures, due to its high G content, the single-stranded 3' overhang can potentially form G-quadruplexes. In humans, G-quadruplexes are thought to be important in telomere protection, suppression of recombination, and inhibition of accessibility of telomerase to telomeres [13].

A.2. The Shelterin Complex

The linear nature of chromosomes causes two main problems for the cells: 1) How to protect the ends of chromosomes from degradation and fusion, the "end-protection problem" and 2) How to replicate the extreme ends of the chromosomes, the "end-replication problem" (discussed below in section 2).

The end-protection problem is defined by the inability of DNA-damage recognition and repair pathways to distinguish natural ends of chromosomes from damage-induced chromosomal double stranded breaks. Mammalian cells have two different signaling pathways that are activated by double-stranded breaks. While the ATM (Ataxia Telangiectasia Mutated) kinase signaling pathway is activated by double-stranded DNA ends, the ATR (Ataxia Telangiectasia and Rad3 related) kinase pathway is activated by the single-stranded overhang DNA generated by trimming or resection of the 5'-end of double-stranded breaks. Activation of these pathways can lead to cell cycle arrest and cell death. Thus, it is important to keep these pathways repressed at telomeres in order to maintain genome stability and cell proliferation. Moreover, double-

stranded breaks are repaired in cells either by homology-directed repair (HDR) or by the nonhomologous end joining (NHEJ) pathway, which can result in chromosome fusions. Therefore, cells also need to protect their chromosome ends from these repair pathways. In summary, failure to distinguish natural chromosome ends from double-stranded DNA breaks can result in cell cycle arrest (resulting from activation of ATM and/or ATR pathways), chromosome end-to-end fusions (resulting from activation of NHEJ), and sequence exchanges among telomeres or between telomeres and other regions of the genome (resulting from HDR activation) [14].

The solution to the end protection problem in mammals is provided by the shelterin complex, which is composed of six known components: TRF1, TRF2, Rap1, TIN2, POT1 and TPP1 (Figure 1.1). Although shelterin, in general, functions in shielding the chromosome ends from being recognized as damaged DNA, each component of the shelterin complex has its own unique contribution to the protection of telomeres, as well as to telomere length maintenance [15], as discussed in following sections.

TRF1

TRF1, encoded by *TERF1*, was the first identified component of the shelterin complex. It specifically binds to TTAGGG repeats in double stranded telomeric DNA giving it the name TTAGGG repeat-binding factor 1 (TRF1)(Figure 1.1) [16]. The structure of TRF1 is divided into three domains; an acidic N-terminus, a central TRF homology (TRFH) domain and a C-terminal DNA-binding domain [17],[18].

The acidic N-terminal domain differentiates TRF1 from TRF2. Through this domain, TRF1 binds to different accessory proteins. For instance, it harbors the RxxADG sequence that can bind to tankyrase 1 and tankyrase 2 [19]. Parsylation of TRF1 by tankyrases is proposed to open the shelterin complex, thereby enhancing telomerase-mediated telomere elongation [20, 21].

The C-terminal DNA binding domain is an approximately 50-amino acid long SANT/Myb-type region. The SANT/Myb-type region is a structurally conserved DNA-binding domain. Belonging to same protein family, the Myb and SANT domains are structurally similar; however, they are known to be divergent in their functions (i. e the

Myb domain binds to DNA but the SANT domain does not bind to DNA) [22, 23]. TRF1 binds to DNA as a dimer, and dimerization is mediated by the central TRFH domain [24], [10]. Although TRF1 and TRF2 are structurally very similar, they recruit different sets of proteins to telomeres through their interactions. The TRFH domain of TRF1 harbors a specific docking sequence recognized by the FxLxP motif of several specific accessory proteins. TRF1 binds to the FxLxP motif in the C-terminus of TIN2 [25, 26]

The consensus DNA binding sequence of TRF1 was shown to be a half-site of 5'-YTAGGGTTR-3' by SELEX (systematic evolution of ligands by exponential enrichment) and interestingly, TRF1 can bind as a dimer to two distantly related half-sites even in opposite directions [27]. From these studies, it was concluded that TRF1 has a high spatial flexibility, presumably conferred by the flexible linker region.

TRF1 is primarily implicated in telomere length maintenance in cells. In telomerase positive cells, it is a negative regulator of telomere length. Overexpression of TRF1 causes telomere shortening, whereas inhibition of TRF1 with a dominant negative form causes telomerase-dependent telomere elongation, presumably by affecting telomerase action [28-30]. In the mouse, TRF1 is indispensable. Targeted deletion of *Terf1* in mice results in early embryonic lethality (at E5-E6). In this *Terf1* $^{-/-}$ mouse, severe growth defects and apoptosis of the inner cell mass of blastocycts was detected. The embryonic lethality could only be briefly delayed by deletion of *p53* [31]. Conditional deletion of *Terf1* in mouse embryonic stem cells causes loss of TRF2 and TIN2 at telomeric ends, leading to telomere fusions with reduced telomere signal. These data indicate that TRF1 plays a key role in stabilizing telomere structure by interacting with other telomeric proteins [32]. Conditional deletion of *Terf1* in stratified epithelial cells causes severe tissue degeneration due to telomeric damage, independent of telomere length maintenance [33]. In addition, TRF1 is suggested to prevent formation of fragile telomeres by contributing to efficient replication of telomeres [34], although its role in this process is currently unknown.

TRF 2

TRF2, encoded by *TERF2*, is another double-stranded telomeric DNA binding protein present at mammalian telomeres (Figure 1.1). It was identified based on its shared SANT/Myc motif with TRF1 [18, 35]. In addition to the SANT/Myc domain, it also shares a central TRF homology (TRFH) domain with TRF1. These domains are connected by a flexible hinge domain, which is not structurally conserved between the two proteins [18, 27, 35, 36]. TRF1 and TRF2 also differ significantly in their N-terminal domain. While TRF1 has an acidic N-terminal domain, TRF2 has a basic N-terminal domain containing a Gly/Arg-rich region, also referred to as a GAR domain [18].

The TRFH domain mediates the dimerization/ oligomerization of both TRF1 and TRF2. Both proteins bind to telomeric repeats as dimers but they cannot interact with each other due to differences in their TRFH domain. Interestingly, TRF2 has a tendency to be involved in higher order oligomerization, such as t-loop formation[37]. Although TRF2 is capable of mediating t-loop formation *in vitro*, it is not clear whether it has the same capability *in vivo* [10, 37]. Recently, Doksani et al. demonstrated direct evidence for the formation of t-loops and the requirement of TRF2 for the formation and maintenance of t-loops [11].

Differences in the TRFH domain of TRF1 and TRF2 result in recruitment of different sets of proteins to telomeres. Similar to TRF1, the TRFH domain of TRF2 also harbors a docking motif for binding its partners, but this motif is recognized by a different sequence, YxLxP, in accessory proteins. TRF2 binds to the YxLxP motifs of several accessory proteins, including Apollo (also known as Snm1b), XPF, Mre11, MCPH1 and PNUTs [25, 26]. TRF2 also interacts with Rap1 through its TRFH domain [38]. TRF2 also binds to a region in the N-terminus of TIN2 via its hinge region [26].

TRF2 is primarily known for its role in telomere capping and end-protection. Like TRF1, deletion of *Terf2* is not compatible with life in mice. Embryonic lethality occurs before E13.5 in *Terf2*$^{-/-}$ mice [39]. Because it is known that TIN2 and TRF1 both participate in stabilization of TRF2 at telomeres [40-42], the embryonic lethality of TRF1 null and TIN2 null mice can also be explained by the loss of TRF2 at the telomeres. Conditional deletion of *Terf2* in mouse embryonic fibroblasts (MEFs) showed senescence like-arrest in the presence of *p53*. In *Terf2*$^{-/-}$ *p53*$^{-/-}$ MEFs, genome-wide

telomeric fusions and DNA damage responses were detected, demonstrating the importance of TRF2 in telomere end-protection [39]. Expression of a dominant negative mutant of TRF2 also results in loss of telomeric overhangs due to either failure to protect the 3' overhang from degradation or deficiency in generating new 3' overhangs after replication. As a consequence of the loss of 3' overhangs, telomere end-to-end fusions were generated through activation of the ATM/p53 DNA damage response pathway[43, 44]. TRF2 directly interacts with ATM, and removal of TRF2 from telomeres causes localization of phosphorylated ATM to the unprotected telomere ends to initiate an ATM-dependent damage response. Thus, TRF2 represses ATM-dependent damage responses by directly interacting with ATM [45, 46].

TRF2 is also important for telomere length maintenance by restricting the access of telomerase to telomeres via t-loop formation. Overexpression of TRF2 induces telomere shortening, independent of the telomerase status of the cells [29, 44], and knocking down TRF2 leads to telomere elongation [47].

Rap1

The mammalian ortholog of Rap1 was identified as a TRF2-binding partner (Figure 1.1) [38]. Human Rap1 forms a complex with TRF2 through its RCT domain in a 1:1 stoichiometry[48]. Although Rap1 has not been fully characterized, there are four distinguishable domains; an N-terminal BRCT domain, a single Myb domain, a coiled region, and a Rap1 carboxy-terminal (RCT) domain. The Myb domain is proposed to confer protein-protein interactions, whereas the RCT domain mediates the interaction of Rap1 with TRF2 in addition to homodimeric interactions. Additionally, there is a putative nuclear localization signal (NLS) in the C-terminus of Rap1[38].

The yeast counterpart of mammalian Rap1 is known to bind directly to telomeres through its two Myb domains. Despite the presence of a Myb domain, human Rap1 requires TRF2 to bind telomeres. Recent ChIP analysis showed that Rap1 and TRF2 have both distinct and overlapping binding sites on chromosomes. More specifically, although TRF2 recruits Rap1 to telomeres [39], Rap1 binds some extra-telomeric sequences that do not have consensus $(TTAGGG)_2$ motifs, and this binding is thought

to be independent of TRF2 [49, 50]. Rap1 is proposed to form complexes with other factors thought to be involved in its extra-telomeric functions, including subtelomeric gene silencing and transcriptional regulation [49].

Rap1 is also implicated in telomere length regulation. Based on deletion mapping studies, the BRCT and Myb domains are proposed to recruit one or more putative accessory factors that play a role in the negative regulation of telomere length. In addition, deletion of the BRCT domain reduced the heterogeneity of telomere length, indicating that the BRCT domain of Rap1 is implicated in telomere length distribution [51]. Rap1-deficient mice are viable but display increased recombination due to the role of Rap1 in repression of Homology-directed Repair (HDR) [49, 52].

TIN2

TIN2, encoded by *TINF2*, is a central component of the shelterin complex. It was identified in a two-hybrid screen as a binding partner of TRF1 [53]. It binds TRF2 and TPP1 as well as TRF1 and provides a bridge between the double-stranded telomeric complex (TRF1 and TRF2/Rap1) and the telomeric complex (POT1 and TPP1) found at the G-rich single-stranded overhang (Figure 1.1)[53].

TIN2 is a 354-amino acid (40kDa) protein. It binds to the TRFH domain of TRF1 through its central domain (amino acids 195-284) and to the N-terminus hinge region of TRF2 through its amino terminal domain (amino acids 1-195). TIN2 also binds to the C-terminal TIN2-binding domain of TPP1 through its N-terminal domain. By deleting the N-terminal domain of TIN2, a recent study revealed that TIN2 is the only link between TPP1-POT1 heterodimers and telomeres. If TPP1-POT1 fails to bind to TIN2, the connection to the shelterin complex is lost, and the heterodimer can no longer function in the end-protection of telomeres [54].

TIN2 can bind to TRF1 and TRF2 simultaneously and is important in stabilizing both proteins *in vivo* [40, 55]. Mutational studies reveal that destabilization of either TRF1 or TRF2 causes induction of a DNA damage response. Thus, TIN2 contributes to the telomere capping function of both TRF1 and TRF2 by stabilizing them or their binding at telomeres [41].

Loss of TIN2 in mice causes early embryonic lethality, emphasizing the role of TIN2 in end-protection [56, 57]. Conditional deletion of *Tinf2* in MEFs results in decreased localization of all shelterin components to telomeres. In these cells, an ATR-mediated DNA damage response (mimicking the absence of Pot1a/b) was induced, indicating that TIN2 is critical for the protective functions of TPP1-POT1, presumably via recruitment of TPP1 (and therefore POT1) to telomeres. There was also a weak ATM-mediated DNA damage response in these cells, supporting the role of TIN2 in the end-protection function of TRF2 [57].

TIN2 was the first shelterin component in which mutations were identified in a human disease [58]. Approximately 10% of patients with dyskeratosis congenita (DC) have a *TINF2* mutation (described in more detail be in section B.5). DC patients with *TINF2* mutations have extremely short telomeres, indicating a defect in TIN2-dependent telomere length control. Although Yang et al. showed that the telomere shortening phenotype due to *TINF2* mutations is caused by defects related to telomerase recruitment in human cells, Frescas and de Lange demonstrated that the effects of the mouse counterparts of specific human mutations are telomerase independent [59, 60]. Thus, the mechanism by which *TINF2*-associated DC mutations lead to telomere shortening is still unclear.

POT1

POT1 is the single stranded telomeric repeat-binding component of shelterin (Figure 1.1). It was first cloned based on its homology to the TEBPα (telomere end-binding protein alpha) subunit of *Oxytricha nova* [61]. Like TEBPα, the DNA-binding domain of POT1 contains two OB (oligosaccharide/oligonucleotide-binding) fold domains [62, 63]. Human POT1 has two OB fold domains that recognize the telomeric decamer TTAGGGTTAG; the first OB fold binds to the first six nucleotides (TTAGGG) of the decamer and the second binds to and protects the four nucleotides (TTAG) at the 3' end of this single stranded DNA sequence [63].

The C-terminal domain of POT1, which immediately follows the two N-terminal OB domains, binds the central POT1-binding domain of the shelterin component, TPP1.

TPP1 is required for recruitment of POT1 to telomeres *in vivo* [42, 64, 65]. Although POT1 itself can bind to DNA *in vitro* [63, 66], TPP1 increases the affinity of POT1 for DNA by ~10 fold [67]. Furthermore, TPP1 binding, but not DNA binding, of POT1 is required for POT1 recruitment to telomeres.

POT1 is known to shield telomeres from DNA damage responses. It represses ATR-dependent DNA damage responses and regulates nucleolytic processing of telomere ends. POT1 is also involved in two contrasting aspects of the regulation of telomere elongation in the presence of telomerase. First, it is proposed that POT1 functions in a negative feedback mechanism for telomere elongation, whereby it binds to the telomeric 3' overhang and prevents telomeric DNA from being elongated by telomerase [68]. Secondly, POT1 together with TPP1 increases the processivity of telomerase; thus, it also functions in favor of telomere elongation [69, 70].

There are two Pot1 paralogs in mouse; Pot1a and Pot1b. Both are highly homologous, having 71-75% amino acid identity to each other and to human POT1. They can both bind to DNA, but they have different roles in cells. While *Pot1a* is known to repress the ATR-dependent DNA damage response, Pot1b is responsible for regulation of 5'-end resection [71-73]. Pot1a null mice exhibit early embryonic lethality, while *Pot1b* null mice exhibit milder phenotypes such as growth retardation, hyperpigmentation, infertility, and intestinal apoptosis [72, 73]. *Pot1a/Pot1b* double knock-out MEFs exhibit growth arrest, endoreduplication, and loss of chromosome end-protection [64]. Human POT1 is thought to combine the features of Pot1a and Pot1b [74]. Interestingly, rescue of Pot1a deficiency in mice with human POT1 also requires co-expression of human TPP1. This observation suggests a degree of species specificity exists in the interaction between POT1 and TPP1 [65]

TPP1

TPP1, encoded by the *ACD* gene, is the last identified component of shelterin (Figure 1.1). It was identified independently, by 3 different groups using mass spectrometry analysis of the TRF1-TIN2 complex and two-hybrid screens with TIN2. The name was ultimately changed from TINT1, PTOP and PIP1 to TPP1 (resulting from

the combination of the first letters of the three former names) [42, 75, 76]. TPP1 is the mammalian homolog of the *Oxytricha nova* chromosome binding protein TEBPβ subunit [67]. Human TPP1 is a 544-amino acid (~58 KDa) protein with a debatable N-terminal region (1-86 amino acids) (Figure 2.2). The human TPP1 protein is currently thought to initiate at Met87, such that the mRNA coding for the preceding 86 residues is now believed to be a part of the 5' UTR of the gene. This is supported by several observations. First, amino acids 1-86 lack homology to most mammalian TPP1 orthologs, including those from mouse, dog, monkey and rat [42]. Second, none of the mass spectrometry data that led to discovery of human TPP1 recovered any peptides that belonged to the amino acid 1-86 region. Third, the first 86 amino acids are dispensable for all known functions of human TPP1 [77].

In light of the above mis-annotation of the N-terminus of TPP1, the TPP1-OB fold domain (87-250 amino acids) is the most N-terminal domain of TPP1 (Figure 2.2). Although the crystal structure of the TPP1-OB domain demonstrated that it shares typical architecture of the OB-domain containing DNA-binding proteins [69], it does not bind DNA directly. The TPP1-OB domain functions in telomerase recruitment to telomeres [67, 78, 79]. In addition to its role in telomerase recruitment, the POT1-TPP1 heterodimer also plays a role as a processivity factor for telomerase by reducing the dissociation rate of telomerase from the DNA primer and increasing the translocation efficiency (Figure 1.2) [69, 70]. Zaug et al. further demonstrated that species-specificities exist between mammalian telomerases and their TPP1 (and POT1) counterparts [80].

Mutagenesis studies revealed a surface of the OB domain of TPP1 including seven critical amino acids (E168, E169, E171, R180, L183, L212 and E215), called the TEL patch (TPP1 glutamate (E) and leucine (L)-rich patch), that is responsible for the interaction between TPP1 and telomerase and recruitment of telomerase to telomeres. This domain was also demonstrated to be critical for the processivity of telomerase [81]. A subset of these residues was independently identified by two other labs as being critical for these aspects of telomerase function [79, 82].

The centrally located POT1-binding domain (250-334 amino acids) resides immediately C-terminal to the OB-fold domain (Figure 2.2). As mentioned earlier, TPP1 binds to the C-terminal TPP1-binding domain of POT1 through this domain and recruits it to telomeres [42, 64, 65]. Conditional deletion of TPP1 in MEFs causes release of Pot1a and Pot1b from telomeres, resulting in an identical phenotype to conditional *Pot1a/b* double knock out (DKO) cells. These data further highlight the requirement of TPP1 for recruitment of POT1 to telomeres [64].

Based on similarities between the crystal structure of TPP1-OB and *Oxytricha nova* TEBPβ (in the TEBPα/β heterodimer), it was proposed that TPP1 is the missing beta-subunit of the TPP1/POT1 complex. As in the case of TEBPα/β, TPP1 is responsible for increasing the affinity of POT1 for single-stranded telomeric DNA [64, 67].

The C-terminal terminal domain of TPP1 (425-544 amino acids) is the TIN2-binding domain (Figure 2.2) [75]. Truncation studies in two-hybrid assays revealed that the last 22 residues of TPP1 are critically important for TIN2 binding [83], and the presence of TPP1 at telomeres depends on TIN2. As indicated previously, TIN2 functions as a bridge between double-stranded and single-stranded telomeric regions.

Although referred to as TPP1 at the protein level, the gene encoding TPP1 is named *ACD*, based on the mouse adrenocortical dysplasia (*acd*) phenotype, which results from a spontaneous autosomal recessive splice site mutation in the *Acd* gene. Homozygous *acd* mutant mice exhibit pleiotropic phenotypes including defects in the adrenal glands, kidneys, and gonads in adult mice as well as caudal regression and strain-dependent perinatal lethality [84]. *acd* mutant embryos and MEF cells exhibit evidence of telomere dysfunction and widespread apoptosis in the caudal portion of the embryo [85, 86]. The caudal regression phenotype is thought to be caused by telomere dysfunction with subsequent p53-dependent apoptosis during caudal development [86]. Due to the splice site defect, the *acd* allele produces ~2% wild type *Acd* transcript, thus functioning as a hypomorphic allele [85]. MEFs from *acd* mutant embryos exhibit mild telomere deprotection phenotypes, probably due to the small amount of wildtype Tpp1; however, knock-down of the remaining Tpp1 in these MEFs results in phenotypes,

similar to *Pot1a/b* DKO, including strong induction of TIFs, an increased amount of single stranded telomeric DNA, and a higher frequency of telomere fusions [65]. These data indicate that TPP1 is a unique shelterin component that is not only involved in protecting chromosome ends, but is also critical for the extension of these same ends by telomerase.

B. TELOMERASE

Toward the end of the 20th century, Greider et al. showed a novel activity in Tetrahymena cell-free extracts that could add tandem TTAGGG repeats onto telomeric primers[87]. It was first proposed that this activity was coming from a telomere terminal transferase in eukaryotes. However, in 1989 a novel ribonucleoprotein complex, adding *de novo* telomeric repeats to the end of human telomeres, was identified. This ribonucleoprotein complex was named telomerase [88]. In 2009, Elizabeth Blackburn, Carol Greider and Jack Szostak were awarded Nobel Prize in Physiology or Medicine "for the discovery of how chromosomes are protected by telomeres and the enzyme telomerase". In particular, Elizabeth Blackburn and Carol Greider were awarded for the discovery of telomerase.

One problem that emerges due to the linear nature of eukaryotic chromosomes is the end-replication problem, because DNA polymerases cannot fully replicate the extreme end of chromosomes. DNA polymerases depend on small RNA primers during replication. In the growing replication fork, the leading strand is synthesized continuously in the 5’ to 3’ direction with one RNA primer starting from origin of replication. However, synthesis of the lagging strand is in the opposite direction with the growing replication fork; thus, 5’ to 3’ synthesis must be completed in fragments, called Okazaki fragments, with multiple RNA primers. As one fragment approaches the 5’ end of the adjacent fragment, the RNA primer is removed and the two fragments are ligated together. At the very ends of the chromosomes, even if the RNA primer binds to the most extreme end of the chromosome, once the RNA primer is removed, it leaves a gap at the 5’-end of the lagging strand that cannot be filled by DNA polymerases. Thus, chromosomes shorten with each division due to loss of DNA from the 5’ end of the lagging strand. In most eukaryotes, the end-replication problem is solved by telomerase,

which synthesizes telomeric DNA *de novo* to compensate the DNA loss from the 5` end of the lagging strand during each cell division. Telomerase is a ribonucleoprotein composed of a reverse transcriptase protein subunit (TERT) that catalyzes telomere repeat addition using templating information provided by its RNA subunit (TERC) [89] (Figure 1.2).

B.1. Telomerase RNA (TERC)

Telomerase RNA or TERC is one of the major components of the telomerase ribonucleoprotein. It is a non-coding RNA containing a region that acts as template for the reverse transcriptase subunit, TERT, to synthesize telomeric DNA [90]. The size and nucleotide sequence of the RNA component is highly variable in different organisms. The length of TERC is ~150 nucleotides in ciliates, ~500 nucleotides in vertebrates and ~ 1300 nucleotides in yeast. Although the nucleotide sequence and length differs in different organisms, the structure of TERC in different organisms shares similar secondary structural features [91]. There are 3 different conserved elements in the structure of TERC: the core domain, the trans-activating domain (conserved regions 4 and 5) and the domains required for stability of TERC *in vivo*, including the box H/ACA domain (conserved regions 6 and 7) (Figure 1.3A). TERC interacts with TERT through the core domain and the trans-activating domain independently [92, 93].

The core domain contains a template region (conserved region 1), a pseudoknot (conserved regions 2 and 3), and a 5' boundary element for the template (Figure 1.3A). The template region contains a primer alignment region that functions in positioning the 3' end on the template for telomere synthesis. The telomeric 3' G-stranded overhang acts as a primer, which anneals to the primer alignment region via Watson-Crick base-pairing. The templating region, which resides immediately upstream or 5' of the primer alignment region, is used to synthesize telomeric DNA at the 3' end of the annealed telomeric primer. It is important to note that the primer alignment region does not function as a template for telomeric repeat synthesis; it only positions the primer accurately for extension. Therefore, mutations in the primer alignment region impair telomeric repeat synthesis but do not result in non-telomeric mis-incorporations in the telomeric primer. The extent of base pairs between the primer and template alters the

processivity of telomerase by affecting the translocation efficiency in human and mouse telomerase [94].

The pseudoknot is the most intensely studied element of telomerase RNA. Recent studies showing the structural elements of this domain via NMR spectroscopy and molecular modeling demonstrated that the folding dynamics of the pseudoknot are important for the proper functioning of telomerase [95, 96]. Mutational studies also showed that reduction in telomerase activity caused by mutations in the pseudoknot domain can be reversed by compensatory mutations that restore the tertiary structure [97].

While the 3' boundary of the template is defined by its complementary sequence to the telomere, the 5' boundary of the template is defined by a specific RNA element located immediately before the template domain. It specifies the site where translocation occurs in the process of telomere elongation (Figure 1.2). This element shows a high degree of divergence in difference species. For instance, in human TERC, the structure and position of a specific motif, called theP1b helix, are important for specifying the 5' boundary [98], whereas in ciliate TERC, the 5' boundary element is a conserved sequence motif upstream of the template region [99].

The trans-activating domain exhibits a high level of homology among different organisms. This domain is important in the nucleotide addition processivity of telomerase [100]. Entire or partial truncations of this domain cause loss of telomerase activity. The effect is due, at least partly, to the role of this domain in interaction with TERT [101]. Interruptions in the interaction between TERC and TERT abolish telomerase activity [92] . The trans-activating domain of TERC was shown to be functional in *trans* when expressed separately from the core domain of human TERC [102]. A stem-loop region, termed P6.1, within the trans-activating domain is essential for TERC`s interaction with the telomerase RNA binding domain (TRBD) of TERT. Mutational studies revealed that the general structure of this loop is important for interaction with TERT. However, there are still specific sequences in the loop structure that are important telomerase function [93]. Crosslinking studies mapping the interface of interaction between the trans-activating domain of TERC and the TRBD of TERT

suggested that the loop is involved in proper folding of TERT by interacting with both the TRBD and the C-terminus domain of TERT [103]. The recently reported crystal structure of the trans-activating domain of TERC in complex with the TRBD domain of TERT from teleost fish *Oryzias latipes* revealed that both the sequence and the conformation of the trans-activating domain are important for this interaction [104].

The H/ACA domain is located toward the 3'-teminus of mature TERC in conserved region 7(CR7) (Figure 1.3A). It contains a hinge box (H box, consensus sequence of ANANNA) and a 5'-ACA-3' sequence. These two sequence motifs serve as binding sites for proteins involved in TERC processing, stability, nuclear localization, and telomerase activity [100, 105-107]. Specifically, four proteins, Dyskerin, Nhp2, Nop10 and Gar1 bind the H/ACA domain to stabilize TERC in cells [108, 109]. In addition to the H/ACA domain, CR7 contains a four-nucleotide motif (5'-UGAG-3') called the Cajal body localization (CAB) box [110]. Cajal bodies are nuclear compartments in proliferating/metabolically active cells where snRNPs biogenesis and processing occurs. They are implicated in the recruitment of telomerase to telomeres [111]. It is known that TERC localizes to Cajal bodies transiently via its CAB box depending of the phase of the cell cycle [112]. A WD40 repeat-containing protein WDR79 (TCAB1) facilitates localization of telomerase to Cajal bodies, presumably via binding to the CAB box of TERC [113, 114]. CR7 also harbors a domain called biogenesis box (BIO box, 5'-CUGU-3'). As stated in the name, the BIO box functions in the biogenesis and assembly of the telomerase RNP [115].

Human TERC is synthesized by RNA Pol II and therefore contains a trimethyl guanosine cap at its 5' end. It also contains a guanosine tract that forms a G-quadruplex, which is proposed to protect it against degradation by nucleases [116]. This G-quadruplex is opened up by the helicase DHX36/RHAU during the process of TERC maturation and telomerase RNP assembly [117].

B.2. Telomerase Reverse Transcriptase (TERT)

TERT is the catalytic component of the telomerase RNP. It was first identified in the ciliate *Euplotes aediculatus* as an RT-like polypeptide shown to have homology with the yeast Est2 protein [118, 119]. To date, the only existing crystal structure of a TERT protein is from a homolog present in the flour beetle, *Tribolium castaneum*. The *T. castaneum* TERT (TcTERT) structure displays the three characteristic domains of DNA polymerases and reverse transcriptases, namely, the thumb, fingers, and palm domain. Indeed, comparison of the crystal structure of TcTERT and HIV RT showed a high level of structural similarity. In contrast to TERC, the TERT protein sequence shows a high level of conservation among different species. Sequence analysis revealed several conserved domains grouped into four structural elements: the N-terminal extension domain (containing the telomerase essential N-terminal domain, TEN; and the telomerase RNA-binding domain, TRBD), the RT domain (RT), and the C-terminal extension (CTE) domain (Figure 1.3B) [120]. It is interesting to note that *T. castaneum* TERT lacks the TEN domain, suggesting that this loss is compensated by the gain of additional features in the remaining domains of TERT.

N-terminal Extension

The N-terminal extension is the domain containing DNA- and RNA- binding sub-domains; the telomerase essential N-terminal domain (TEN) and telomerase RNA binding domain (TRBD). These two domains are connected via an unstructured linker, which confers conformational flexibility to the holoenzyme.

The TEN domain is the least evolutionarily conserved domain of TERT. It is required for telomerase activity *in vitro* and telomere maintenance *in vivo* in human, yeast and ciliated protozoa [121, 122] . Although it has non-specific RNA binding properties, the TEN domain mainly functions in binding single stranded telomeric DNA repeats. A region called “dissociates activities of telomerase” (DAT) directs telomerase to telomeric substrate in human cells. Mutational studies indicate that the DAT region plays a role in affinity of telomerase for its substrate and may serve as an anchor-site for telomerase to bind its telomeric substrate. In addition, there are some amino acid residues in the TEN domain that are crucial for telomerase activity and telomere maintenance, independent of its role in DNA binding. The TEN domain has also been

proposed to be involved in the recruitment of telomerase to telomeres [79, 123, 124]. Recently, Schmidt et al. identified specific residues in the TEN domain that are necessary for recruitment of telomerase to telomeres [125].

The TRBD, the highly conserved domain located between the TEN and RT domains, is required for functioning of telomerase both *in vivo* and *in vitro.* Through its cognate RNA recognition motif, it is responsible for RNA binding that results in the formation of the telomerase RNP complex [126, 127]. The TRBD domain interacts with the trans-activating domain of TERC, and mutational studies based on the crystal structure of the TRBD domain of TERT in complex with the trans-activating domain of TERC suggested that trans-activating domain-TRBD recognition is common to most eukaryotes [104]. Moreover, a sub-domain, called the T domain, of human TRBD contributes to the rate of repeat extension in substrate primer elongation and translocation (Figure 1.2). Crosslinking of the trans-activating domain of TERC to the TRBD domain of TERT in teleost fish *Oryzias latipes* revealed that there is a distinct binding pocket on TRBD for TERC to bind [103].

RT domain

The catalytic RT domain of TERT is composed of 7 universally conserved reverse transcriptase (RT) motifs (Motif 1, 2, A, B', C, D, E). Motifs 1 and A are organized in a putative sub-domain, called "fingers". This sub-domain is responsible for interaction with nucleic acid substrates. Motifs B' and E are organized in the "palm" domain containing the catalytic active site (Figure 1.3B) [120]. There is a triad of conserved aspartic acid residues in motifs A and C. As in the case of other polymerases, these residues are important for the activity of telomerase by directly contributing to nucleotide addition via coordination of two-metal ions [128-130]. The palm and fingers sub-domains are connected with a "primer grip" region of Motif E. According to molecular models, this loop interacts with the DNA-RNA heteroduplex and contributes to single-stranded DNA binding [120, 131, 132].

The RT domain of TERT can be distinguished from other retroviral or retrotransposon reverse transcriptases by a domain called insertion in finger domain

(IFD) (Figure 1.3B). Mutational studies reveal that the structural integrity of the IFD is important for enzymatic activity through both protein-RNA interaction and RNA-DNA interactions. In yeast, a mutation in this domain was shown to abolish multiple repeat synthesis by affecting the repositioning of the DNA product relative to the RNA template [133].

Carboxy-Terminal Extension (CTE)

In addition to the palm and finger domains present in the RT domain of TERT, the thumb domain is located within the CTE (Figure 1.3B). Conservation of the motifs in this domain is weaker compared to the conservation in the other two domains, suggesting the CTE domain may have species-specific functions. Supporting the species specificity, CTE is essential for telomerase activity in humans and in Tetrahymena but not in yeast and it is predicted to be absent in *C. elegans*.

The C-terminus is composed of a helical bundle that harbors several surface-exposed loops. These loops are thought to participate in the formation and stability of the DNA-RNA heteroduplex in the catalytic site [120, 134]. Mutations in this domain of TERT affect enzymatic activity and processivity of human and yeast telomerase. Some of these mutations are found to influence the subcellular localization of TERT and telomere maintenance in human cells [132, 135-138].

Interestingly, addition of epitope tags to the C-terminus of human TERT, as well as mutations near the C-terminus, disrupt telomere elongation *in vivo*, but have no effect on *in vitro* catalytic activity [139]. This indicates that the extreme C-terminus of TERT is important for steps of telomere biology other than its catalytic step.

B.3. Telomerase recruitment to telomeres

One prerequisite for telomerase functionality is its localization to telomeres. The single stranded binding function of telomerase is known to be governed by the POT1-TPP1 [65].Because POT1 and telomerase bind the same G-rich sequences found at chromosome ends, POT1 is thought to be an inhibitor of telomerase. Indeed, the addition of POT1 protein decreases telomerase activity *in vitro* [63]. Interestingly, Wang

et al showed that addition of both POT1 and TPP1, but not POT1 or TPP1 alone, stimulates telomere processivity by 2-3 fold [69]. This suggests that TPP1 is involved in the positive regulation of telomerase. Pull-down experiments showed that TPP1 binds to TERT; specifically, the OB fold domain of TPP1 is necessary and sufficient for TPP1-TERT interaction [67]. It was also demonstrated by Immunofluorescence and Fluorescent *In Situ* Hybridization (IF-FISH) and chromatin immunoprecipitation (ChIP) experiments that TPP1 is required for recruitment of telomerase to telomeres, because deletion of the OB fold domain of TPP1 disrupts the recruitment of telomerase to telomeres [78]. It was also shown that the OB fold domain is sufficient for recruitment of telomerase to an artificially constructed non-telomeric locus in the human genome [79]. Nandakumar et al. investigated the residues of the OB fold domain that are important for interactions with telomerase and via mutagenesis studies, and demonstrated that an acidic patch of amino acids on the surface of TPP1, termed the TEL patch, binds to telomerase. The TEL patch specifically enables telomerase to be recruited to telomeres and to extend telomere ends with high processivity [81]. In addition to data from *in vitro* pull-down and telomerase activity assays showing the importance of the TEL patch for telomerase function, it was also shown that the TEL patch mutations decrease the extent of telomere elongation by telomerase in cultured human cells [81]. Two independent groups have also shown that portions of the TEL patch are required for telomerase recruitment and activity [79, 140]. It was suggested that the TEL patch is not only important for telomerase recruitment, but also functions as a telomerase activator, independent of it role in telomerase recruitment [82]. In addition, by using separation-of-function mutations, Schmidt et al. recently identified specific residues on the TEN domain of telomerase that are necessary for interaction of telomerase with TPP1 and for recruitment of telomerase to telomeres [125]. In this study, it was also shown that the interaction between the OB-fold of TPP1 and telomerase is a direct interaction by rescuing the interaction defect caused by TEN mutations with compensatory mutations in the TEL-patch [125].

B.4. The role of telomerase in stem cells

It is known that in most human somatic cells, except for stem cells and lymphocytes, telomerase activity is diminished after birth. Thus, telomeres shorten with each cell division, resulting in limited proliferation capacity of most somatic cells. Considering the high self-renewal capacity of stem cells, it is not surprising that stem cells have at least a low level of telomerase activity.

Stem cells are pluripotent or multipotent cells. They have self-renewal capability and multi-linage differentiation potential [141, 142]. In mammals, there are three general types of stem cells: embryonic, germinal, and adult stem cells. Embryonic stem cells (ESCs) reside in the inner cell mass of blastocysts that gives rise to the primary germ layers: ectoderm, endoderm and mesoderm. Germinal stem cells (or primordial germ cells, PGCs) are the origin of eggs and sperm. Adult stem cells (ASCs) divide and differentiate to replenish damaged tissues. For sustained and indefinite proliferation potential, all stem cells must maintain their telomere length, which is accomplished by expressing telomerase.

ESCs are immortal with indefinite proliferation capability *in vitro*. They have high levels of telomerase and long stabilized telomeres. As ESCs differentiate, TERT expression is down-regulated, resulting in repressed telomerase activity. Thus, in cells differentiated from ESCs, telomeres start to shorten as they proliferate. It has also been suggested that telomerase activity confers a stemness factor to ESCs. Inhibition of telomerase activity leads to decreased proliferation, and the suppression of TERT results in differentiation of ESCs. In contrast, overexpression of TERT in ESCs leads to increased cell proliferation and colony-forming ability [143, 144]. It has been shown that multiple stemness factors and signaling pathways play roles in maintaining high levels of telomerase activity in ESCs. For instance, Kruppel-like factor 4(KLF4), an essential component of the pluripotency transcriptional network, is involved in the regulation TERT expression in ESCs [145].

Telomere length is also maintained in the germline. Telomerase activity is observed in both immature and mature oocytes in females and in testis in males [146, 147]. Spermotogonial stem cells were demonstrated to grow in cell culture and differentiate into multiple lineages. These observations support the notion that

telomerase activity in stem cells can be correlated to self-renewal and multi-lineages differentiation capabilities. Loss of telomerase activity leads to telomere shortening and male sterility in successive generations. Although spermatogonial stem cells have telomerase activity, spermatozoa lack telomerase activity. When spermatogonia reach the growth arrest phase in development, telomerase expression is repressed [148-150].

ASCs maintain their reservoir of cells by self-renewal and differentiate to more specialized tissues to regenerate damaged tissues/organs. These two general properties of ASCs are the key to generation of tissues/organs during embryonic development and maintenance of tissue/organ homeostasis in adults [141, 142, 151]. In aging and degenerative diseases, tissue/organ homeostasis gradually declines, eventually resulting in loss of the supply of cells for regeneration upon damage [152]. One of factors likely playing a role in this decline is telomere shortening due low level telomerase activity observed in ASCs. For instance, in HSCs and also in non-hematopoietic stem cells, a low level of telomerase activity was detected [153]. Both stem cell types still undergo age-dependent telomere shortening in humans, suggesting that the level of telomerase activity is not sufficient to maintain telomere length in these cells. In particular, there are several lines of evidence confirming the insufficiency of telomerase in HSCs. First, HSCs isolated from adult bone marrow exhibit shorter telomeres than HSCs from fetal liver and cord blood. Secondly, HSCs from younger individuals have longer telomeres than those of older individuals. Third, telomere length comparisons between donor and recipient after bone marrow transplantation reveal that cells from different lineages undergo telomere loss in response to extensive cell division for expansion [154]. In addition to HSCs, stem cell function is known to decline naturally with age in various other organs including the forebrain [155-157], skeletal muscle [158, 159] and skin [160]. Although enhancing telomerase function in aging stem cells has been proposed as an avenue to counteract aging, the risk of predisposing toward cancer would be expected to outweigh the potential benefits of this approach.

The critical role of telomerase in stem cells in mice has been demonstrated from studies using telomerase knockout/transgenic mice. Deletion of *Terc* (telomerase RNA component) causes reduced tissue renewal efficiency and shorter life span in mice. In

addition, male and female infertility, immune-senescence, and reduced regeneration in highly proliferative organs including the digestive system, the skin and hematopoietic system have been shown in the absence of *Terc*. It is important to note that because mice have very long telomeres; phenotypes associated with telomere shortening can only be observed in late generations of telomerase knockout mouse models [161-164]. On the other hand, *Tert* overexpression leads to a decrease in aging-associated degenerative and inflammatory processes and an increase in the median survival rate of mice [165]. Moreover, Jaskelioff et al. showed that the multi-system degeneration in late-generation telomerase-deficient adult mice (with severe telomere dysfunction) can be stopped or reversed by reactivation of telomerase without increasing cancer incidence [166]. In humans, telomerase deficiency-related diseases including dyskeratosis congenita (DC) are relevant to studies of the role of telomerase in stem cells. Although these diseases are mostly caused by mutations in a number of different genes, the cause of the disease is generally considered to be deficiency of telomerase and telomere shortening, leading to reduced function of stem cells.

In addition to telomere lengthening, recent studies revealed that telomerase or TERT functions in multiple different processes that may be important for the function of stem cells. Mouse ESCs with TERT overexpression are more resistant to apoptosis and oxidative stress *in vitro* [144]. Moreover, loss of TERT causes mitochondrial defects leading to increased levels of reactive oxygen species in mice [167]. Interestingly, TERT is also implicated in genome-wide epigenetic regulation of cell differentiation [168].

B.5. Telomerase Deficiency and Human Diseases

The role of telomerase activity in human stem cells has been recently highlighted in human diseases caused by mutations in telomerase-associated protein genes, including dyskeratosis congenita, aplastic anemia, and idiopathic pulmonary fibrosis. Although the pathophysiology of these diseases is not very clear, telomere attrition due to telomerase deficiency, causing dysfunctional stem cells, is thought to underlie the disease process.

Dyskeratosis Congenita (DC)

DC is a rare inherited multisystem disorder with an estimated prevalence of 1 in 1,000,000 (http://ghr.nlm.nih.gov/condition/dyskeratosis-congenita). It was initially described by Zinsser in 1906 and recognized as a clinical entity by Engman (1926) and Cole (1930). Although it is a rare disease, it is the second-most- common type of inherited bone marrow failure syndrome (IBMFS). Bone marrow failure is found in approximately 80 % of DC patients and is known to be the leading cause of death, followed by pulmonary disease and cancer.

DC is a clinically heterogeneous disease. In addition to bone marrow failure, DC is often characterized by the triad of nail dystrophy, reticular skin pigmentation of the neck/upper chest and oral leukoplakia (Figure 1.4). Although this triad is classical for the diagnosis of DC, it may be observed in late stages or it may not be observed at all due to variable expressivity and/or incomplete penetrance. Variable expressivity is a genetic phenomenon that is used to describe the range of phenotypes for a given genotype. It indicates that the phenotype is expressed in varying degrees in different individuals. Incomplete penetrance is another genetic phenomenon describing incomplete genotype-phenotype correlation. In other words, incomplete penetrance indicates that each individual with a given genotype may not exhibit the phenotype associated with that genotype.

Patients with DC may also present with several other clinical features including pulmonary fibrosis, liver disease, bone abnormalities, dental defects, esophageal stricture, immune deficiency, and endocrine, urological or neurological problems. Cancer predisposition is another manifestation of DC. Myelodysplatic Syndrome (MDS), acute myeloid leukemia (AML), head and neck squamous cell cancer, lymphoma, gastrointestinal tract cancer and liver cancer have also been seen in some patients with DC. Despite the limitations in sample size and retrospective nature, a study from NCI`s DC cohort demonstrated an 11-fold increased risk of cancer in DC patients, and this risk is 40% by age of 50 [169]. Since cells from DC patients are characterized by inability to maintain their telomeres due telomerase deficiency, it may seem surprising that they have increased cancer susceptibility. However, critically shortened telomeres (as in the case of DC patients) result in genomic instability leading to telomere fusions, which is

implicated in cancer. Moreover, it is noteworthy that DC patients are specifically at the risk of developing cancer affecting tissues with high turnover rate [170]. Accumulation of mutations due to high turnover rate may also be another underlying mechanism of cancer susceptibility in these patients.

DC is also genetically heterogeneous. It can be inherited in X-linked, autosomal dominant (AD), and autosomal recessive (AR) patterns (Table 1.1). In addition, there are several *de novo* germ line mutations that are observed in DC patients such as in *TERC* and *TINF2*.

AD-DC exhibits genetic anticipation associated with progressive telomere shortening. Genetic anticipation is a phenomenon defined as an increased severity and decreased age of disease onset in successive generations. In DC families with *TERC* mutations, genetic anticipation is observed due to progressive telomere shortening as described below.

Currently, the genetic basis is identified in ~70% of DC cases. In these patients, DC is caused by germ-line mutations in genes responsible for maintenance of telomere length and function. Prior to work reported in this dissertation, nine DC-associated genes (*DKC1, TERT, TERC, TINF2, TCAB1, NOP10, NHP2, CTC1 and RTEL1*) had been identified (Table 1.1, Figure 1.5). In Chapter 2, my work demonstrates that *ACD* is a novel DC-associated gene.

***DKC1*, *NOP10* and *NHP2* mutations**

Dyskerin (encoded by *DKC1*), NOP10 and NHP1 are components of H/ACA snoRNP complexes. These complexes are known to be involved in the modification of specific uridine residues in newly synthetized ribosomal RNA. H/ACA snoRNPs consist of 1 snoRNA and 4 proteins; dyskerin, NOP10, NHP2 and GAR1. While the snoRNA guides the complex to the target site of pseudouridylation, dyskerin functions as an active pseudouridine synthase enzyme, and NOP10, NHP2 and GAR1 assist in the assembly and stability of the complex.

In vertebrates, dyskerin, along with NOP10, NHP1 and GAR1, binds to the H/ACA box located at the 3' end of telomerase RNA. This H/ACA complex functions in the assembly of telomerase in the nucleus. Knock-down of dyskerin, NOP10 and NHP2 (but not GAR1) cause a reduction in levels of TERC. Thus, it is not surprising that mutations of *DKC1*, *NOP10* and *NHP2* have been identified in DC patients.

DKC1 mutations:

The most commonly diagnosed form of DC is the X-linked form (Table 1.1). Mutations in *DKC1* are almost always point mutations causing a single amino acid change. However, there are also exceptions, including a 2kb deletion (producing a truncated protein), a splice site mutation and a putative promoter mutation. Point mutations are usually clustered in 2 regions of the gene: the PUA RNA-binding domain and a region near the N terminus. Crystallographic studies have revealed that in the archael ortholog of dyskerin, Cbf5, these two regions are in close proximity in the three dimensional structure, suggesting that they are involved in the same function [171-173]. Thus, it is not surprising that DC mutations in these regions would affect the same function of dyskerin.

Although the underlying mechanism by which dyskerin mutations cause DC is not clear, they are known to cause telomere shortening in DC patients. In both humans and mice, DC mutations in *DKC1* result in low levels of TERC [174-176]. It is proposed that low levels of TERC fail to maintain telomere length in stem cells, causing stem cell exhaustion in highly renewable tissues, including bone marrow, skin, and fingernails. Thus, stem cell exhaustion likely explains the clinical manifestations of DC. Interestingly, DNA damage foci formation was observed in mouse cells with pathogenic *Dkc1* mutations [177]. This suggests that these mutations cause a transient capping defect at the telomere, which in turn causes telomere loss.

As mentioned above, dyskerin is known to be involved in the uridylation of newly synthesized rRNA. Although dyskerin mutations do not seem to affect ribosome biogenesis in DC patients, they cause defects in ribosome biogenesis and

psuedouridylation in mouse cells [174, 176, 178, 179]. Thus, these defects may still be playing an undefined role in the DC phenotype in humans.

Mutations in *DKC1* that cause DC have a broad range of severity. In general, affected boys develop the characteristic triad of mucocutaneous manifestations in the first decade, bone marrow failure in the second decade, and they die from complications of bone marrow failure, bleeding and infections in their third decade. There are very severe cases in which patients display intrauterine growth retardation, immune deficiency and cerebellar aplasia, a syndrome called Hoyeraal Hreiderson Syndrome (HH), although there are also less severe cases [180-182]. The variable expressivity of a given *DKC1* mutation in different individuals suggests the contribution of other genetic and/or environmental factors in DC

***NOP10* mutations:**

An autosomal recessive mutation in *NOP10* was found in a large consanguineous family with 3 affected children. All three children showed the classical triad of mucocutaneous features of DC, but only one had bone marrow failure. The affected children were homozygous for a R34W mutation and had very short telomeres and low levels of TERC. Interestingly, although heterozygous carrier family members were asymptomatic, they also had shorter telomeres and lower levels of TERC in comparison with healthy controls. However, the effect was not as severe as in the affected children [183].

***NHP2* mutations:**

Two families with autosomal recessive DC and *NHP2* mutations have been identified. In the first family, the patient was homozygous for a Y139H mutation. The patient showed nail dystrophy, thrombocytopenia, growth and mental retardation along with other DC manifestations. The second patient was compound heterozygous (V126M and X154Arg causing loss of the natural stop codon and extending the protein by 51aa) for *NHP2* mutations. This patient presented at the age of 12 with classical DC with pancytopenia. As expected, short telomeres and low levels of TERC were observed in

these two patients, suggesting that the mechanism of disease mimics that of DC patients with *DKC1* mutations [184].

TERC mutations

In a large 3-generation family with autosomal dominant DC, a 74-base pair deletion at the 3' end of the gene encoding the RNA component of telomerase, TERC, was first identified in 10 members of the family. Their approach was to map the location of the gene to chromosome 3q by linkage analysis. Given the role of telomerase deficiency previously identified in the X-linked form of DC, *TERC* was the best candidate gene in that region [185]. Since their first description, TERC mutations have been found in about 6 % of DC families (Table 1.1). The disease phenotype associated with TERC mutations is generally milder than in the X-linked disease [186, 187]. However, the severity of the disease increases in successive generations, consistent with genetic anticipation due to inheritance of already-shortened telomeres from the affected parent [188]. Anticipation is also observed in *Terc*-null and *Tert*-null mice. In order for *Terc*-null and *Tert*-null mice to display abnormalities similar to those found in humans, they require breeding for several generations, due to longer telomeres in mice [161].

Up until now, more than 40 additional TERC mutations, including nucleotide substitutions, small/large deletions and insertions have been reported (http://telomerase.asu.edu/diseases.html). Although mutations can be found in all domains of TERC, most are located in the pseudoknot domain/template domain containing sequences required for catalysis, TERT binding, and templating of DNA synthesis. Most TERC mutations, including large deletions, cause a reduction of TERC levels. The resulting haploinsufficiency is likely a mechanism for pathogenesis of these mutations [189]. Haploinsufficiency is also supported by *in vitro* reconstitution experiments, in which expression of mutant TERC in TERC and TERT null cells produces only 50% of telomerase activity with respect to that of wild type TERC [190, 191]. Other TERC mutations mostly results in loss of function through a variety of mechanisms, such as reduced TERC stability, reduced association with TERT, decreased catalytic activity of telomerase, and changes in the accuracy of telomere

repeat addition [189, 192]. Marrone et al. reported two *TERC* mutations (G178A and C180T) that were proposed to be acting on telomerase activity in a dominant negative manner [193]. These mutations reside in a region of the pseudoknot that is thought to be important for homodimer formation by trans-base pairing [190]. Moreover, patients with these two *de novo* mutations presented with aplastic anemia in first generation while published cases with happloinsufficiency require several generations to display clinical phenotypes [194]. Surprisingly, these mutations did not show a dominant negative effect when they were co-expressed with wild type TERC in telomerase negative cells [195]. Thus, TERC happloinsufficency is considered to be the primary mechanism of pathogenicity for TERC mutations, similar to the heterozygous *TERC* knockout mouse model [196, 197].

TERT **mutations**

After the discovery of *TERC* mutations in DC and aplastic anemia, *TERT*, as a component of telomerase, became a good candidate gene to screen for mutations in patients with no *DKC1* or *TERC* mutations. In general, lower penetrance and higher level of heterogeneity are seen in disease caused by *TERT* mutations, compared to disease caused by *TERC* mutations [198]. Several groups found pathogenic *TERT* mutations in patients with aplastic anemia, DC or HH syndrome [199-201]. Since then, more than 50 disease–associated mutations have been reported in *TERT.* These mutations have been mapped to different domains of the protein with a slight clustering in the reverse transcriptase and the CTE domains (http://telomerase.asu.edu/diseases.html). As expected from their localization in *TERT*, most of these mutations affect the catalytic activity or repeat processivity of telomerase [186, 192, 193, 199, 202, 203]. *TERT* mutation thus far has been reported to have dominant negative effects; thus the mechanism of pathogenesis in TERT-associated diseases is generally accepted to be due to haploinsufficiency [199].

Disease caused by *TERT* mutations differs from TERC-associated diseases in terms of penetrance and heterogeneity. Although individuals who are homozygous or compound heterozygous for *TERT* mutations present with severe manifestations of disease, heterozygous *TERT* mutations generally have lower penetrance with

asymptomatic or mildly affected carriers. The heterogeneity of TERT-associated diseases is also higher than in TERC-associated diseases. It has been suggested that there are fewer *TERT* null mutations identified in patients, thereby, most patients with *TERT* mutations still have residual telomerase activity, contributing to the low penetrance and variable expressivity. Genetic anticipation and other genetic/ environmental factors likely also play role in the reduced penetrance and the highly heterogeneous phenotype[198].

***TINF2* mutations**

Germline mutations in *TINF2*, encoding the shelterin protein TIN2, are known to cause autosomal dominant DC. For the first time, Savage et al. identified a mutation in the *TINF2* gene, causing DC in a large family (with no mutations in *TERT*, *TERC* or *DKC1*) via genetic linkage analysis [58]. Affected members of the family had a heterozygous K280E mutation and very short telomeres. Subsequently, the same group found mutations in four of eight additional patients with genetically unidentifiable DC; three with R282H and one with R282S. All of the probands presented with severe DC-like features earlier than four years of age and had very short telomeres. One patient with R282H had Revesz Syndrome [204], characterized by bilateral retinopathy, developmental delay, the DC triad, and cerebellar hypoplasia. In order to further establish the role of *TINF2* mutations in DC, Walne et al. sequenced a large cohort of patients with genetically uncharacterized DC [205]. They identified TINF2 mutations, mostly *de novo*, in 33 out of 175 DC patients. Strikingly, 21 of the mutations were identified in amino acid R282, changing it either to H (14) or to C(7). Interestingly, 32 of the 33 patients had severe forms of DC with very short telomeres compared to other DC subtypes. Most of them had developed aplastic anemia by the age of 10. In addition to missense mutations, there are also patients with severe DC, including Revesz syndrome, who have nonsense and frameshift mutations [206]. Although the general trend of increased severity in DC patients with *TINF2* mutations was confirmed by other studies [206, 207], rare individuals with *TINF2* mutations were found to be silent carriers or to present with less severe forms of DC [58, 205].

As mentioned above, the mechanism of action of pathogenic *TINF2* mutations has yet to be elucidated. Although very short telomeres in patients with *TINF2* mutations is a clue that the effect is on telomere length maintenance, there are contradicting data on the subject in human and mouse cells. While overexpression of pathogenic *TINF2* mutations in human cells was found to mimic the telomere shortening phenotype of DC through deficiency in TERC association, no decrease in telomere length was observed in human cells with these mutations in an independent study [59]. The latter study also revealed that the effect of *TINF2* mutations is independent of telomerase in mouse cells [60].In a separate study, TIN2 was shown to bind a protein called HP1γ. HP1γ binds to telomeres in S phase, where it functions to maintain cohesion of sister chromatids by interacting with cohesin protein complexes. Thus, it prevents sister telomere loss. The HP1γ binding site on TIN2 was shown to be required for sister telomere cohesion, and pathogenic mutations in this region of TIN2 cause failure in telomere length maintenance. Interestingly, *TINF2* mutations in DC cluster at the consensus binding site for HP1γ, and these mutations have been shown to block HP1γ binding. Furthermore, DC patient cells were found to be defective in sister telomere cohesion. These observations suggest that defects in HP1γ binding, and hence defective sister telomere cohesion, likely play a significant role in the pathogenesis of the disease [208, 209]. When pathogenic *TINF2* mutations were overexpressed in human cells, the resulting telomere shortening was less drastic compared to the very short telomere lengths observed in patient cells [208]. In order to explain this discrepancy, the authors speculated that the effect of *TINF2* mutations could be on embryonic telomere maintenance, in which sister telomere cohesion is involved in a recombination like mechanism [210, 211].

***TCAB1* mutations**

TCAB1, also known as *WDR79* or *WDR53*, is a WD40 repeat-containing protein that binds to the CAB box within the H/ACA domain of TERC [114, 212]. As mentioned, the CAB motif is required for trafficking of telomerase to Cajal bodies. The accumulation of telomerase in Cajal bodies is crucial for translocation of telomerase to telomeres [213]. Depletion of TCAB1 by RNA interference causes disruption of the association of

TERC with both Cajal bodies and telomeres. Thus, TCAB1 plays a key role in the trafficking and translocation of telomerase. TCAB1 depletion also leads to telomere shortening in cancer cells, suggesting its involvement in the control of telomere synthesis [113].

Zhong et al. sequenced the *TCAB1* gene in a cohort of DC patients with no known DC-associated mutations [214]. Two patients with telomere lengths below the first percentile were found to be compound heterozygous for *TCAB1* mutations. Both of the patients presented with classic DC, including the triad of mucocutaneous features and bone marrow failure. *TCAB1*-associated DC was inherited in an autosomal recessive manner in these two families. The mother and father of each proband carried one of the *TCAB1* mutations, although they had no clinical manifestations and normal telomere lengths. The mutations (F164L and R398W; H376Y and G435R) are in conserved residues of TCAB1. Epitope-tagged proteins with the pathogenic mutations were found to exhibit reduced expression in HeLa cells compared to the wild type protein, and the localization of mutant proteins to Cajal bodies was impaired. Similar mislocalization defects were observed in patient-derived cells. In addition to TCAB1 mislocalization, dyskerin failed to localize in Cajal bodies, and TERC mislocalized to nucleoli instead of Cajal bodies in patient-derived cells [214]. Thus, pathogenic *TCAB1* mutations impair the trafficking of telomerase, causing the failure of telomerase to be localized in Cajal bodies for its subsequent translocation to telomeres.

CTC1 mutations

Conserved telomere maintenance component 1 (CST telomere maintenance component 1 or CTC1) is a component of a trimeric complex, called CST (CTC1/STN1/TEN1). The CST complex localizes to telomeres and functions in telomere maintenance through telomere replication [215, 216] but the exact mechanism by which it functions has not yet been elucidated. Although it is involved in the inhibition of telomerase function both *in vivo* and *in vitro* [217], the CST complex was proposed to function mainly in priming the filling of the C-strand gap by recruiting pol α primase, subsequent to extension of the 3'overhang by telomerase [218, 219]. In particular, CTC1 is known to bind single stranded DNA and stimulate pol α primase activity [215,

216, 220]. In addition, Gu et al. suggested that CTC1 contributes to efficient telomere replication at telomeres by promoting the restart of lagging strand telomere synthesis at stalled replication forks [221].

Two independent studies revealed that compound heterozygous mutations in *CTC1* cause Coats plus syndrome, which is characterized by short telomeres and other phenotypes overlapping with DC [222-224]. Subsequently, Keller et al. identified compound heterozygous mutations in *CTC1*, in a patient with DC [225]. Interestingly, the mutations found in the DC patient are identical to the mutations found in patients with Coat plus syndrome [222, 223], thus strengthening the role of *CTC1* mutations in the pathogenesis of both diseases. The differences in the phenotypic presentations of these patients are likely due to genetic and/or environmental modifying factors [225, 226] also identified biallelic *CTC1* mutations in 6 patients with DC and related bone marrow failure syndromes. Interestingly, the spectrum of phenotypical features in these patients with *CTC*1 mutations was highly variable, even with regard to telomere length.

Phenotypes observed in *Ctc1* knockout mice are similar to the clinical manifestations of some patients with *CTC1* mutations, including bone marrow failure. Moreover, defective telomere replication and massive telomeric loss observed in cells from *Ctc1* knockout mice may also account for the effect of *CTC1* mutations in patients with short telomeres [221, 226]. Chen et al. functionally characterized disease-causing *CTC1* mutations, including point mutations and small deletions, and showed that they are generally defective in the telomere replication function of the CST complex, leading to accumulation of single-stranded gaps at telomeres [227]. All patients described to date have missense mutations; none of them carry two loss of function mutations, suggesting that complete loss of CTC1 function might be lethal. When mutant proteins with missense mutations were co-expressed with wild type CTC1, they showed a dominant–negative effect on the telomere replication function of CST. In conclusion, all *CTC1* mutations result in the accumulation of single-stranded gaps at telomeres, indicating that the replication defect is the most common mechanism of pathogenesis.

RTEL1 mutations

Regulator of telomere elongation helicase 1 (*RTEL1*) is an evolutionarily conserved DNA helicase, playing at least 2 critical roles in telomeric integrity [228]. First, it prevents replication fork stalling during telomeric DNA replication by removing the telomeric G-quadruplex, thereby suppressing telomeric fragility. Second, it is thought to be involved in the disassembly of t-loop structures at certain stages of the cell cycle to prevent catastrophic telomere loss [34, 229].

RTEL1 mutations were recently identified in a small cohort of DC patients by whole-exome sequencing [230]. Probands from two families had Hoyeraal Hreidarsson (HH) syndrome and a proband from a third family had a DC-like syndrome. Siblings with HH in the first family showed autosomal dominant inheritance of a R1010X mutation. Their mother, who has short telomeres, also carries the mutation. The proband in the second family had compound heterozygous mutations in *RTEL1* (E615D and R998X) with autosomal recessive inheritance. Genetic anticipation was observed in both families associated with telomere shortening. The proband from the third family had an A645T mutation associated with short telomeres. Both R1010X and R998X are predicted to result in loss of PIP (PCNA-interacting peptide) motifs in RTEL1. The phenotypes produced by these mutations are predicted to be similar to RTEL1-PIP box mutant mouse-like phenotypes, including replication fork instability [231]. E615 and A645 are highly conserved residues in the C-terminal helicase domain, which plays a key role in the helicase activity of RTEL1 and may explain the telomere shortening phenotypes [230].

In an independent study of 7 families, 11 biallelic *RTEL1* mutations with autosomal recessive inheritance were identified in 10 individuals with HH syndrome. Cells harboring these mutations showed defects in resolution of t-loops, which may be a mechanism for telomere shortening in these patients [232]. In a third study of two families, using an approach combining whole-genome linkage analysis and exome sequencing, compound heterozygous *RTEL1* mutations were identified in three patients with HH syndrome. The mutations reside either at the catalytic core of RTEL1 or in the cysteine rich consensus sequence, C4C4-type RING-finger motif [233]. Although the

role of the C4C4-type RING-finger motif is not fully known, it is involved in protein-protein interactions and is predicted to be important for the metal ion binding function of RTEL1 [234].

In conclusion, there are a number of DC mutations identified throughout the *RTEL1* gene. The underlying pathogenic mechanism of each mutation remains to be determined but is likely associated with either increased telomeric fragility or increased t-loop excision.

Aplastic Anemia (AA)

AA is characterized by peripheral blood pancytopenia due to inefficient hematopoiesis and hypocellular bone marrow. Mutations in telomerase components (TERT: [201]; *TERC:* [235]) are common in AA patients and accordingly, reduced telomerase activity and telomere loss are characteristic of AA. Indeed, AA is a common manifestation in DC patients. In addition to exhibiting significantly short telomeres, AA patient cells display an increased frequency of chromosomal breaks and aberrations, including monosomy 7 in some cases [236]. As with DC, clinical features of AA can be explained by a reduction in stem cell reserves, caused by the failure of self-renewal capacity of stem cells due to telomerase deficiency. Given the primary clinical manifestations in blood cells and bone marrow, hematopoietic stem cells are the most significantly affected stem cell population in AA patients.

Idiopathic Pulmonary Fibrosis (IPF)

IPF is a chronic, progressive, fatal lung disease characterized by dyspnea, lung scarring and abnormal gas exchange. It is also a common manifestation of other telomerase-related diseases, specifically, the autosomal dominant form of DC. Mutations in *TERT* and *TERC* are currently the most identifiable genetic cause of IPF, with germline mutations in *TERT* and *TERC* observed in up to one-sixth of patients with IPF [237]. However, one study suggested that the prevalence of sporadic mutations in *TERC* and *TERT* in IPF patients is considerably lower [238]. Two independent studies using different approaches have demonstrated that patients with heterozygous *TERT* and *TERC* mutations have shorter telomere lengths in their white blood cells compared

to age-matched controls. Continuous shortening of telomeres leads to premature senescence in alveolar epithelial cells, which explains the underlying basis of the disease. Due to the time that is needed for telomeres to reach critical shortening, differences in mean telomere lengths between carriers and age- matched controls are higher in older mutation carriers of a given family. This also explains the age-dependent nature of IPF. In addition, it was proposed that IPF and bone marrow failure form a syndrome complex [239]. Parry et al. showed that in 10 patients from 10 families, co-occurrence of IPF and bone marrow failure were predictive of germline mutations of TERT or TERC with 100% accuracy [240]. In these families, it was proposed that the pattern of disease switches from being lung-predominant to being bone marrow-predominant in successive generations [240].

B.6. The role of telomerase in cancer

The earliest connection between telomeres and cancer was from studies in primary human fibroblast cells. Hayflick showed that fibroblasts have limited replicative potential such that they undergo ~60-80 population doublings before they enter a non-replicative senescent state [241]. On the other hand, cancer cells keep dividing indefinitely in cell culture. Moreover, progressive telomere shortening was observed in normal fibroblast cells but not in cancer cells. The connection between these two observations provided the first clue for the association between telomere length maintenance and cancer. Since the first observation of telomerase expression in association with cancer in 1994, the number of studies on this subject has increased exponentially [242].

The canonical role of telomerase in cancer is to maintain telomere length. Normal somatic cells, as mentioned above, have limited replicative potential. Due to the lack of telomerase expression, they undergo telomere shortening with each division and enter replicative senescence. Cells with defective cell cycle check points such as inactivated p53, Rb, or p16, bypass this senescence state and continue to divide. As they divide, telomere erosion persists until the cells reach a crisis state, in which chromosome ends become uncapped and shortened ends fuse together. This sequence of events results in chromosomal instability and eventually apoptosis. Replicative senescence and crisis

are mechanisms used by the cell to protect against cancer. However, in some cases cells can acquire a mechanism to maintain the length of their telomeres before crisis. The most common way of maintaining telomeres is to activate telomerase expression, which is believed to be an important step in the progression towards carcinogenesis.

In addition to its role in telomere length maintenance, telomerase has been suggested to have other roles in carcinogenesis. It is known that telomerase-negative tumor-derived cells maintain their telomere length by a mechanism called Alternative Lengthening of Telomeres (ALT). Stewart et al. used a cell line that maintains telomere length by ALT to demonstrate that the role of telomerase activity in carcinogenesis cannot be substituted by the ALT mechanism [243]. Thus, telomerase is thought to have additional, probably extra-telomeric roles in tumorigenesis. It was demonstrated that telomerase can also affect proliferation of epithelial cells by modulating the expression of growth-promoting genes. Ectopic expression of telomerase in human mammary epithelial cells leads to a decrease in the requirement of mitogens to promote cell growth. This effect was shown to be mediated through the inhibition of expression of growth-promoting genes such as EGFR [244]. Moreover, telomerase functions as a transcriptional modulator of Wnt/β catenin signaling, which is implicated in several different cancer types. In addition to its putative role in cell proliferation, TERT is also involved in the suppression of apoptosis. Taken together, these observations support the hypothesis that telomerase has telomere-independent roles in tumorigenesis [49].

Deregulation of telomerase is a common feature of cancer cells. In approximately 90% of cancers, telomerase expression is upregulated. Although the exact mechanism is not clear in all cases, it is thought to occur through several different mechanisms including epigenetic deregulation and amplification of the *TERT* gene locus [245]. Another interesting hypothesis is that normal stem cells, which naturally exhibit telomerase activity, are progenitors in tumors [246]. Recently, two independent groups discovered causal promoter mutations in the *TERT* gene creating *de novo* Ets/TCF transcription factor binding motifs. Horn et al. identified a *TERT* promoter mutation in a large family with melanoma. In reporter gene assay studies, this mutation was shown to result in a two fold induction in transcription of *TERT* [247]. When they screened tumors

from unrelated families with melanoma, they identified recurrent mutations in the *TERT* promoter, resulting in the creation of Ets/TCF transcription factor binding motifs. Huang et al also identified two independent highly recurrent mutations in promoter region of the *TERT* gene, which generate *de novo* Ets/TCF transcription factor binding motifs and induce a two-to four fold induction in transcription of *TERT* in reporter gene assay studies [248]. Moreover, they found these mutations in cell lines from different types of tumors, including bladder and hepatocellular cancer cells. These two studies demonstrated that promoter mutations in the *TERT* gene leading to telomerase activation are an important tumorigenic mechanism [247, 248]. In addition, the role of telomerase reactivation in the rapid progression of prostate cancer was demonstrated in a mouse model with short dysfunctional telomeres [249]. The same group also showed that in identical telomere dysfunction settings, when reactivation of telomerase is inhibited, cancer cells reprogram their transcription of mitochondrial genes to adapt to the loss of telomerase activity and acquire the ALT mechanism to maintain telomere length [250].

Considering the role of telomerase in tumorigenesis, there has been a lot of effort to devise telomerase-based therapies against cancer. One strategy is vaccination against tumor associated antigens, although the results of clinical trials have not yet been very successful. For instance, vaccination with GV1001, a 16-mer TERT peptide, seemed to generate a specific immune response in non-small cell lung cancer [251], whereas no immune or tumor response was seen in patients with hepatocellular carcinoma and cutaneous T cell lymphoma [252, 253]. Another popular approach is gene therapy involving targeting either the RNA of TERC or TERT expression by antisense oligonucleotides (ASOs). The most well-studied ASO is imetelstat (GRN163L), a lipid-modified 13-mer oligonucleotide complementary to TERC [254]. Studies in preclinical models showed therapeutic potential of imetelstat; thus, it is currently being tested in clinical trials [255, 256].

Future studies in the field of telomeres and telomerase will provide new insights into the regulation and maintenance of stem cells as well as the complex relationship between telomeres and cancer development.

C. INTRODUCTION TO DISSERTATION

As discussed in previous sections, DC is an inherited bone marrow failure disorder, characterized by short telomeres. Although the genetic cause of DC is not always identified; in 70% of cases, DC is the result of germline mutations in nine telomere biology genes including *TERC*, *TERT*, *DKC1*, *NHP2*, *NOP10*, *TCAB1*(*WRAP53*), *RTEL1*, *TINF2* and *CTC1* (Figure 1.5).

In Chapter 2, I report for the first time that mutations in *ACD/TPP1* can cause of DC. We identified a single-amino-acid deletion in the TEL patch and a missense mutation in the TIN2-binding domain of TPP1 in a patient with a severe variant of DC, Hoyeraal-Hreidarsson (HH) syndrome. Functional characterization of these mutations revealed that the deletion in the TEL patch abrogates telomerase recruitment and also impairs the enzymatic processivity of telomerase, whereas the missense mutation has milder effects characterized by reduced binding to TIN2.

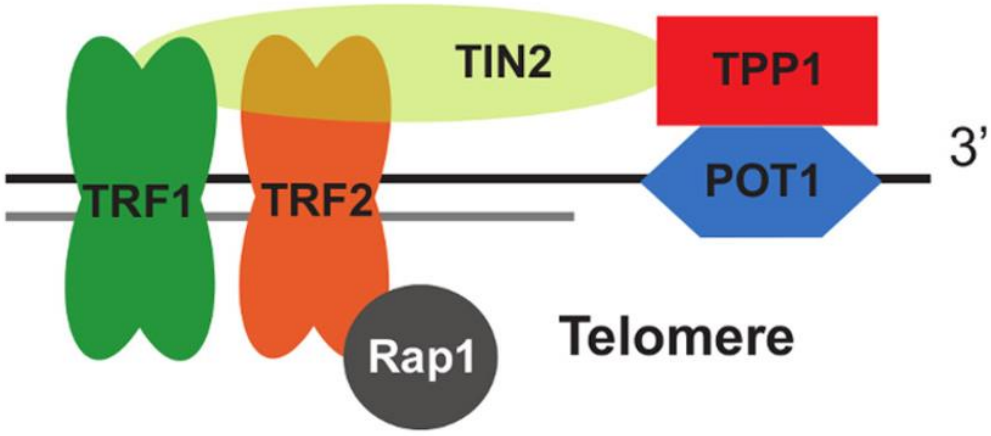

Figure 1.1: Schematic diagram of shelterin complex. There are six known subunits of shelterin. TRF1 and TRF2 bind to double-stranded telomeric DNA. TIN2 can bridge TRF1 and TRF2. POT1 binds to single-stranded telomeric DNA. POT1 is recruited to telomeres by TPP1. TPP1 is recruited to telomeres by TIN2. Rap1 is a binding partner of TRF2.

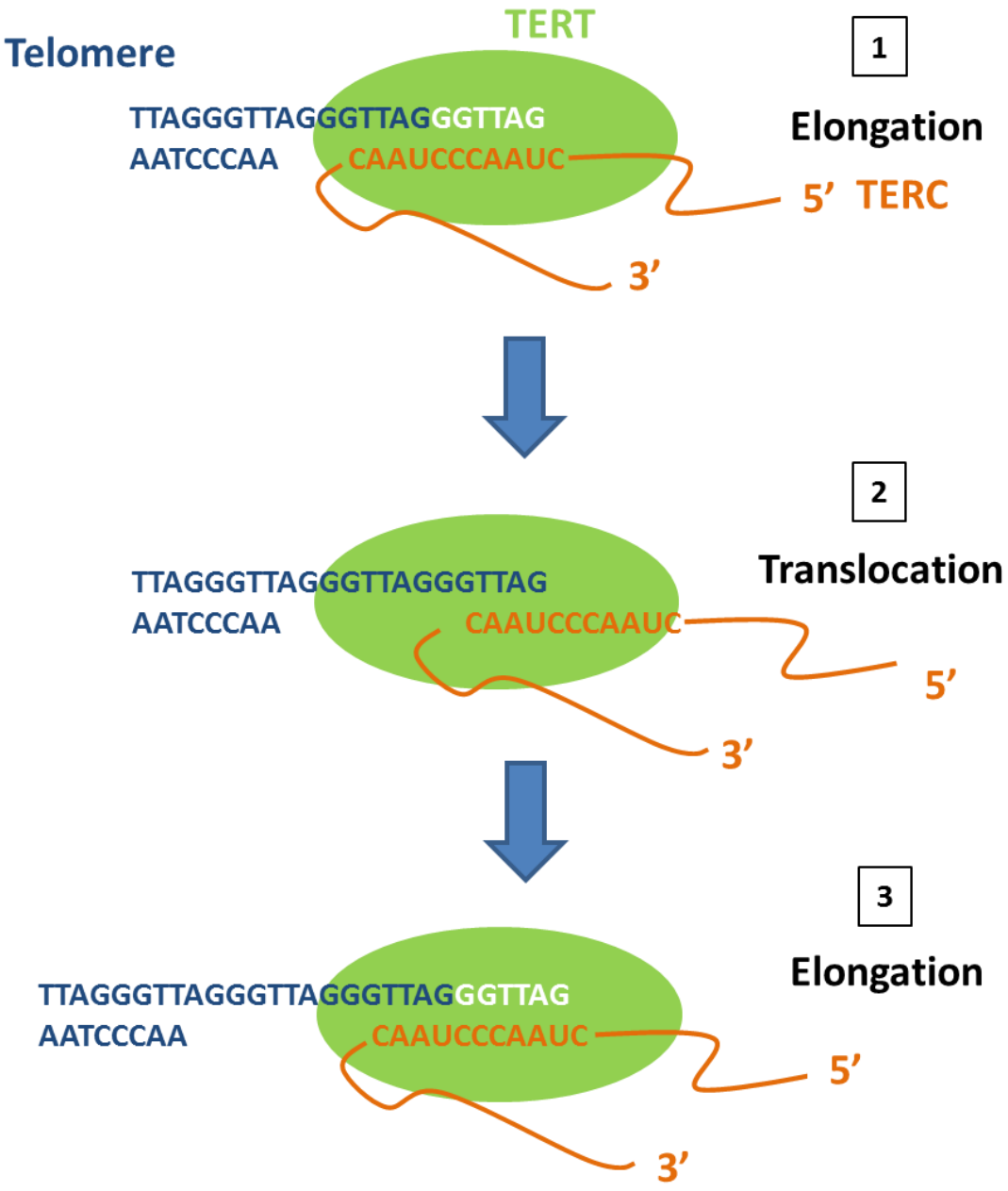

Figure 1.2: Telomeric repeat synthesis by telomerase. RNA component of telomerase (TERC, shown in orange) functions as template for the synthesis of 3' end. Reverse transcriptase component of telomerase (TERT, shown in green) synthesizes the complementary strand until 5' end of template is reached (1). Then, telomerase translocates to newly synthesized 3' end (2). After the translocation of telomerase, second round of synthesis is performed by TERT (3). Primase and DNA polymerase synthesize the complementary strand of 3' overhang.

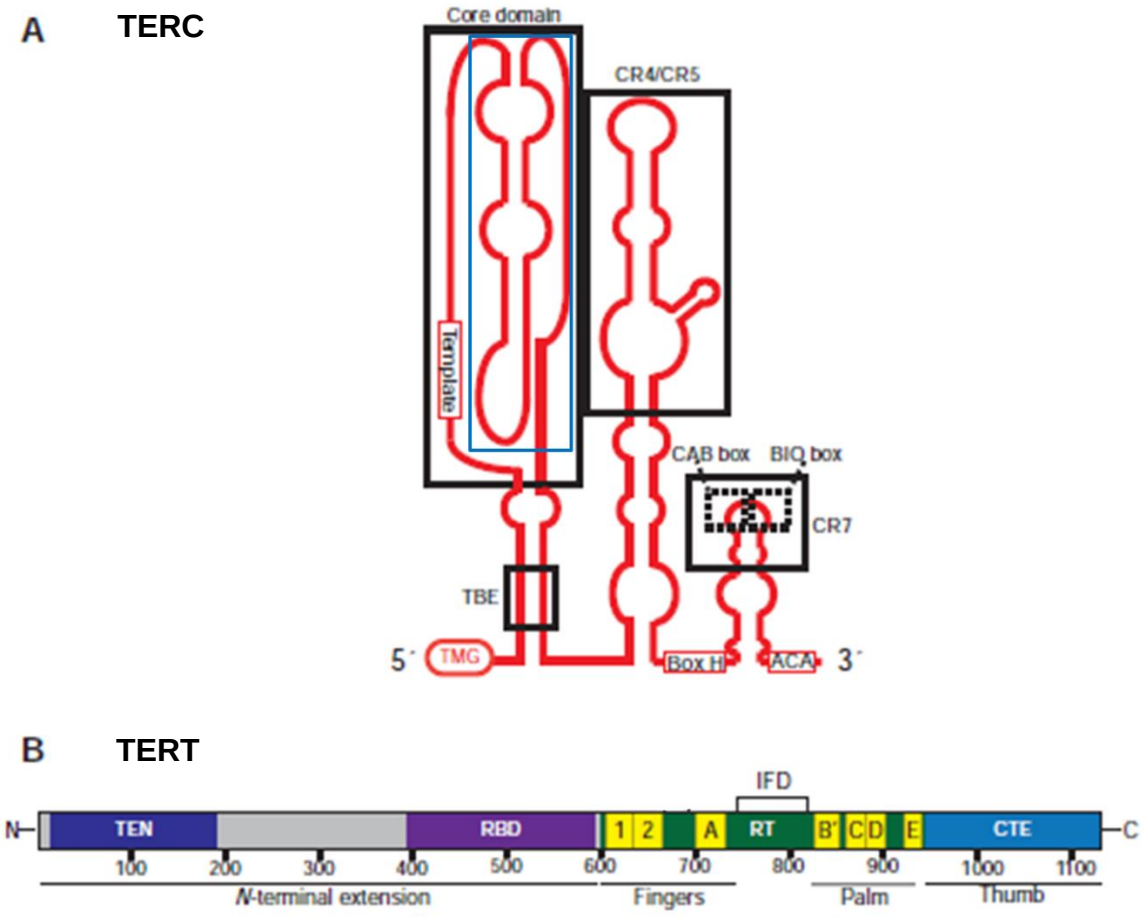

Figure 1.3: Domain structure of human TERC and TERT. (A) Schematic representations of the secondary structures of TERC. CR4/CR5, CR7, BIO box, CAB box, H/ACA domains, template boundary element (TBE), and 5' trimethylguanosine (TMG) cap are indicated. Pseudoknot is indicated with blue box. TMG (B) Domain structure of human TERT. The N-terminal extension, telomerase RNA-binding domain (RBD), fingers, palm, thumb, and IFD are shown. Adopted from Hukezalie and Wong (2013)[3].

Figure 1.4: DC diagnostic triad. A. Dystrophic fingernails. B. Lacey, reticular pigmentation of the neck and upper chest. C. Oral leukoplakia. Adopted from Savage and Alter (2009) [2]

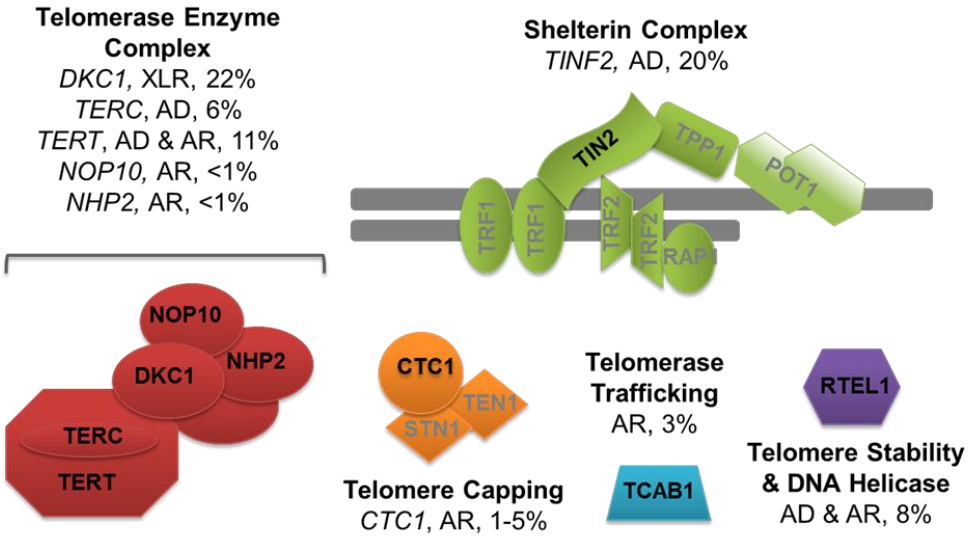

Figure 1.5: DC genetics. Germline mutations in telomerase subunit genes (*TERC* and *TERT*) or genes involved in telomerase biogenesis (*DKC1*, *NOP10*, *NHP2*, and *WRAP53*) are commonly associated with DC. Additionally, mutations in telomere biology genes (*TINF2*, *CTC1*, and *RTEL1*) are also observed in certain cases of DC. XLR: X-linked recessive, AD: Autosomal dominant, AR: Autosomal recessive. Adopted from Savage (2014) [1]

Table 1.1: Known genetic causes of DC

Gene, gene product name(s)	Inheritance	%DC
DKC1, Dyskerin	X-linked recessive	22
NOP10, NOP10, NOLA3, Nuclear protein family A, member 3	Autosomal recessive	<1
NHP2, NHP2, NOLA2, Nuclear protein family A, member 2	Autosomal recessive	<1
TERC, TERC, Telomerase RNA	Autosomal dominant	6
TERT, TERT, Telomerase Reverse Transcriptase	Autosomal dominant Autosomal recessive	11
TINF2, TIN2, TERF1 (TRF1)-Interacting Nuclear Factor 2	Autosomal dominant	20
TCAB1, TCAB1, Telomerase Cajal Body Protein 1	Autosomal recessive	3
CTC1, CTC1, Conserved Telomere Maintenance Component 1	Autosomal recessive	1-5
RTEL1, RTEL1, Regulator of Telomere Elongation Helicase 1	Autosomal dominant Autosomal recessive	8

CHAPTER 2: HOYERAAL-HREIDARSSON SYNDROME CAUSED BY A GERMLINE MUTATION IN THE TEL PATCH OF THE TELOMERE PROTEIN TPP1

ABSTRACT*

Germline mutations in telomere biology genes cause dyskeratosis congenita (DC), an inherited bone marrow failure and cancer predisposition syndrome. DC is a clinically heterogeneous disorder diagnosed by the triad of dysplastic nails, abnormal skin pigmentation, and oral leukoplakia. Hoyeraal-Hreidarsson syndrome (HH), a clinically severe variant of DC, also includes cerebellar hypoplasia, immunodeficiency, and intrauterine growth retardation. Approximately 70% of DC cases are associated with a germline mutation in one of nine genes, the products of which are all involved in telomere biology. Using exome sequencing, we identified mutations in *Adrenocortical Dysplasia Homolog* (*ACD*) (encoding TPP1), a component of the telomeric shelterin complex, in one family affected by HH. The proband inherited a deletion from his father and a missense mutation from his mother, resulting in extremely short telomeres and a severe clinical phenotype. Characterization of the mutations revealed that the single-amino-acid deletion affecting the TEL patch surface of the TPP1 protein significantly compromises both telomerase recruitment and processivity, while the missense

* Material in this chapter is modified from:

Kocak H, Ballew BJ, Bisht K, , Boland JF, Eggebeen R, Hicks BD, Suman S, O'Neil A, Giri N, NCI DCEG Cancer Genomic Research Laboratory; NCI DCEG Cancer Sequencing Working Group, ; Maillard I, Alter BP, Keegan C , Nandakumar J, Savage SA (2014) "Hoyeraal-Hreidarsson syndrome caused by a germline mutation in the TEL patch of the telomere protein TPP1". *Genes Dev.* 28(19):2090-102.

The experiments shown in figures 2.4B, 2.5, 2.6, 2.7, 2.8 were performed by me. The experiments shown in figures 2.9A, D, 2.10 and figure 2.11A, B were performed by me in collobaration with Kamlesh Bisht. I contributed to the experiments in figures 2.11C, D by doing transient transfections for the ChIP assay.

mutation in the TIN2-binding region of TPP1 is not as clearly deleterious to TPP1 function. Our results emphasize the critical roles of the TEL patch in proper stem cell function and demonstrate that TPP1 is the second shelterin component (in addition to TIN2) to be implicated in DC.

INTRODUCTION

Dyskeratosis congenita (DC) is a rare cancer-prone inherited bone marrow failure syndrome caused by dysfunctional telomere maintenance [170, 257]. It is diagnosed clinically by the presence of the classic triad of nail dysplasia, lacy skin pigmentation, and oral leukoplakia. Substantial clinical heterogeneity exists among DC patients, even within affected families: Patients may also have pulmonary fibrosis; liver disease, esophageal, urethral, or lacrimal duct stenosis; developmental delay; dental and ophthalmologic abnormalities; and/or other complications [170]. Patients with DC are at a very high risk of bone marrow failure and cancer, particularly myelodysplastic syndrome, acute myelogenous leukemia, and solid tumors (usually squamous cell carcinoma of the head/neck, skin, or anogenital region) [258]. DC is characterized on a molecular level by blood leukocyte telomere lengths less than the first percentile for age, the result of germline mutations in telomere biology genes [259].

Multiple modes of inheritance are associated with DC [183, 184, 225, 226, 232, 233, 260, 261]. X-linked recessive (XLR) DC is caused by *DKC1* (MIM 300126) mutations. Autosomal dominant (AD) DC can be caused by mutations in *TERC* (MIM 602322; encodes the telomerase RNA template TR), *TERT* (MIM 187270; encodes the telomerase reverse transcriptase), *RTEL1* (MIM 608833), or *TINF2* (MIM 604319). Autosomal recessive (AR) inheritance of mutations in *TERT*, *RTEL1*, *CTC1* (MIM 613129), *NOP10* (MIM 606471), *NHP2* (MIM 606470), or *WRAP53* (MIM 612661) also cause DC. Germline mutations in these genes account for ~70% of DC cases.

Hoyeraal-Hreidarsson (HH) syndrome is a clinically severe variant of DC marked by immunodeficiency [262], intrauterine growth retardation (IUGR), developmental delay, and cerebellar hypoplasia; the latter is characteristic of HH [263]. HH patients have extremely short telomeres, even in comparison with other DC patients [259].

Mutations in a subset of DC-associated genes (*DKC1* [XLR], *TINF2* [AD], *TERT* [AR], and *RTEL1* [AD and AR]) have been shown to cause HH.

TPP1, a protein encoded by the *Adrenocortical Dysplasia Homolog* (*ACD*) gene (MIM 609377), is one of the core components of the telomeric shelterin complex (Figure 2.1). TPP1 performs multiple functions at the telomere, mediated by distinct protein domains (Figure 2.2A). The central domain of TPP1 facilitates formation of a heterodimer with POT1 (MIM 606478); this complex binds and protects the single-stranded tail found at all chromosome ends [63, 75, 76]. Via the C-terminal domain, TPP1 binds TIN2, forming a bridge between POT1 and the dsDNA-binding TRF1/TRF2 (MIM 600951/602027) components of shelterin [57]. By physically linking two critical shelterin components, TPP1 plays a central role in protecting chromosome ends [264].

In addition to its critical role in end protection, TPP1 is also responsible for recruiting telomerase to chromosome ends, thereby facilitating telomere extension (Figure 2.1). A group of surface-exposed amino acids in the N-terminal OB domain of TPP1 (TPP1-OB), collectively termed the TEL patch, mediates the interaction of TPP1 with telomerase, facilitates telomerase recruitment to telomeres, and stimulates telomerase enzymatic processivity (Figure 2.2A; [67, 69, 70, 78, 79, 81, 140]. An intact TEL patch is required for both telomere lengthening and HeLa cell proliferation [81, 265]. Because TPP1 depends on binding to TIN2 for its own recruitment to telomeres, the TPP1–TIN2 interaction described above is also important for telomerase recruitment [67, 78, 79].

Here, we report the identification of a single-amino-acid deletion in the TEL patch of TPP1 and a missense mutation in the TIN2-binding domain of TPP1 in an HH proband who is negative for mutations in other DC-associated genes. Characterization of these mutants revealed that the deletion in the TEL patch severely compromises both telomerase recruitment and processivity, whereas the missense mutation has less severe effects.

MATERIALS AND METHODS

Patients

Patient NCI-275-1 and his family were participants in an institutional review board (IRB)-approved longitudinal cohort study at the National Cancer Institute (NCI) entitled "Etiologic Investigation of Cancer Susceptibility in Inherited Bone Marrow Failure Syndromes" (NCI 02-C-0052, ClinicalTrials.gov Identifier: NCT00027274). This study includes comprehensive family history and individual history questionnaires, detailed medical record review, and biospecimen collection [258]. The proband, his older sister, younger twin sisters, mother, and father were evaluated at the National Institutes of Health (NIH) Clinical Center by the Inherited Bone Marrow Failure Syndromes (IBMFS) study team. Telomere length was evaluated by flow cytometry with fluorescent *in situ* hybridization (flow FISH) in leukocytes [266].

Exome Sequencing and Analysis

Whole exome sequencing for family NCI-275 was performed at the NCI's Cancer Genomics Research Laboratory as previously described [261], with the following modifications. Genomic DNA libraries were prepared and amplified with the Bioo Scientific NEXTflex™ Pre-Capture Combo Kit (Bioo Scientific, Austin, TX, USA) according to the manufacturer's protocol, then cleaned with Agencourt AMPure XP Reagent (Beckman Coulter Inc, Brea, CA, USA) according to the Bioo-provided protocol. Amplified sample libraries were quantified using Quant-iT™ PicoGreen dsDNA Reagent (Life Technologies, Carlsbad, CA, USA). Prior to hybridization, four amplified sample libraries with unique index adapters were combined in equal amounts (275 ng) into 1.1 µg pools for multiplex sequence capture. Exome sequence capture was performed with NimbleGen's SeqCap EZ Human Exome Library v3.0, targeting 64 Mb of exonic sequence (Roche NimbleGen, Inc., Madison, WI, USA). Exome-enriched libraries were amplified and purified as above. The resulting post-capture enriched multiplexed sequencing libraries were sequenced as described [261]. Approximately 90% of all targeted bases were covered at a depth of 15X or greater (Table 2.3).

Sequence reads were trimmed using the Trimmomatic program [267], then aligned to the hg19 reference genome using Novoalign software version 2.07.14 (http://www.novocraft.com), Picard software version 1.67 (http://picard.sourceforge.net/) and the Genome Analysis Toolkit (GATK, http://www.broadinstitute.org/gatk/) [268] as described previously [261]. Variant discovery, genotype calling, and annotation were performed as described [261] using data from the UCSC GoldenPath database (http://hgdownload.cse.ucsc.edu/goldenPath/hg19/database/), the ESP6500 dataset from the Exome Variant Server, NHLBI Exome Sequencing Project (ESP), Seattle, WA (http://evs.gs.washington.edu/EVS/) (accessed August 2012), the Institute of Systems Biology KAVIAR (Known VARiants) database (http://db.systemsbiology.net/kaviar/) [269], the National Center for Biotechnology Information dbSNP database (http://www.ncbi.nlm.nih.gov/projects/SNP/) [270] build 137, and the 1000 Genomes (http://www.1000genomes.org/); [271]. Variants were also annotated for their presence in an in-house database consisting of over 1400 whole exomes that were sequenced in parallel with our DC families. Variants within each family were filtered and categorized as indicated in Table 2.4.

Ion semiconductor sequencing

Validation of exome sequencing findings in the NCI-275 family was performed by sequencing the entire genomic locus surrounding TPP1 (chr16:67690393-67695778). A targeted, multiplex PCR primer panel (Table 2.6) was designed using the custom Ion AmpliSeq Designer v3.0 (Life Technologies, Carlsbad, CA, USA). The primer panel covered 95.85% of the ACD gene, including introns and up- and down-stream sequence. Average amplicon size was 224bp. DNA was amplified using this custom AmpliSeq primer pool, and libraries were prepared following the manufacturer's Ion AmpliSeq Library Preparation protocol (Life Technologies, Carlsbad, CA, USA). Individual samples were barcoded, pooled, templated, and sequenced on the Ion Torrent PGM Sequencer using the Ion PGM Template OT2 200 and Ion PGM Sequencing 200v2 kits per manufacturer's instructions. Mean read length after sequencing was 140bp.

Sanger sequencing

EBV-transformed lymphoblastoid cells derived from family members were cultured in IMDM media containing 20% FBS and 1% L-alanyl-L-glutamine. Fibroblast cells derived from the family members were cultured in DMEM containing 10% FBS. Genomic DNA was isolated from the above cells with PUREgene Blood Core Kit B using the manufacturer's instructions (Qiagen). The genomic region of interest was amplified by PCR with sequence-specific primers (Table 2.6). PCR products were sequenced by the University of Michigan DNA Sequencing Core and resulting data were analyzed using the Sequencher 5.1 DNA sequence analysis software (Gene Codes Corporation, Ann Arbor, MI).

***In silico* analysis**

PolyPhen-2 [272] (http://genetics.bwh.harvard.edu/pph2), SIFT [273] (http://sift.jcvi.org), PROVEAN [274] (http://provean.jcvi.org), MutationAssessor [275] (http://mutationassessor.org), MutationTaster [276] (http://mutationtaster.org), and FATHMM [277] (http://fathmm.biocompute.org.uk), and CADD [278] were used to predict the severity of TPP1 mutations. Multiple sequence alignments were generated for homologous TPP1 protein sequences using COBALT [279] (http://www.st-va.ncbi.nlm.nih.gov/tools/cobalt) and viewed in Jalview [280](www.jalview.org) to evaluate conservation. Alignments were generated with proteins NP_001075955.1 (*Homo sapiens*), EPQ14055.1 (*Myotis brandtii*), AAI49588.1 (*Bos taurus*), ELR55817.1 (*Bos mutus*), EHH31762.1 (*Macaca mulatta*), NP_001032270.1 (*Rattus norvegicus*), NP_001012656.1 (*Mus musculus*), EGV97050.1 (*Cricetulus griseus*), ELV12230.1 (*Tupaia chinensis*), EHB17028.1 (*Heterocephalus glaber*), ELK14507.1 (*Pteropus alecto*), ELK25602.1 (*Myotis davidii*), EPY84197.1 (*Camelus ferus*), NP_001089068.1 (*Xenopus laevis*), and NP_001124265.1 (*Danio rerio*).

Site-directed mutagenesis

Oligonucleotides for site-directed mutagenesis were purchased from Integrated DNA Technologies (Coralville, IA). Indicated variants for expression in cultured human cells were introduced into the *ACD* gene using fully complementary mutagenic primers

(QuickChange® Site-Directed Mutagenesis Kit; Agilent Technologies, Santa Clara, CA). The p3X-FLAG-TPP1-CMV plasmid was used as the template in the PCR reaction. The *ACD* genes in the mutant plasmids were sequenced completely to confirm the presence of the intended mutation and to exclude the acquisition of unwanted nucleotide changes.

Expression and purification of recombinant proteins

Purified wild-type and K170Δ Smt3-TPP1-N fusion proteins were obtained upon lysis of isopropyl β-d-thiogalactopyranoside-induced BL21(DE3) cells after nickel–agarose chromatography, treatment with Ulp1 protease (MTA with Cornell University for pUlp1 vector) to cleave the Smt3 tag, and size exclusion chromatography (Superdex 75, GE Life Sciences) as reported previously [69]. The full-length human POT1 gene was cloned into a His-Sumostar-containing baculoviral expression vector (Life Sensors) and expressed in baculovirus-infected High Five cells (Life Technologies) using vendor recommendations. POT1 protein was purified from these insect cell lysates using nickel–agarose chromatography, treatment with SUMOstar protease (Life Sensors), anion exchange (HiTrap Q HP, GE Life Sciences), and size exclusion chromatography (Superdex 200, GE Life Sciences).

HeLa and HEK293T cell culture

A clonal HeLa cell line called HeLa-EM2-11ht [81] was used for all transient transfection experiments reported here involving HeLa cells. HeLa-EM2-11ht was obtained from Tet Systems Holdings. KG upon signing an MTA. HeLa1.2.11 cells were used only in the telomere ChIP experiments. Both HeLa cell lines and the HEK293T cells were cultured at 37°C in the presence of 5% CO_2; they were propagated in growth medium containing DMEM, 10% FBS, 1 mM sodium pyruvate, 2 mM L-glutamine, 100 U/mL penicillin, and 100 µg/mL streptomycin. Doxycycline was added to a final concentration of 200 ng/mL for expression of the human POT1 (or TIN2) gene that is driven by a tetracycline-inducible promoter from the p3X-Flag-POT1-BI4 (or p3X-Flag-TIN2-BI4) plasmid in HeLa-EM2-11ht cells [81].

Culture and manipulation of EBV-transformed lymphoblasts from proband and family members

EBV-transformed lymphoblastoid cells derived from family members were cultured in IMDM medium containing 20% FBS and 1% L-alanyl-L-glutamine. They were centrifuged at 1200 rpm for 3 min and washed with 1× PBS to pellet the cells. The cells were then resuspended in 1% BSA–PBS to a final concentration of ~200 cells per microliter. To prepare slides for FISH analysis, a cytocentrifuge (Rotofix 32A, Hettich Lab Technology) was used. One-hundred microliters of cell suspension was aliquoted into cytocentrifuge funnels and centrifuged at 800 rpm for 3 min. After dissembling the centrifugation setup, a hydrophobic circle was drawn on each slide around the smear using a hydrophobic pen. Cells were fixed with 4% formaldehyde in PBS for 8 min and stored at −20°C. Slides were thawed to room temperate immediately prior to FISH experiments.

Immunofluorescence and Fluorescent *In Situ* Hybridization (IF/FISH)

IF/FISH experiments to measure telomerase recruitment were performed using published protocols [81]. Briefly, confluent six-well plates containing HeLa-EM2-11ht cells were transfected with 1 µg of p3X-Flag-TPP1-CMV (wild-type or indicated mutant) plasmid [265], 1 µg of TERT-cDNA6/myc-HisC plasmid, and 3 µg of phTR-Bluescript II SK(+) plasmid using Lipofectamine 2000 (Life Technologies) following the manufacturer's recommendations. Three days post-transfection, cells were fixed with 4% formaldehyde in PBS for 8 min. After fixative removal, the cells were permeabilized with PBS containing 0.5% Triton X-100 (PBS-T), blocked in PBS-T containing nuclease-free 3% BSA, and incubated with mouse monoclonal anti-Flag M2 (1:500; F1804, Sigma) and rabbit polyclonal anti-coilin (1:100; sc-32860, Santa Cruz Biotechnology) in PBS-T containing nuclease-free 3% BSA for 1 h. The cells were then washed in PBS and incubated with Alexa Fluor 488-conjugated anti-mouse IgG (Life Technologies) and Alexa Fluor 568-conjugated anti-rabbit IgG (Life Technologies) diluted 1:500 in PBS-T containing nuclease-free 3% BSA for 30 min in the dark. The cells were washed in PBS and fixed again in 4% formaldehyde in PBS for 10 min at room temperature. The fixative was removed, and the cells were incubated successively in 70%, 95%, and 100%

ethanol. Upon removal of ethanol, cells were rehydrated in 50% formamide in 2× SSC buffer for 5 min. The coverslips were prehybridized with solution containing 100 mg/mL dextran sulfate, 0.125 mg/mL *Escherichia coli* tRNA, 0.5 mg/mL salmon sperm DNA, 1 mg/mL nuclease-free BSA, 1 mM vanadyl ribonucleoside complexes, and 50% formamide in 2× SSC for 1 h at 37°C in a humidified chamber. Prehybridization buffer was then removed, and the coverslips were incubated overnight at 37°C in a dark humidified chamber in hybridization solution containing a mixture of three Cy5-conjugated TR probes (90 ng of each probe per coverslip) [281]. The next morning, the cells were washed with 50% formamide in 2× SSC followed by PBS, and the coverslips were mounted on microscope slides using ProLong Gold anti-fade reagent containing DAPI (Life Technologies). The coverslips were sealed using transparent nail polish and stored at −20°C. Imaging was performed using a laser-scanning confocal microscope (SP5, Leica) and a 100× oil objective. Images were processed using ImageJ and Adobe Photoshop. Pseudocolored representative cells are shown in figure panels. Mean and standard deviations of three experiments, each involving 100–150 telomeric foci, were plotted for each TPP1 construct. For IF experiments to detect RAP1, rabbit polyclonal anti-RAP1 (1:500; NB100-292, Novus Biologicals) was used. Telomere FISH of EBV-transformed lymphoblasts was performed with a red fluorescence probe: Cy3-OO-CCCTAACCCTAACCCTAA-3′ (Bio-Synthesis, Inc.).

Telomerase activity assays

Both versions of the direct primer extension experiments to measure telomerase processivity shown in Figures 2.9 and 2.10 were based on published protocols [81]. Briefly, for the experiments shown in Figures 2.9A, C, D, and 2.10, HeLa-EM2-11ht cells grown in the wells of a six-well plate were transfected with the indicated plasmid DNA using Lipofectamine 2000 (Life Technologies) using the manufacturer's recommendations. One microgram of TERT-cDNA6/myc-HisC, 3 µg of phTR-Bluescript II SK(+), 1.5 µg of p3X-Flag-POT1-BI4, and 0.5–0.7 µg of p3X-Flag-TPP1-CMV (wild type or mutant) were added per transfection. In control transfections where POT1 and TPP1 were omitted, 2 µg of empty vector was included. Two days post-transfection, the cells were trypsinized, washed with PBS, lysed in 100 µL of CHAPS lysis buffer [70],

and centrifuged (13,600 rpm for 10 min) to remove cell debris. The clarified lysates were flash-frozen in liquid nitrogen and stored at −80°C. Telomerase reactions were carried out in 20-µL volumes containing 50 mM Tris-Cl (pH 8.0), 30 mM KCl, 1 mM spermidine, 1 mM $MgCl_2$, 5 mM β-mercaptoethanol, 1 µM primer a5 (TTAGGGTTAGCGTTAGGG), 500 µM dATP, 500 µM dTTP, 2.92 µM unlabeled dGTP, 0.33 µM radiolabeled dGTP (3000 Ci/mmol), and 3 µL of HeLa-EM2-11ht cell extracts for 60 min at 30°C. Reactions were stopped with buffer containing 100 µL of 3.6 M ammonium acetate and 20 µg of glycogen and precipitated with ethanol. The pellets were resuspended in 10 µL of H_2O and 10 µL of loading buffer containing 95% formamide, heated for 10 min at 95°C, and resolved on a 10% acrylamide, 7M urea, and 1× TBE sequencing gel. Gels were dried and imaged on a PhosphorImager (Storm; GE), and the data were analyzed using Imagequant TL (GE Life Sciences) software. Processivity calculations were performed exactly as described previously [70]. Briefly, the intensities of individual bands in the ladder generated by telomerase activity in each lane were quantified and divided by the number of added guanosine nucleotides. For a given band *n*, the fraction left behind (FLB), which is the sum of counts for repeats (1 − *n*) divided by the total counts in the lane, was calculated. Next, *ln*(1 − FLB) was plotted against repeat number for each lane, and the plot was fit with a linear regression equation with slope *m*. The processivity value, which is plotted in Figures 2.9C and E, equals −0.693/*m*.

For telomerase activity assays shown in Figures 2.9B, E, and F, HEK293T cells were transfected with TERT-cDNA6/myc-HisC and phTR-Bluescript II SK(+) plasmids as described for HeLa, but plasmids encoding POT1 and TPP1 were omitted. Telomerase extracts were prepared exactly as detailed above for HeLa lysates. The telomerase assay was also performed exactly as above with the exception that purified POT1 and TPP1-N proteins (wild type or K170Δ) were preincubated with the DNA primer for 5 min on ice prior to addition of the telomerase extract. All subsequent steps of the assay, including electrophoresis, gel-drying, imaging, and processivity analyses, were performed exactly as detailed above for telomerase assays with HeLa extracts.

Co-immunoprecipitation (Co-IP) assay

HeLa-EM2-11ht cells were seeded and transfected with 1 µg each of plasmids encoding Flag-TIN2 and wild-type or mutant Flag-TPP1. After 24 h of transfection, cells were washed with PBS, dislodged with a cell scraper using 400 µL of ice-cold lysis buffer (50 mM Tris-Cl at pH 7.4, 20% glycerol, 1 mM EDTA, 150 mM NaCl, 0.5% Triton X-100, 0.02% SDS, 1 mM dithiothreitol, 2 mM phenylmethylsulfonyl fluoride, complete protease inhibitor cocktail [Roch]), and kept on ice. After 5 min, 20 µL of 5 M NaCl was added and mixed. After another 5 min on ice, 420 µL of ice-cold water was added and mixed before immediate centrifugation (13,600 rpm for 10 min). Supernatants were collected and used directly for immunoprecipitation. Lysate (40 µL) added to 40 µL of 4× SDS gel loading buffer was kept aside for analysis of “input” samples. Five microliters of anti-TIN2 antibody was added, followed by incubation overnight at 4°C. Fifty microliters of protein A/G sepharose beads (Pierce; Thermo Scientific) preincubated with 100 mg/mL BSA in PBS was added, and samples were mixed with rocking on a nutator for 2 h at 4°C. Beads were washed three times with 1:1 diluted lysis buffer, and proteins were eluted by adding an equal volume of 2× SDS gel loading buffer for analysis of “bead” samples. All “input” (10 µL) and “bead” (15 µL) samples were heated for 12–14 min at 90°C and analyzed by SDS-PAGE and immunoblotting using HRP-conjugated anti-Flag antibody. The fraction of TIN2 that is bound by TPP1 (normalized against the ratio of wild-type TPP1: wild-type TIN2) was determined by quantification of the chemiluminescence signal using a ChemiDoc MP gel imager (Bio-Rad) and subsequent analysis using AlphaView software (ProteinSimple). Results from four independent experiments were used to generate means and standard deviations.

For Co-IP assays in Figure 2.5, HeLa-EM2-11ht cells were seeded and transfected with 1 µg of TERT-cDNA6/myc-HisC, 3 µg of phTR-Bluescript II SK(+), 1.5 µg of p3X-Flag-POT1-BI4, and 1 µg of p3X-Flag-TPP1-CMV (wild type or mutant) were added per transfection. In control transfections where TPP1 were omitted, 2 µg of empty vector was included. Lysates were prepared exactly as detailed above. Lysate (40 µL) added to 40 µL of 4× SDS gel loading buffer was kept aside for analysis of “input” samples. Fifty microliters of anti-FLAG M2-agarose (Sigma) preincubated with 100

mg/mL BSA in PBS was added in the presences of a5 (TTAGGGTTAGCGTTAGGG) oligonucleotide, and samples were mixed with rocking on a nutator for 2 h at 4°C. Beads were washed three times with 1:1 diluted lysis buffer, and proteins were eluted by adding an equal volume of 2× SDS gel loading buffer for analysis of “bead” samples. All “input” and “bead” samples were heated for 12–14 min at 90°C and analyzed by SDS-PAGE and immunoblotting using rabbit monoclonal antibody TERT(C-term) antibody (Abcam) or HRP-conjugated anti-Flag antibody. Horse-radish peroxidase-conjugated goat antiboesd against rabbit (Santa Cruz Biotechnology) was used to reveal the primary antibody using chemiluminescence detection by ECL plus reagents (GE Healthcare Life Sciences). Quantification was performed using a ChemiDoc MP gel imager (Bio-Rad) and subsequent analysis using AlphaView software (ProteinSimple).

Telomere ChIP

HeLa1.2.11 cells were transfected with the p3X-Flag-TPP1-CMV (either wild type or P491T) as detailed above for HeLa-EM2-11ht. Transfected cells were processed for ChIP as described previously [282]. Following cell lysis, 15% of the lysates were kept aside to serve as “input” samples. Immunoprecipitation on the remaining 85% of the lysates was performed by addition of 4 µg of mouse anti-TRF2 4A794.15 (NB100-56506, Novus Biological) and 4 µg of monoclonal anti-ACD (H00065057-M02, Abnova) antibodies. Hybridization was performed in Church buffer (0.5 M sodium phosphate buffer at pH 7.2, 1% BSA, 1 mM EDTA, 7% SDS) as described previously (de Lange 1992) using ^{32}P-labeled $(TTAGGG)_4$ or an oligonucleotide probe to detect Alu repeats [78]. Following hybridization, membranes were washed to reduce nonspecific binding of the probe, imaged using a PhosphorImager (Storm, GE Life Sciences), and quantified using ImageJ software. The percentage of input DNA that was pulled down was plotted.

Structural modeling

The Web-based Swiss Model software (http://swissmodel.expasy.org; [283]) was used to create a homology model for TPP1-OB K170Δ and TPP1-OB Q205R based on the crystal structure of TPP1-OB wild type (PDB: 2I46). The homology model was subjected to energy minimization using the crystallography and NMR (nuclear magnetic

resonance) system (CNS) program (http://cns-online.org/v1.3; [284]) to furnish the model displayed in Figure 2.12.

RESULTS

Clinical characterization

The male proband NCI-275-1 is an identical twin born at 29-week gestation with IUGR. Clinical features consistent with HH were noted during the first year of life and included microcephaly, cerebellar hypoplasia, developmental delay, oral leukoplakia, nail dystrophy, and esophageal stenosis (Table 2.1). By age 20 mo, the proband required regular platelet and red blood cell transfusions for bone marrow failure. Fanconi anemia and Shwachman-Diamond syndrome were excluded based on a normal chromosomal breakage test and the absence of mutations in *SBDS (*Shwachman-Bodian-Diamond syndrome) *gene*, respectively. Despite extremely short blood leukocyte telomere length, as demonstrated by flow cytometry with FISH (Figure 2.4A) and by FISH/confocal microscopy of EBV-transformed lymphoblasts (Figure 2.4B), sequencing did not identify mutations in any of the nine known DC-associated genes. The proband underwent successful matched unrelated hematopoietic stem cell transplantation at 3 yr of age.

The proband's identical twin, NCI-275-2, was also affected by IUGR and died at 4 mo from complications of pertussis. The proband's older sister, NCI-275-3, is healthy and has no clinical features of DC but has very short telomeres (Figure 2.4A). The proband has two healthy younger sisters who are identical twins, NCI-275-4 and NCI-275-5, with telomeres at the first percentile (Figure 2.4A, B). Although the twins' telomeres are at the low end of the normal range, they do not meet the stringent criteria for a DC diagnosis (three out of four leukocyte subsets, excluding granuloctyes, below the first percentile) [259]. Both parents (father, NCI-275-6, and mother, NCI-275-7) are healthy, although the father has very short telomeres, premature gray hair, and minor dental abnormalities (Figure 2.3 and 2.4A; Table 2.1).

Sequence analysis

DNA from the proband (NCI-275-1), his older sister (NCI-275-3), and both parents (NCI-275-6 and NCI-275-7) (Figure 2.3) was analyzed by whole-exome sequencing, resulting in ~300,000 reported variants. We used a custom filtering algorithm to identify likely causal variants. Based on data from the National Institutes of Health Heart, Lung, and Blood Institute (NHLBI) Exome Sequencing Project (ESP), the 1000 Genomes Project, and an in-house database of 1400 exomes, we identified the rarest variants in accordance with the low prevalence of DC (Table 2.4). We further filtered variants by family structure using telomere length as the phenotype of interest to minimize the effect of variable expressivity: Because the proband (NCI-275-1), older sister (NCI-275-3), and father (NCI-275-6) all have short telomeres, we hypothesized that they must share a contributing variant despite the fact that they are not equally affected clinically. This resulted in a list of 40 variants (Table 2.5), only one of which was in a telomere biology gene: *ACD* (*ACD*), chr16:67693689–67693691delCTT (genomic coordinates correspond to GRCh37/hg19). A second *ACD* variant, chr16:67691750G>T, shared by the proband (NCI-275-1) and mother (NCI-275-7), was also present. The presence or absence of each of the two variants was validated in all six family members by both ion semiconductor sequencing of the entire gene locus and Sanger sequencing of the region around the mutations; the healthy twins (NCI-275-4 and NCI-275-5) carry neither mutation. The healthy paternal grandmother is also wild type at both of these loci; DNA was not available on any other family members.

The 3-base-pair (3-bp) deletion results in an in-frame deletion of a single amino acid, K170 (based on NM_001082486.1/NP_001075955.1). This residue is located in the OB fold of TPP1 (Figure 2.2A; [69]). The deletion affects a conserved solvent-accessible charged loop, a likely site of molecular interaction. This is supported by reports describing the TEL patch of TPP1 (Figure 2.2A), a cluster of residues encompassing this deletion that mediates interactions required for telomerase recruitment and telomerase processivity [79, 81]. K170 is implicated in the interaction between TPP1 and telomerase [79], and mutation of adjacent amino acids (E169 and

E171) has been shown to severely impede both telomerase recruitment and processivity [81]. Deletion of K170, a residue that is strictly conserved in mammals (Figure 2.2B), is predicted to be deleterious by in silico algorithms (Table 2.2). This mutation is not reported in National Center for Biotechnology Information Single Nucleotide database build 137 (dbSNP 137), the ESP database, or the 1000 Genomes Project and is not present in our internal non-DC population.

The missense variant chr16:67691750 G>T results in the replacement of a proline by a threonine at amino acid position 491 (P491T; NM_001082486.1/NP_001075955.1). The P491T mutation resides in the C-terminal TIN2-interacting domain of TPP1 (Figure 2.2A); this interaction is required for TPP1 localization (and hence telomerase recruitment) to telomeres [59]. P491 is also well conserved in mammals (Figure 2.2B), and four of six in silico prediction algorithms list this mutation as deleterious (Table 2.2). This variant is listed in dbSNP as rs201441120 and is present in the ESP database (n = 6496 individuals) with a MAF of 0.0002; however, it is not present in the 1000 Genomes Project or our internal non-DC population (total $n \approx 9900$ individuals).

TPP1-Telomerase Interaction

To examine the effect of deletion of K170 on the interaction of TPP1 and telomerase, we performed Co-IP assays (Figure 2.5). HeLa cells were transiently transfected with plasmids encoding TERT, TR, and Flag-tagged POT1 and TPP1 (wild type, K170∆) and immunoprecipitated with Flag beads. We did not observe a significant reduction in the interaction of TPP1 and TERT in the presence of K170Δ. These studies demonstrated that K170Δ does not cause a significant defect in the interaction between TPP1 and telomerase.

Telomerase recruitment

To test the effect of deletion of K170 on telomerase recruitment, we conducted an IF/FISH-based telomerase recruitment assay. HeLa cells transiently transfected with plasmids encoding TERT, TR, and Flag-tagged TPP1 (wild type, K170∆, P491T) were fixed and stained/probed for Flag, TR, and coilin (a marker of Cajal bodies). Flag-tagged

TPP1, TPP1-K170Δ, TPP1-P491T were visualized as punctate foci (Figure 2.6A). As in previous studies [81], the Flag foci observed here represent telomeres insofar as they colocalize with the shelterin component RAP1 (Figure 2.7). FISH probes for TR indicated the localization of telomerase in the same nuclei. As expected, we observed that a large fraction of the TR foci localized to telomeres in the presence of wild-type TPP1 (Figure 2.6A). Quantification of data collected from triplicate experiments for each TPP1 construct revealed that 54% of all telomeric foci in wild-type cells contain TR foci (Figure 2.6B), confirming efficient recruitment of telomerase to telomeres by wild-type TPP1. In addition, we observed coilin (Figure 2.6A) colocalizing with both telomerase and telomeres in structures referred to as neo-Cajal bodies, consistent with previous observations [79].

In sharp contrast to cells expressing wild-type TPP1 but akin to TEL patch mutant cells [81], the TR foci in cells expressing TPP1-K170Δ rarely localize at telomeres; only 3% of Flag-TPP1-K170Δ foci colocalize with TR foci (Figure 2.6B). TR foci in TPP1-K170Δ cells maintained their colocalization with coilin, suggesting that the K170Δ mutation interferes with recruitment of telomerase from Cajal bodies to telomeres.

Next, we measured telomerase recruitment in HeLa cells transiently expressing TPP1-P491T, the maternally inherited heterozygous mutation in the proband. TR efficiently colocalized with telomeres in the presence of TPP1-P491T (Figure 2.6A). Quantification revealed that 65% of all telomeric foci in TPP1-P491T-expressing cells contain TR foci (Figure 2.6B), suggesting that the P491T mutation does not severely interfere with the interaction of telomerase and Flag-tagged TPP1-P491T at telomeres.

Previously our collaborator at NCI identified another variant in *ACD* in a different family with DC using a candidate gene strategy, Q205R. The patient also harbors a TERC mutation in close vicinity to the RNA templating region. Q205 is also located in the OB-fold domain but it is far from the TEL patch; thus, Q205R is unlikely to be the cause of DC in this patient. However, it was still of interest to functionally characterize this mutation. Therefore, we also measured telomerase recruitment in HeLa cells transiently expressing TPP1-Q205R. We observed that TR colocalized with telomeres

in the presence of TPP1-Q205R (Figure 2.8A). Although quantification revealed that 29% of all telomeric foci in TPP1-Q205R-expressing cells contain TR foci (Figure 2.8B), the difference between WT-TPP1 and Q205R-TPP1 expressing cells was not significant (P= 0.09).

Telomerase processivity

The TEL patch of TPP1 has also been shown to stimulate telomerase processivity [81], enabling telomerase to synthesize long DNA products containing multiple telomeric repeats. To test the effect of TPP1-K170Δ on telomerase processivity, direct telomerase primer extension assays were performed using two methods. The first method involves using lysates of HeLa cells expressing Flag-TERT, TR, Flag-POT1, and Flag-TPP1 (wild type or mutant) as reported previously [81]. Although the use of HeLa extracts provides limiting amounts of Flag-POT1 and Flag-TPP1 for the telomerase activity assay, the proteins are coexpressed with telomerase in human cells, more closely recapitulating what occurs in vivo. Compared with the untransfected control, transfection of wild-type TPP1 resulted in an increase in processivity [69], indicated by the appearance of higher-molecular-weight (slower-migrating) products (Figure 2.9A). However, the deletion of K170 led to the disappearance of the slowest-migrating bands observed with wild-type TPP1 (Figure 2.9A). Quantification of the data from multiple experiments further indicates a telomerase processivity defect in the presence of TPP1-K170Δ (Figure 2.9C). The deleterious effect of TPP1-K170Δwas not a result of varying protein levels, as Flag-TERT, Flag-POT1, and Flag-TPP1 protein levels were comparable in all cell lines tested (Figure 2.9D). The P491T mutation does not cause a significant defect in telomerase processivity (Figure 2.10), consistent with the nonessential nature of the TIN2-binding domain for stimulation of telomerase processivity [69].

We repeated the analysis of telomerase processivity using purified, recombinant POT1 and TPP1-N (a TPP1 construct that binds POT1 as well as telomerase) [69]. These proteins were added at high concentrations (see the Materials and Methods) to lysates from HEK293T cells transiently overexpressing telomerase (supertelomerase); the increased POT1/TPP1 concentrations allow for a larger stimulation of telomerase

processivity [70]. Using this approach, we saw the characteristic threefold to fourfold increase in telomerase processivity in the presence of the POT1–TPP1 complex containing wild-type TPP1-N but not with POT1–TPP1-N (K170Δ) (Figure 2.9B, E). Because both TPP1-N (wild type) and TPP1-N (K170Δ) proteins were purified to similar levels (Figure 2.9F) and were added to the assay at the same concentrations, we conclude that the TPP1-K170Δ mutation reduces the ability of POT–TPP1 to stimulate telomerase processivity.

TPP1–TIN2 interaction

Because the P491T mutation resides in the TIN2-interacting domain of TPP1, this mutation may affect TIN2–TPP1 binding. To assess the interaction between TIN2 and mutant TPP1, we performed Co-IP assays (Figure 2.11A, B). Whereas wild-type TPP1 and TPP1-K170Δ efficiently precipitated with TIN2, TPP1-P491T showed a modest (approximately twofold) reduction in TIN2 association.

Disruption of the TIN2–TPP1 interaction can indirectly cause a reduction in telomerase recruitment to telomeres; however, we did not see evidence of this in the telomerase recruitment assay (Figure 2.6). To monitor the effect of the P491T mutation with regard to TPP1 recruitment to telomeres, we conducted telomere ChIP experiments. Our results show that TPP1 (as well as TRF2, a positive control) binding to telomeres is unaffected by the P491T mutation, at least under the conditions of this assay (Figure 2.11C, D).

TPP1 structural modeling

To gain insight into the structural implications of this deletion, we constructed a model for TPP1-OB lacking K170 based on the TPP1-OB wild-type crystal structure (Protein Data Bank [PDB]: 2I46) using homology modeling and energy minimization (see the Materials and Methods for details). The crystal structure for the wild-type protein (Figure 2.12A, B; [69]) reveals that while E168, E169, and E171 amino acid side chains are surface-exposed and available for binding telomerase, K170 is buried and directed toward the core of the wild-type protein. Strikingly, deletion of K170 results in a structural model in which the amino acid side chain of E169 is withdrawn from the

surface and buried in the core of the protein structure (Figure 2.12A). In comparison, a model of the missense mutation K170A does not exhibit any gross conformational changes in E168, E169, or E171 (data not shown), suggesting a structural basis for the modest effect of K170A on telomerase recruitment [79]. In summary, our structural modeling suggests that deletion of K170 occludes E169 from telomerase binding and reduces the extent of the acidic patch on TPP1-OB, thereby compromising telomerase recruitment and processivity. On the other hand, Q205R does not exhibit a significant change in the structure of TPP1-OB (Figure 2.12B), supporting the lack of a recruitment defect in the presence of TPP1-Q205R (Figure 2.8A, B).

DISCUSSION

Here we describe an individual affected by the severe DC variant HH who harbors two *ACD* mutations affecting two distinct TPP1 domains. TPP1 interacts with both POT1 and TIN2, forming a bridge between the ssDNA-binding and dsDNA-binding components of the shelterin complex, thereby enabling proper chromosome end protection [264]. TPP1 recruits telomerase via its TEL patch, allowing efficient extension of chromosome ends in actively replicating cells. The mutation affecting the TEL patch, K170Δ, abrogates telomerase recruitment and reduces telomerase enzymatic processivity. The TIN2-binding domain mutation P491T showed a modest reduction in the interaction between TPP1 and TIN2 but did not significantly affect telomerase recruitment or processivity.

To understand the functional significance of the K170Δ mutation of TPP1, we performed telomerase recruitment assays using IF/FISH (Figure 2.6) and telomerase activity assays (Figure 2.9). Our results demonstrated that K170Δ compromises both telomerase recruitment and processivity. K170 is located adjacent to the TEL patch amino acids E168, E169, and E171, which form an acidic patch on the TPP1-OB structure that is critical for telomerase function. Our structural modeling suggests that deletion of K170 occludes E169 from telomerase binding and reduces the extent of the acidic patch on TPP1-OB, which compromises telomerase recruitment and processivity (Figure 2.12). However, in the absence of a crystal structure for K170Δ, we cannot rule out additional disruptive changes in the TEL patch caused by deletion of K170.

P491 resides in the TIN2-binding domain of TPP1, which is important for recruiting TPP1 (and hence telomerase) to telomeres but is dispensable for telomerase processivity. As expected, the P491T amino acid change did not result in a significant reduction in telomerase processivity (Figure 2.10) or interaction with telomerase at telomeres (Figure 2.6). However, we observed that P491T significantly inhibited the interaction between TIN2 and TPP1 (Figure 2.11A, B). The physiological relevance of this partial TIN2-binding defect is unclear; TPP1-P491T is present at telomeres at wild-type levels by ChIP, suggesting that the reduction in TIN2 binding is not sufficient to impact TPP1 recruitment in vivo (Figure Figure 2.11C, D). Because our analysis of P491T was done using transient transfections, it is possible that subtle phenotypes were masked via overexpression. Additionally, our analyses assessed the defects of TPP1-K170Δ and TPP1-P491T individually, while the severely affected proband harbors both variants; it is possible that the combination of these two alleles is more deleterious than the presence of either single allele. Therefore, we cannot exclude the possibility that TPP1-P491T is a disease modifier in the proband, although any potential contribution of P491T to the disease in the proband is likely minor compared with that of the K170Δ mutation.

The data indicating that TPP1-K170Δ severely compromises telomerase recruitment and processivity while TPP1-P491T has no significant effect on telomerase recruitment are consistent with the phenotypes associated with the family members having one or both of these mutations. The heterozygous carriers of TPP1-K170Δ (the father and older sister), while clinically healthy at this time, are affected on a molecular level: Their telomeres are below the first percentile for age, an important consideration for family planning and potential bone marrow donation to affected relatives. The mother, a carrier of P491T, is currently unaffected and has telomeres between the 10th and 50th percentiles, suggesting that P491T does not cause a significant change in telomere length; this is consistent with the minimal defects that we observed for this allele. The healthy twins do not harbor either TPP1 mutation, although their telomeres are at the low end of the normal range for their age; this is presumably a consequence of inheritance from at least one parent with very short telomeres [285]. The proband, the most severely affected individual in this family, is also the only one to harbor both

K170Δ and P491T. The two TPP1 mutations may have a synergistic relationship in which a modest defect with the P491T allele is magnified in an environment where TPP1 is already deficient due to the K170Δ mutation. Alternatively, a minimal P491T defect may be sufficient to drop TPP1 function below a certain functional threshold in the context of the K170Δ mutation, resulting in disease. Characterization of endogenous TPP1 expression and function in cells derived from the proband and his family members will likely provide further insight into the precise contribution of P491T to telomere maintenance and HH. We cannot rule out the presence of other disease-modifying factors, genetic anticipation, or incomplete penetrance in contributing to development of HH in the proband but not in other K170Δ carriers.

TPP1 has previously been implicated in the proper functioning of the tissues most affected by DC and HH. In mice, the adrenocortical dysplasia (*acd*) mutant phenotype, caused by a hypomorphic allele of Tpp1, includes a number of features of DC, including growth retardation, skin hyperpigmentation, and sparse hair [84]. In caddition, mouse hematopoietic stem cells homozygous for the *acd* allele are profoundly defective in transplantation assays, and complete inactivation of Tpp1 results in severe depletion of hematopoietic progenitors [286]. Deletion of Tpp1 in the epithelial tissue leads to perinatal death, severe skin hyperpigmentation, defective hair follicle morphogenesis, and epithelial dysplasia [287]. While the above studies do not necessarily implicate the TEL patch of TPP1 in stem cell function, a very recent study using genetic engineering of human embryonic stem cells has revealed that deletion of a segment of the TEL patch that includes K170 results in telomere shortening and decreased cell viability [82]. These reports and our current study together suggest that reduced telomerase recruitment and processivity caused by perturbation of the TEL patch of TPP1 result in reduced stem cell function, which provides a mechanism explaining the characteristic mucocutaneous and hematopoietic features of DC.

TPP1 is not the first shelterin component implicated in DC; mutations in exon 6a of *TINF2* result in DC, HH, and the related telomere biology disorders of aplastic anemia and Revesz syndrome [58-60, 208]. However, *TINF2* DC mutations, which do not affect interaction of TIN2 with any of its shelterin-binding partners, cause telomere shortening

via mechanisms that involve both telomerase-dependent and telomerase-independent pathways. In contrast, the deletion in the TEL patch of TPP1 described here provides a more direct model for telomere length shortening resulting from diminished telomerase recruitment to telomeres and reduced telomerase enzymatic processivity. In summary, this is the first report of DC/HH caused by germline mutations in TPP1 and further illustrates the importance of this shelterin component in human telomere biology.

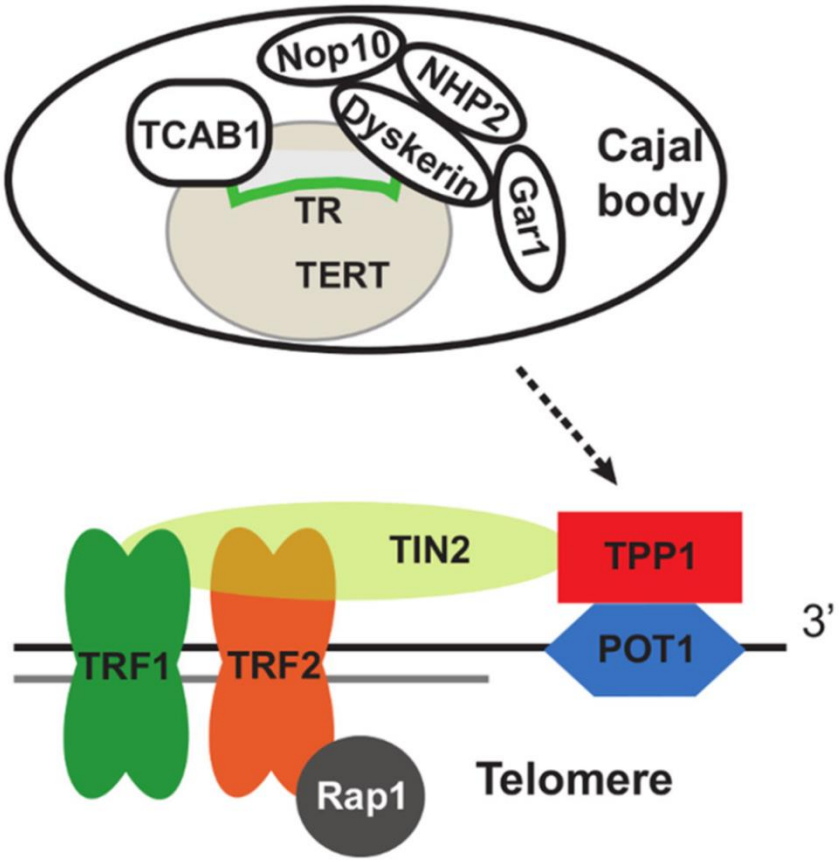

Figure 2.1: Schematic diagram of telomerase recruitment from Cajal bodies to telomeres coated with the shelterin complex. The RNA component of telomerase is indicated as TR, also known as TERC.

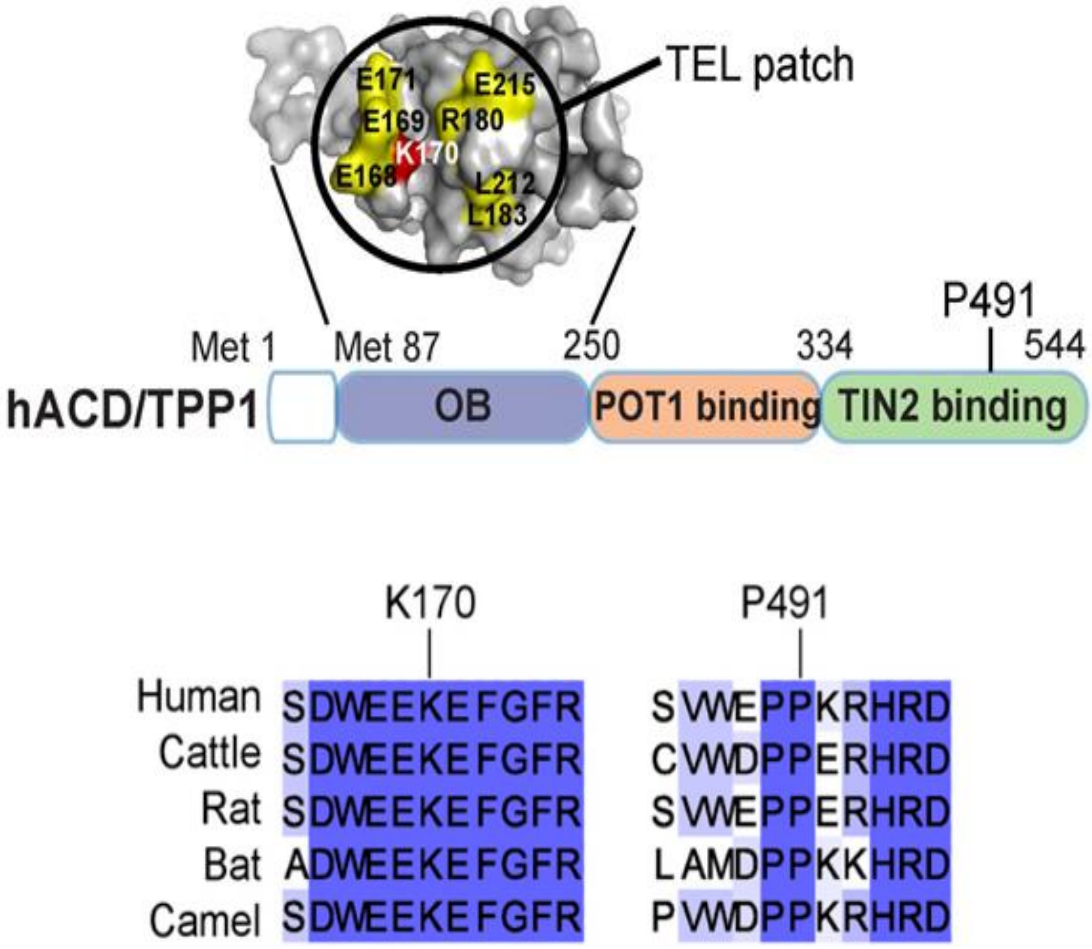

Figure 2.2: The affected TPP1 amino acids in ACD/TPP1. (A) The domain structure of TPP1 is depicted. The TEL patch is highlighted in yellow with K170 in red. The location of the P491T variant is also depicted on the domain diagram. (B) Sequence alignment surrounding the affected amino acids, showing their location in highly conserved regions.

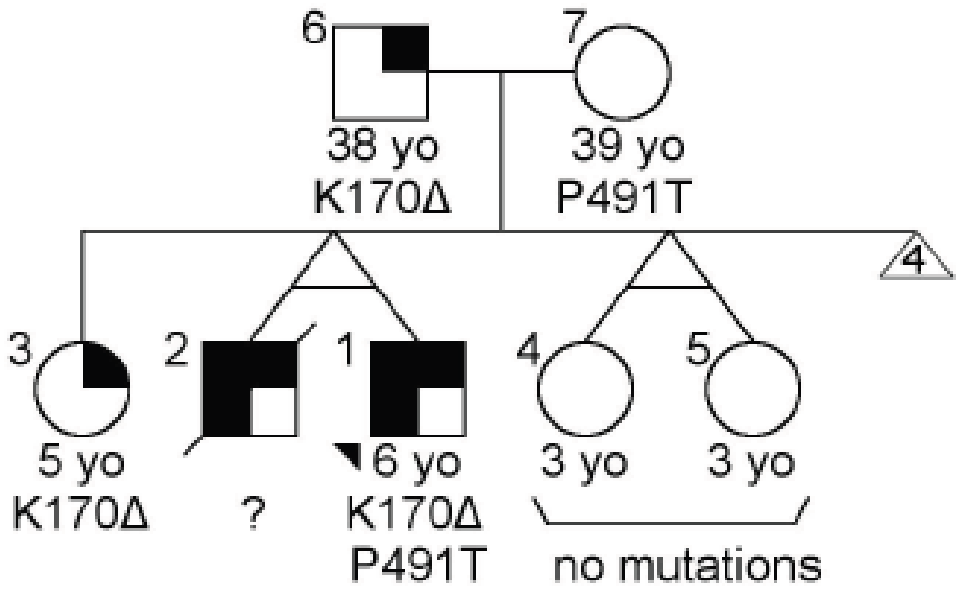

Figure 2.3: The pedigree for NCI-275 showing first-degree relatives of the proband. The proband is indicated by an arrowhead. A diagnosis of HH is indicated by a filled left half, and telomeres below the first percentile are indicated with a filled upper right quadrant. *ACD* genotypes are shown below each symbol.

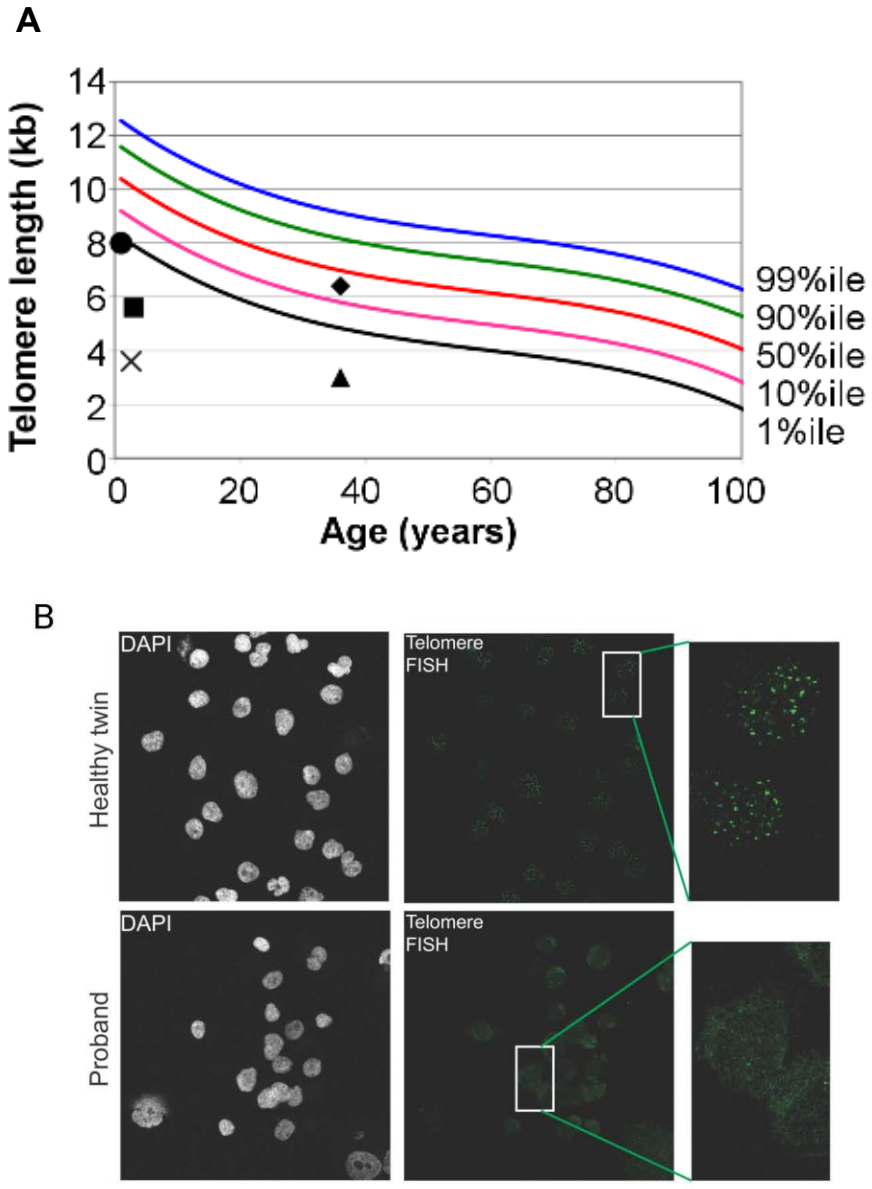

Figure 2.4: Telomere lengths for NCI-275 (A) Lymphocyte telomere lengths for members of family NCI-275. Telomere lengths from the proband (indicated with x), healthy older sisters (indicated with square), healthy twin sisters (indicated with circle), mother (indicated with diamond) and father (indicated with triangle) were measured by flow cytometry with fluorescent *in situ* hybridization. (B) Telomere-FISH of EBV-transformed lymphoblasts derived from proband and his healthy twin sister. Green punctuate staining indicates telomeres.

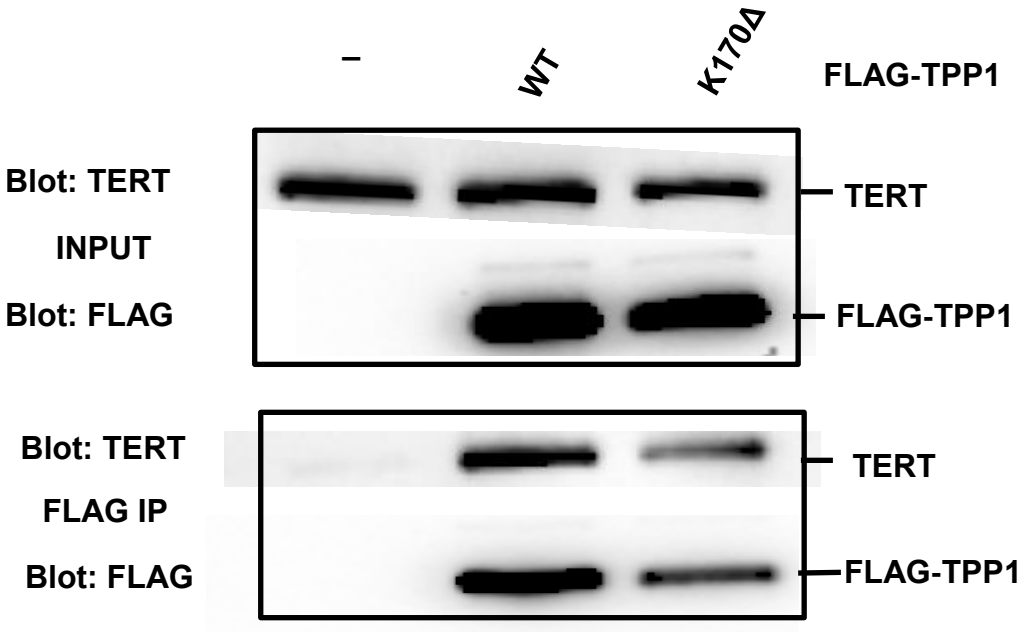

Ratio TERT/TPP1-FLAG	1	0.95

Figure 2.5: The effect of K170Δ on the interaction of TPP1 and telomerase. The comparison of TERT pull down by K170Δ TPP1-FLAG versus wild-type TPP1-FLAG in the presence of a5 primer. Immunoblot using an anti- TERT or HRP-conjugated anti-FLAG antibody of lysates from HeLa cells transfected with FLAG-TPP1, hTERT and POT1-FLAG (INPUT). Immunoblot using an anti- TERT or HRP-conjugated anti-FLAG antibody of lysates from HeLa cells transfected with FLAG-TPP1 after immunoprecipitation using Anti-Flag/M2 affinity gel beads (FLAG IP). The ratio of TERT to TPP1-FLAG is normalized against the ratio of TERT to TPP1-FLAG in wild type.

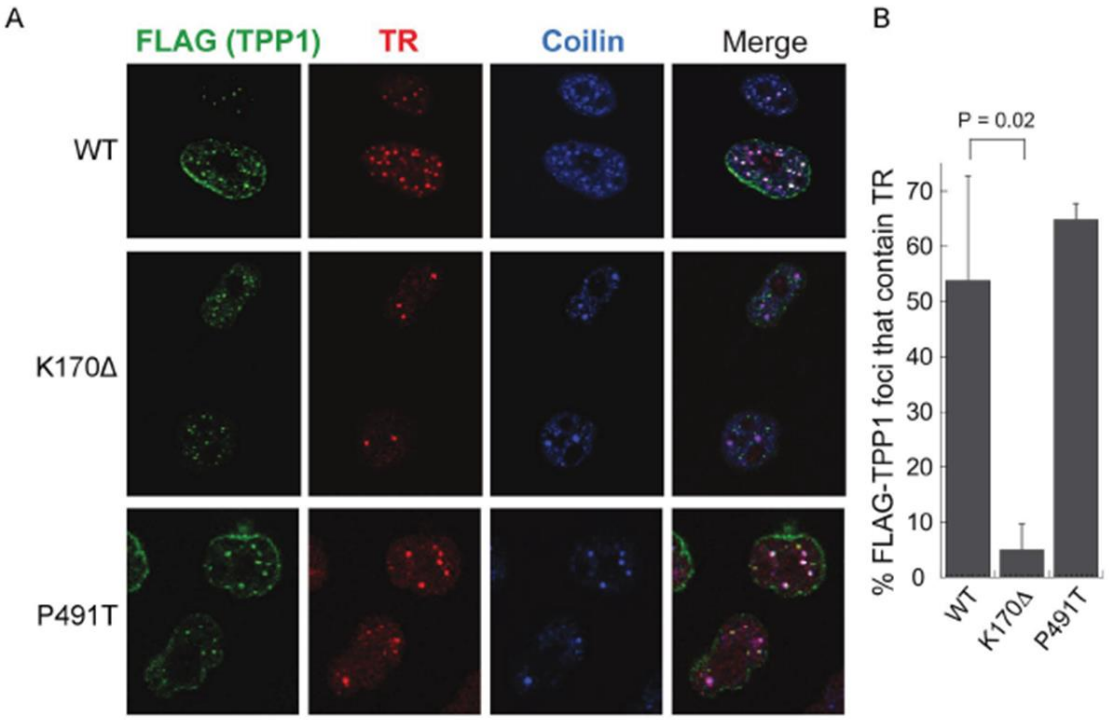

Figure 2.6: TPP1-K170Δ fails to recruit telomerase to telomeres. (A) Data is shown for FISH to detect TR (red) and IF to detect indicated FLAG-TPP1 proteins (green) and coilin (Cajal body marker; blue) for the indicated transfections. *Merge*: White (green + blue + red) spots indicate recruitment of telomerase to telomeres to foci referred to as neo-Cajal bodies. Purple (blue + red) spots indicate telomerase not recruited to telomeres, but rather residing in Cajal bodies. (B) Quantification of telomerase recruitment data of which panel A is representative. The average "% FLAG-TPP1 foci that contain TR" and standard deviations (error bars) were plotted for the indicated transfections. Two-tailed Student t-test with respect to wild-type was used to calculate the P-value for K170Δ.

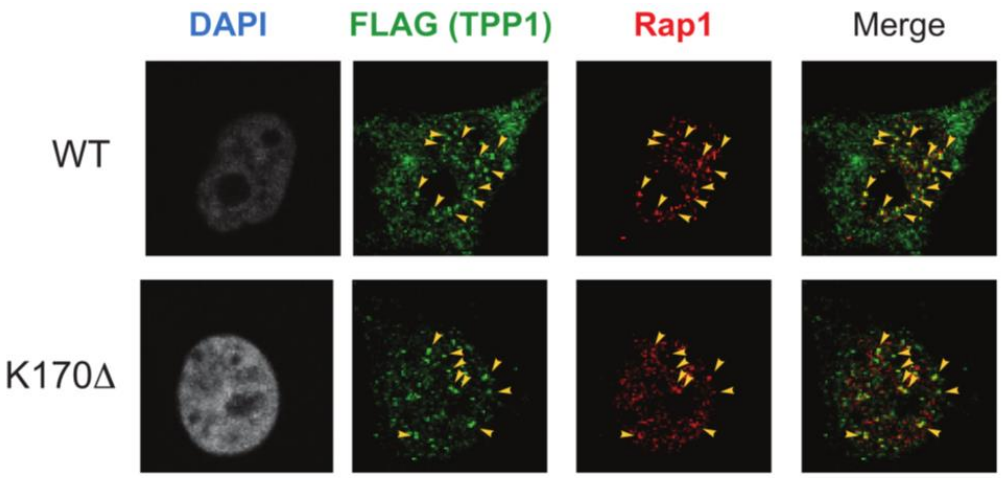

Figure 2.7: TPP1 proteins localize at telomeres. Indirect immunofluorescence of HeLa cells transfected with indicated FLAG-tagged TPP1 constructs and stained with anti-Rap1 and anti-FLAG antibodies.Rap1 is used as telomere marker.

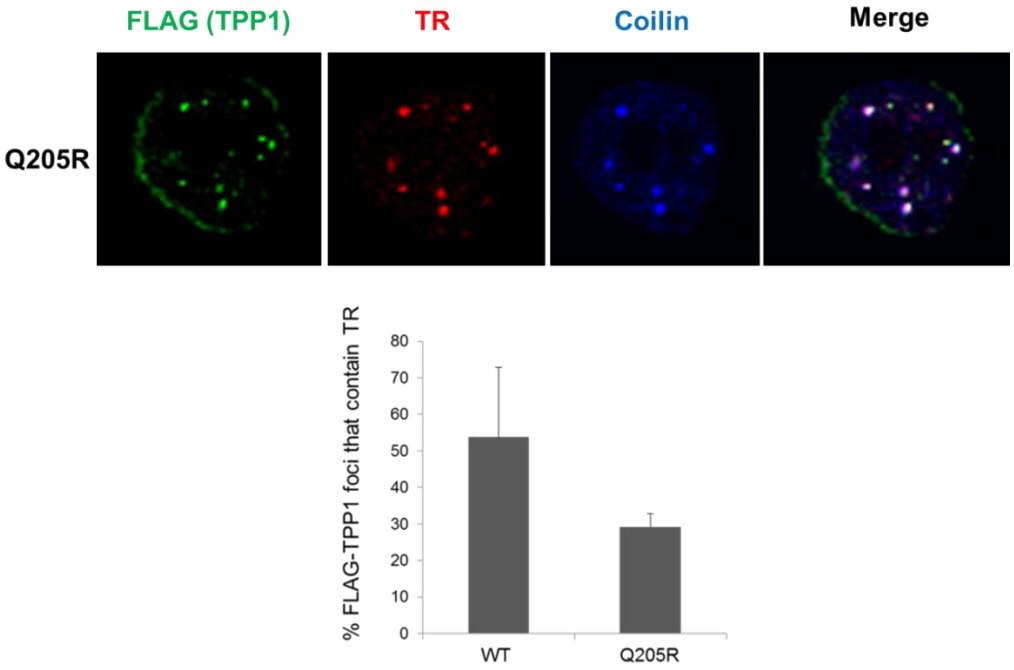

Figure 2.8: TPP1-Q205R does not have a significant effect on the recruitment of telomerase to telomeres. (A) Data is shown for FISH to detect TR (red) and IF to detect indicated FLAG-TPP1 Q205R (green) and coilin (Cajal body marker; blue) for the indicated transfections. *Merge*: White (green + blue + red) spots indicate recruitment of telomerase to telomeres to foci referred to as neo-Cajal bodies. (B) Quantification of telomerase recruitment data of which panel A is representative. The average "% FLAG-TPP1 foci that contain TR" and standard deviations (error bars) were plotted for the indicated transfections.

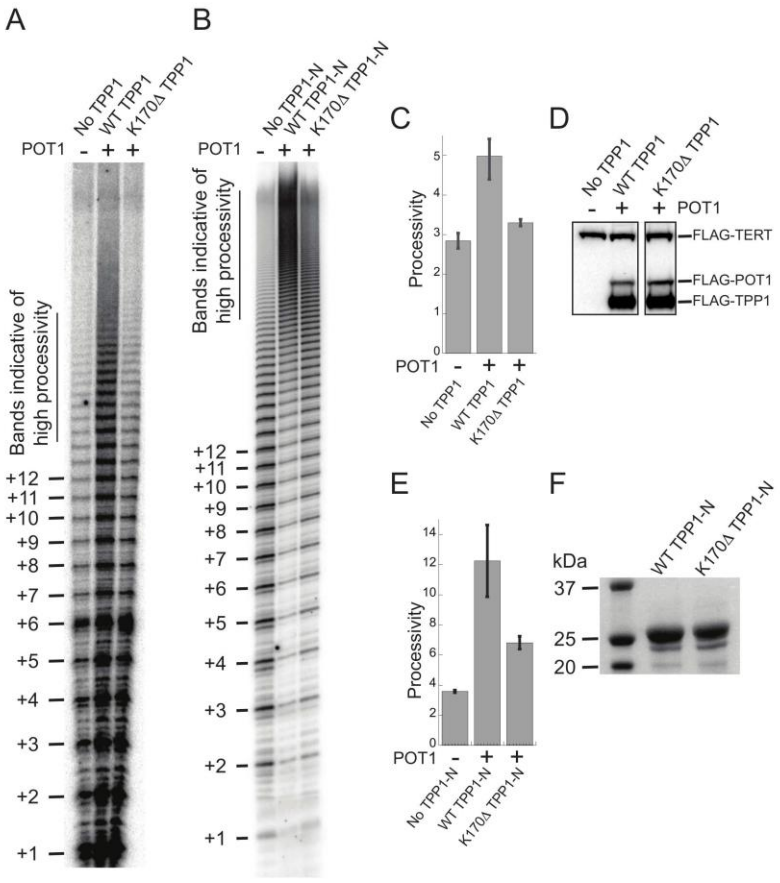

Figure 2.9: TPP1-K170Δ is defective in stimulating telomerase enzymatic processivity. (A) Direct telomerase primer extension assays using lysates from HeLa cells cotransfected with a TR, TERT, and POT1 and the indicated TPP1 plasmids. The number of (hexameric) telomeric repeats added by telomerase is indicated at the left. The region of the gel representing bands indicative of high processivity is indicated by a vertical bar at the left. (B) Direct telomerase primer extension assays using lysates from HEK293T cells supplemented with 500 nM POT1 and the indicated TPP1-N proteins (500 nM each). (C) Quantitation of processivity from three independent sets of experiments of which A is representative; mean values and standard deviations (error bars) were plotted. (D) Immunoblot of lysates used in A probed with anti-Flag antibody– HRP conjugate showing uniform TPP1, TERT, and POT1 protein expression. (E) Quantitation of processivity from three independent sets of experiments of which B is representative. (F) Coomassie-stained SDS-PAGE of 4 mg each of the indicated TPP1-N proteins.

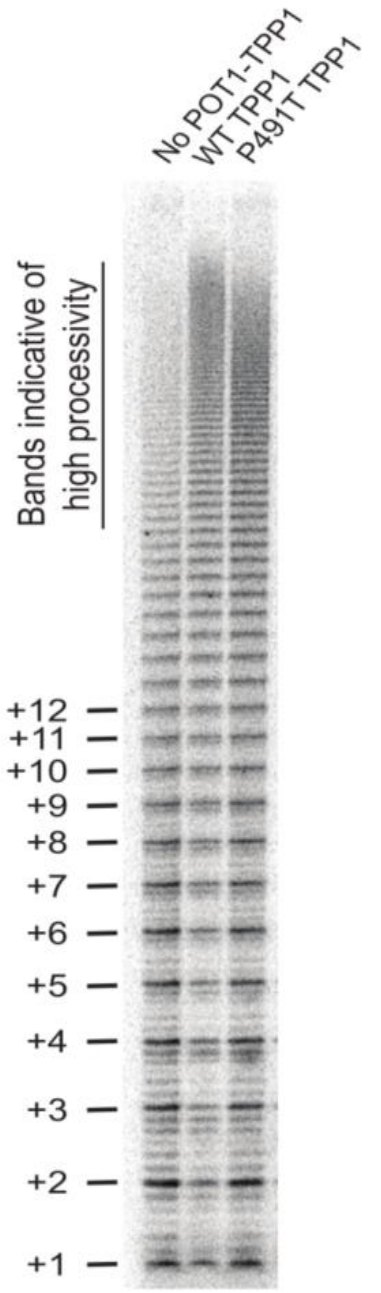

Figure 2.10: TPP1-P491T stimulates telomerase enzymatic processivity. Telomerase activity assay showing stimulation of telomerase processivity by wild-type as well as P491T-TPP1 compared to the 'no POT1-TPP1' control. Direct telomerase primer extension assays using lysates from cells co-transfected with a TR, TERT, POT1 and indicated TPP1 plasmids. "No POT1-TPP1" indicates a transfection without POT1 and TPP1. The number of (hexameric) telomeric repeats added by telomerase is indicated on the left. The region of the gel representing bands indicative of high processivity (>15 repeats added) is indicated with a vertical bar on the left.

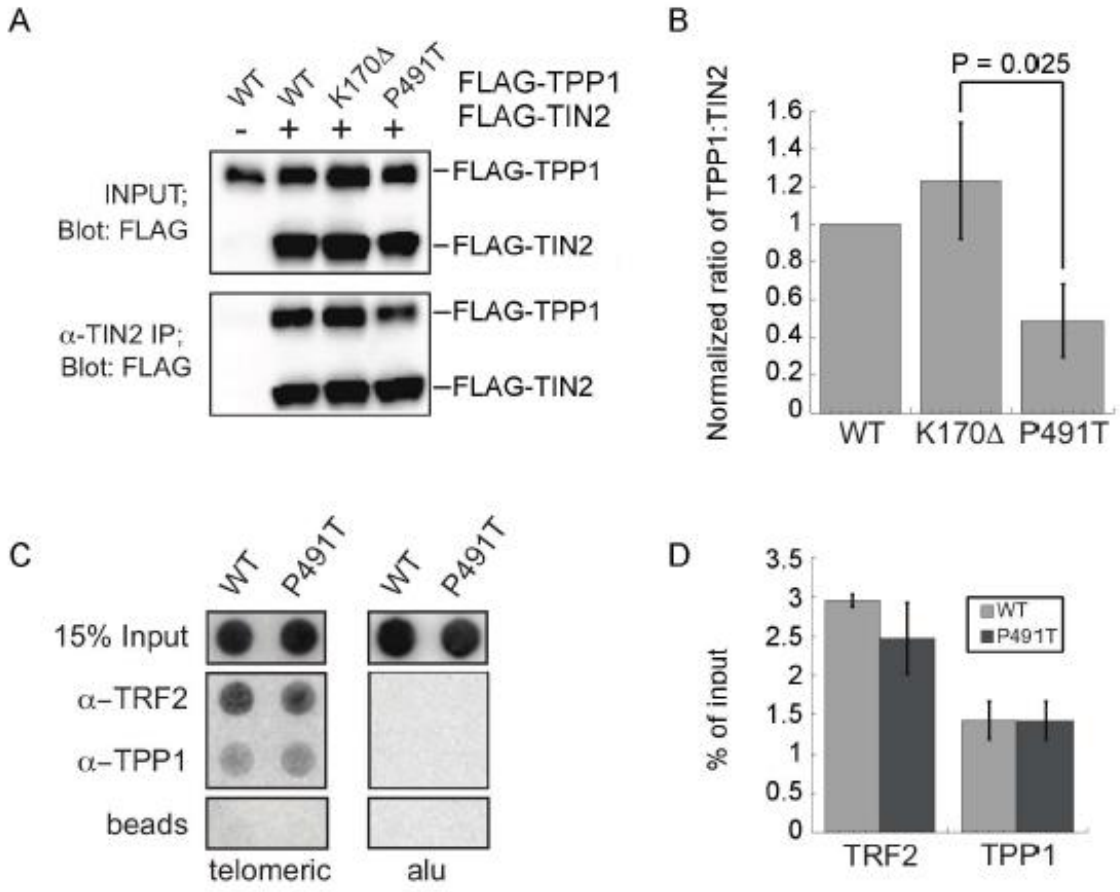

Figure 2.11: Effect of P491T on interaction with telomeres (A) Immunoblot using an HRP-conjugated anti-FLAG antibody of lysates from HeLa cells transfected with FLAG-TPP1 and FLAG TIN2 either before immunoprecipitation (INPUT), or after immunoprecipitation using an antibody against TIN2 (α-TIN2 IP). (B) The Ratio of the FLAG signal for TPP1 versus TIN2 normalized against wild-type TPP1/TIN2 was calculated for four independent experiments, and the mean values and strandard deviations (error bars) were plotted. Two-tailed Student t-test with respect to K170Δ was used to calculate the P-value for P491T. (C) Telomere ChIP was conducted with HeLa 1.2.11 cells transfected with plasmids encoding either TPP1 (wild-type) or TPP1-P491T and immunoprecipitated with antibodies against indicated proteins. The associated DNA was visualized with Southern blotting using either with a ^{32}P-labeled telomeric probe or a probe that recognizes Alu repeats. (D) Quantitation of data from two experiments of which panel C is representative. Mean values and standard errors of the mean (error bars) were

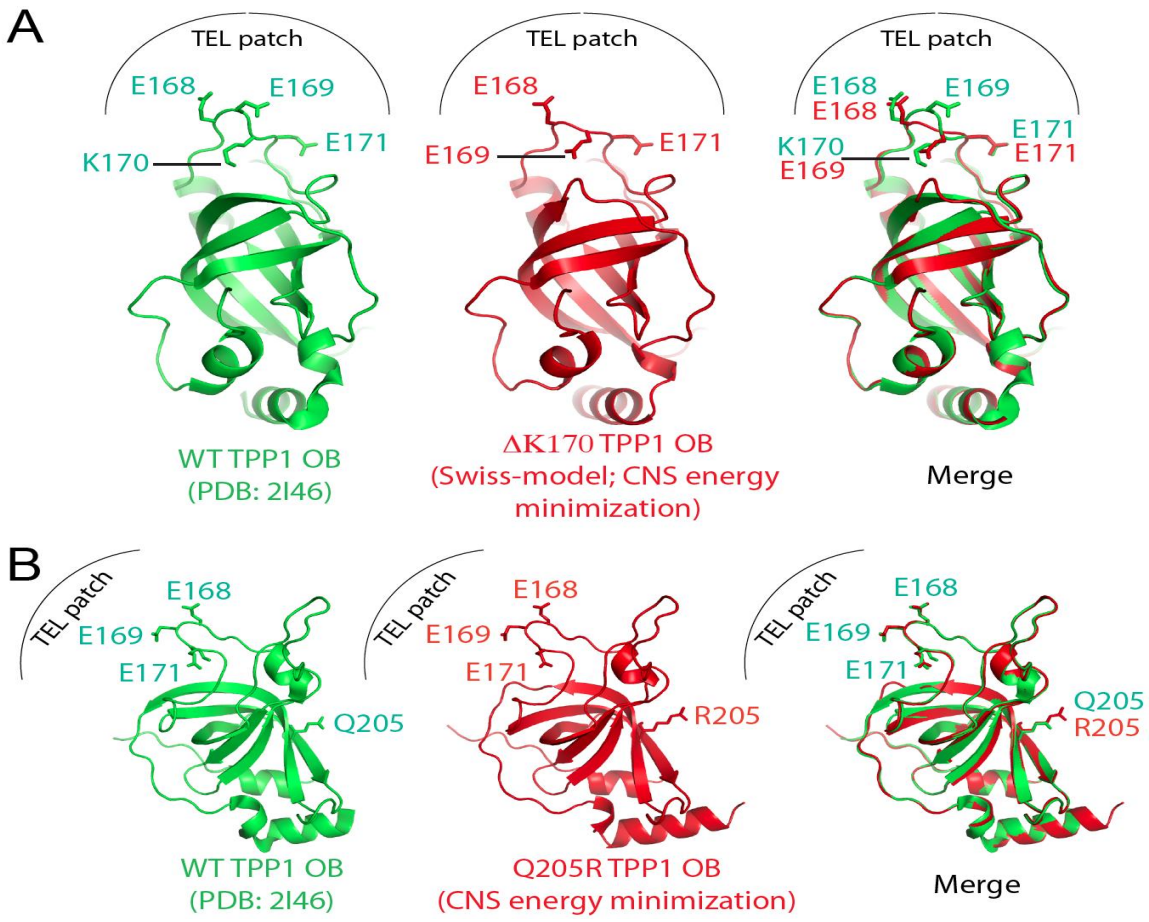

Figure 2.12: Structural modeling of TPP1 mutations in TPP1-OB domain. Ribbon view of wild-type TPP1-OB crystal structure was used to model (A) ΔK170 and (B) Q205R structures. Superposition of each mutant with wild-type structure is shown in Merge. Note how in the absence of K170 in the model, the E169 side chain flips towards the core of the protein in contrast to its surface-exposed conformation in the wild-type structure. On the other hand, Q205R in the model does not cause a significant change in the structure.

Table 2.1: Clinical features

Participant	Gender	Age at study	Diagnosis	DC triad[a]	Initial hematopoietic symptoms	Age at severe BMF (years)	Other clinical features	Telomeres	Genotype
Proband, NCI 275-1	Male	5.1 yr	DC, HH[b]	Oral leukoplakia since age 10 mo, nail dystrophy.	Thrombocytopenia and anemia at 20 mo of age.	1.8	Preterm, one of the twins born at 29 wk, IUGR, oral leukoplakia, esophageal stricture, failure to thrive, developmental delay, microcephaly, cerebellar hypoplasia, and poor speech and balance. Status post-MUD-HSCT at age 3 yr.	<1st percentile	$TPP1^{K170\Delta}$/ $TPP1^{P491T}$
Proband's identical twin, NCI 275-2	Male	0.26 yr		Not available	Not available	N/A	Preterm, second twin born at 29 wk, IUGR, retinopathy for immaturity, bilateral inguinal hernias, and died at age 3 mo from pneumonia as a complication of pertussis.	Not done	N/A
Sibling, NCI-275-3	Female	6.3 yr	Healthy	0	None	N/A	Attention deficit hyperactivity disorder and Tourette's syndrome.	<1st percentile	$TPP1^{K170\Delta}$/TPP1
Sibling (identical twin of NCI-275-5), NCI 275-4	Female	3.3 yr	Healthy	0	None	N/A	None	1st percentile	TPP1/TPP1
Sibling (identical twin of NCI-275-4), NCI 275-5	Female	3.3 yr	Healthy	0	None	N/A	None	1st percentile	TPP1/TPP1
Father, NCI 275-6	Male	38.35 yr	Healthy	0	None; mildly elevated erythropoietin at 32.1 mIU/mL (normal range 3.7-31.5)	N/A	Premature gray hair starting at age 16 yr, diffuse white lichenoid striae in gingiva, and short roots for some teeth.	<1st percentile	$TPP1^{K170\Delta}$/TPP1
Mother, NCI 275-7	Female	38.6 yr	Healthy	0	None	N/A	None	10th–50th percentiles	TPP1/$TPP1^{P491T}$
Paternal grandmother	Female	60 yr	Healthy	0	None	N/A	None	–50th percentiles (data not shown)	TPP1/TPP1
Paternal aunt	Female	26 yr	Healthy	0	None	N/A	None	<1st percentile (data not shown)	Unknown

(DC) Dyskeratosis congenita; (HH) Hoyeraal-Hreidarsson syndrome; (IUGR) intrauterine growth retardation; (MUD HSCT) matched unrelated donor hematopoietic stem cell transplantation; (ADHD) attention deficit hyperactivity disorder; (N/A) not applicable

[a]DC triad features include nail dystrophy, abnormal skin pigmentation, and oral leukoplakia.

[b]The diagnosis of HH requires the presence of cerebellar hypoplasia in addition to features of DC. Patients with HH may also have immunologic abnormalities, growth retardation, and/or microcephaly.

Table 2.2: Description of mutations and *in silico* analyses

Genomic location (hg19)	chr16: 67693691 CTTΔ	chr16: 67691750 G>T
Codon change	AAG/–	CCA/aCA
Transcript change (NM_001082486.1)	c.508_510delAAG	c.1471C>A
Protein change (NP_001075955.1)	p.K170Δ	p.P491T
In silico predictions		
Polyphen-2 (HumDiv/HumVar)	N/A	Probably damaging/probably damaging
SIFT	N/A	Damaging
PROVEAN	Deleterious	Deleterious
Mutation taster	Disease causing	Disease causing
Mutation assessor	N/A	Low functional impact
FATHMM	N/A	Tolerated
CADD	Among the 10% most deleterious mutations (14.89)	Among the 10% most deleterious mutations (18.96)

Table 2.3: Exome coverage statistics

Family	NCI-275				
Individual	NCI-275-1	NCI-275-3	NCI-275-6	NCI-275-7	Average
Target length[a] (bases)	63564604	63564604	63564604	63564604	63564604
Bases on target with at least 15 reads	57867116 91.0%	58354565 91.8%	58457573 92.0%	55964815 88.0%	57661017.3 90.7%
On-target reads	57887518	112161846	39247334	40199476	62374043.5
Off-target reads	16172632	77253622	7557508	6943770	26981883
Percent on-target	78.2%	59.2%	83.9%	85.3%	76.6%

[a]based on UCSC hg19 "known genes" coding regions

Table 2.4: Exome variant filtering strategy

	NCI-275
Total variants called across proband, sibling, father, and mother	361861
Excluding synonymous variants	25527
Excluding variants that appear >3 times in ESP	11181
Excluding variants that appear >2 times in an internal control population	409
Excluding segmental duplications >2[a]	397
Excluding variants that do not appear in the proband	182

Description of remaining candidate variants

	NCI-275
Candidate variants that passed filtering steps	182
Distribution of candidate variants in existing databases	
Listed in dbSNP	49
Listed in 1000 genomes	20
Listed in ESP 3 or fewer times	38
Found in internal control population 2 or fewer times	54
Novel (not in any of the above populations)	88
Candidate variants' effects on the encoded protein	
Substitutions	149
Possible splice variants	22
Frameshifts	9
Premature stops	6
Insertions	6
Deletions	9
Modes of inheritance of candidate variants	
Maternal AD inheritance	69
Paternal AD inheritance	86
De novo	20
X-linked	2
Unclear	5
AR inheritance	0

[a]Based on UCSC genomicSuperDups track

Table 2.5: Rare variants shared by all three short-telomere family members

Location (hg19)	Gene name	Nucleotide change	Amino acid change	Present in other databases
chr1:100680411	DBT	G>A	R>C	1000G, ESP
chr2:79385859	REG3A	A>T	I>N	1000G
chr2:95780861	MRPS5	G>C	P>R	
chr2:98809471	VWA3B	T>G	V>G	
chr2:125671722	CNTNAP5	C>T	R>W	ESP
chr2:138169449	THSD7B	AGATG>A	deletion, frameshift	
chr2:172930353	METAP1D	A>G	I>V	
chr2:197577449	CCDC150,LOC100130452	G>A	A>T	
chr2:202505646	TMEM237	C>T	R>H	
chr2:209219303	PIKFYVE	C>T	R>STOP	
chr3:28454714	ZCWPW2	T>C	V>A	
chr3:50338108	HYAL1	G>A	R>C	
chr4:4389442	D4S234E	C>T	T>M	
chr4:20726464	PACRGL	G>A	E>K	
chr4:146026787	ABCE1	G>A	S>N	
chr5:131811491	C5orf56,IRF1	C>T	S>L	1000G
chr6:29365149	OR12D2	T>C	F>L	
chr6:52147513	MCM3	G>A	P>L	
chr6:88074899	C6orf162,C6orf163	G>A	G>R	
chr6:90089935	RRAGD	C>T	R>K	1000G
chr6:96034415	MANEA	G>T	A>S	1000G
chr7:40277263	C7orf10	C>T	R>STOP	
chr10:23290957	ARMC3	T>C	L>P	
chr10:50960288	OGDHL	T>C	Y>C	1000G
chr11:57313391	SMTNL1	G>A	E>K	
chr11:64977321	CAPN1	G>C	R>P	
chr12:48075570	RPAP3	T>A	Q>H	
chr12:58204204	AVIL	C>T	R>H	ESP
chr12:101703545	UTP20	C>T	P>L	1000G, ESP
chr12:132599028	EP400NL	C>A	L>M	
chr13:114783589	RASA3	T>C	K>R	
chr16:19710891	C16orf62	GCAA>G	deletion	
chr16:67693688	ACD	CCTT>C	deletion	
chr18:9887371	TXNDC2	C>A	L>I	
chr18:47765079	CCDC11	A>C	possible splice variant	ESP
chr21:19653417	TMPRSS15	T>A	R>W	
chr21:34655546	IL10RB	G>A	E>K	
chr21:43259888	PRDM15	T>C	K>E	
chr22:20717934	USP41	C>T	G>R	
chr22:24808628	SPECC1L	A>T	M>L	1000G

Table 2.6: Primers for *ACD* locus used in targeted validation sequencing

Forward primer	Reverse primer	Chr	Start*	Stop*	Platform
5'-GCAGTTGAATGCGGAGCTCA	5'-CTGAGTTCCCAGCAGGAACTC	chr16	67690393	67690618	AmpliSeq
5'-GGTAGGCAGGCACCTGATTC	5'-CTGAGGGAGGCCAGGGAATCAG	chr16	67690547	67690703	AmpliSeq
5'-TGTGCTTGAATGCAGGAGATGT	5'-GGAGCCAGTGCTAGTTGGAAG	chr16	67690805	67690968	AmpliSeq
5'-GTGCAAGGGTTTGACAGCAAG	5'-GCCGTTCTAAGGGACACAGAAA	chr16	67690924	67691147	AmpliSeq
5'-CCAAGCCTTAGCAACCCAC	5'-GCTGGGCTAAGCAGTCCTG	chr16	67691098	67691271	AmpliSeq
5'-CCCAAGCCTAGGTAAGAGGG	5'-GGAGAGGAGAGGATCAGGGATT	chr16	67691208	67691434	AmpliSeq
5'-CCTCACAGGATCTGGCCTTG	5'-AGGACAGATACCGCTCCACA	chr16	67691300	67691498	AmpliSeq
5'-CTCTCCTGCCGCATGAGAT	5'-CTCTGTGCTCGGGTCCAAG	chr16	67691428	67691690	AmpliSeq
5'-CTGGGACTAGTGACCAAGAGTTG	5'-TAGAACAAGGAAGGCCTGAGGTA	chr16	67691621	67691859	AmpliSeq
5'-ATCCAAGGCTACCCATGCTC	5'-AGTCCACACCAGGCTCTTG	chr16	67691805	67692029	AmpliSeq
5'-TTGAACTCCAGGCTAGGTTTCTG	5'-CCACATGTCATCCGAGGAAAGTG	chr16	67691976	67692246	AmpliSeq
5'-GCAGAAGGCTGATGCTGGTA	5'-GCAGGATGCTGTGAAAGGTG	chr16	67692202	67692396	AmpliSeq
5'-TGCAGGGACCGTGTTCATC	5'-ACAGTGCTGATAAGACTTCCTGAAC	chr16	67692343	67692576	AmpliSeq
5'-CTATGAGGGTCAGAGATAGGTCCT	5'-GCCTGTCCTACAGAGTTCATGTC	chr16	67692487	67692748	AmpliSeq
5'-GGGACAGTGTACACAGCTTCT	5'-GCTGCCTCACGATGCAAG	chr16	67692696	67692854	AmpliSeq
5'-CCTGACATCTCCCAAGCAAATCC	5'-CCTTATGCTTCCTCAATAAGCTGTCTTC	chr16	67692797	67693072	AmpliSeq
5'-CCTCCCGCATTTCATCCAGAAG	5'-GTACTGTAGAGCTTGACCAGTGATC	chr16	67692943	67693131	AmpliSeq
5'-AGATCACTGCACAGCGTGTTAG	5'-CCATTAACTACCCTTCTCTTTTTCTTAGCA	chr16	67693084	67693350	AmpliSeq
5'-AGCTTTTTCTGAACATCTAAGTCTTGGT	5'-GACTCTTCGTGACGATTCTGAGAC	chr16	67693292	67693566	AmpliSeq
5'-GTCCACCTGGAGATAGAACTCTG	5'-CAGTGAGGATCCTGCTTGTTG	chr16	67693489	67693722	AmpliSeq
5'-CGGAAGCCGAACTCCTTCTC	5'-CCACGCTGCTTGTGTCTGA	chr16	67693674	67693881	AmpliSeq
5'-CCAGGCATCGGACACTGT	5'-TGGATTCGGGAGCTGATTCTG	chr16	67693836	67694090	AmpliSeq
5'-GGACTGGAGGGTGTCTCTGA	5'-GAGCTTCCTCTTCCGAGGAAAG	chr16	67694046	67694207	AmpliSeq
5'-CTACACCCAGCGGATGCAACG	5'-CCGCGATGAGAGTAAACGGG	chr16	67694131	67694356	AmpliSeq
5'-CGTTCGTCAAGATTCCTGTGGTA	5'-GTGCACTGTGTAGATGAGGAAACT	chr16	67694387	67694584	AmpliSeq
5'-GAACGGTTCAGCACATATTTATTATGACTC	5'-ACGCGGAGTCCACGTTTC	chr16	67694530	67694781	AmpliSeq
5'-CCACGGCTCCGTTTCCTAG	5'-GGAGGAGCCCTTACTTTGCTC	chr16	67694744	67695018	AmpliSeq
5'-CGATAGCATCGTCGAGGTGAA	5'-CTGGAGACCAGCAGTGGAGGAA	chr16	67694976	67695168	AmpliSeq
5'-AGTCCCATTCTGCTTTTCTGCT	5'-TCGGCGTCAAACTGGAAGTC	chr16	67695102	67695368	AmpliSeq
5'-GAGCTGAGGTCTGGGCTTAA	5'-GTCGCCATGAGCATCCGTA	chr16	67695230	67695495	AmpliSeq
5'-CTGGACGTGCTACTTGGCTA	5'-AGAGGGTGACGCTTGGGTA	chr16	67695456	67695680	AmpliSeq
5'-GTCTACAAGGGTTAGTCCATGCC	5'-TGTTGAGATCAGAGACCTGCT	chr16	67695633	67695778	AmpliSeq
5'-CAAGGCAGTCTCACCACTCA	5'-AGAGTAAACGGGCCAGCATC	chr16	67694348	67693584	Sanger (K170Δ)
5'-CAGCCACAGACCAAAGAGG	5'-TGTCATCCGAGGAAAGTGGT	chr16	67692241	67691384	Sanger (P491T)

*Genomic coordinates correspond to GRCh37/hg19.

CHAPTER 3: CONCLUSIONS AND DISCUSSION

TPP1 is one of the components of the shelterin complex, functioning both in end-protection and telomere length regulation. One major role of TPP1 in telomere length maintenance is to recruit telomerase to telomeres. Mutagenesis studies revealed that mutations in a specific surface-exposed acidic cluster, called the TEL patch (E168, E169, E171, R180, L183, L212, E215), in TPP1 disrupt the recruitment of telomerase to telomeres without affecting its end-protection function. In this study, we identified an individual with a severe DC variant HH carrying two *ACD* mutations. One mutation is a deletion of K170 (K170Δ), which is located centrally in the TEL patch region between E169 and E171; the other one is a missense mutation, P491T, which resides in the TIN2-binding domain. The patient is negative for mutations in other DC-associated genes. Considering the role of TPP1 in telomerase recruitment, we hypothesized that these mutations in *ACD* are responsible for HH in this patient. Our goal was to examine the functional consequences of the K170Δ and P491T mutations and to determine the mechanism by which they cause HH. In chapter 2, we showed that K170Δ compromises the recruitment of telomerase to telomeres and significantly reduces the processivity of telomerase. On the other hand, P491T did not have a significant effect on the recruitment and processivity of telomerase, but it disrupts the interaction between TPP1 and TIN2.

K170 resides in the TEL patch of TPP1. Although it is not a surface amino acid, it is located adjacent to TEL patch amino acids E168, E169 and E171. To understand the effect of the deletion of K170 on the function of TPP1, we addressed three different aspects of TPP1 function associated with telomerase that have previously been examined for TEL patch mutations [81]. We examined the effect of ΔK170 on direct interaction of TPP1 with telomerase using Co-IP experiments (Figure 2.5); we monitored recruitment of telomerase to telomeres using IF-FISH experiments (Figure

2.6); and we measured enzymatic processivity using telomerase activity assays (Figure 2.9). Our results demonstrated that ΔK170 compromises the recruitment and processivity of telomerase but it has no detectable effect on the interaction between TPP1 and telomerase. Our structural model (based on homology modeling) of K170Δ dysfunction suggests that deletion of K170 flips E169 into the core of the OB fold domain, disabling it from binding to telomerase (Figure 2.12A); hence, compromising recruitment and processivity of telomerase. However, since we do not have the crystal structure for K170Δ, we cannot rule out the possibility of other disruptive changes caused by K170Δ in TPP1. Moreover, the lack of a significant effect of K170Δ on the interaction between TPP1 and telomerase suggests that there are different interaction points between telomerase and TPP1, which can secure their interaction even when one interaction point is lost. Indeed, it has been proposed that two different domains of TERT (the CTE and TEN domains) are involved in contacting TPP1, providing support for a multi-point telomerase-TPP1 interaction [79].

The P491 amino acid is located in the TIN2-binding domain of TPP1. Since its location is far from the TEL patch, it is not surprising that P491T has no significant effect on telomerase processivity (Figure 2.10) and the recruitment of telomerase to telomeres (Figure 2.6). Indeed, consistent with its location, the P491T mutation inhibits the interaction between TPP1 and TIN2 (Figure 2.11 A, B). The physiological consequence of this inhibitory effect of P491T is still not clear because it does not seem to be affecting TPP1 recruitment to the telomeres *in vivo* (Figure 2.11 C, D). Although ChIP experiments showed that overexpression of P491T does not seem to affect TPP1 recruitment to telomeres *in vivo* (Figure 2.11 C, D), we cannot rule out the possibility that overexpression of P491T masks the TPP1 recruitment defect. In order to better understand the physiological consequence of P491T, using IP experiments, we plan to investigate the interaction between TPP1 and TIN2 in EBV-transformed lymphoblastoid cells from proband, who carries both P491T and K170Δ, compared to cells from his older sister, who carries only K170Δ. Similarly, we can also asses the amount of TPP1 at telomeres in cells from the proband compared to cells from the older sister via telomere ChIP analysis.

The P491T variant exists with an allele frequency of 0.000154 in the general population, and it is predicted to be probably-damaging/damaging by three computer prediction tools (PolyPhen, SIFT, PhastCons). This supports our data showing that P491T inhibits the interaction between TPP1 and TIN2. To further understand how defects in TPP1-TIN2 interaction can result in telomere dysfunction and disease, it is necessary to map the critical amino acid residues of TPP1 that are involved in interaction with TIN2; thus, the next step will be to map the TIN2-binding site of TPP1 using site-directed mutagenesis and/or crystallography. Naturally observed variants, such as P491T and several others, can be used as tools to start dissecting the amino acid determinants of TPP1-TIN2 interaction. The effect of these mutations/variants on the interaction of TPP1-TIN2 will be determined using IP assays. In addition, their effect on the recruitment of TPP1 to telomeres will be determined using either telomere ChIP or IF-FISH experiments.

Our data showing that K170Δ, but not P491T, compromises telomerase recruitment and processivity are also consistent with telomere lengths of the members of the proband`s family. While the family members harboring K170Δ have telomere lengths below the first percentile for their age, the others have normal telomere lengths (Figure 2.4A). As in the case of other telomere shortening-based diseases, anticipation is also seen in the family (from the father to the proband). Interestingly, the heterozygous carriers of K170Δ (the father and the older sister) are clinically unaffected at this time, which cannot be explained only by anticipation. The proband, who is the only member of family carrying both K170Δ and P491T, is also the only family member with HH. On the other hand, the mother, who is a heterozygous carrier of P491T, is healthy and has normal telomere lengths. Therefore, we propose that the proband is a compound heterozygote and that both K170Δ and P491T contribute to the phenotype of the proband, although the contribution of P491T is minor compared to the contribution of K170Δ (Figure 3.1). In order to test that, we plan to examine cumulative effect of K170Δ and P491T on telomerase recruitment by doing IF-FISH experiments (as in figures 2.6 and 2.8) in the presence of both variants. We will also investigate whether any of these variants acts in a dominant negative manner by co-expressing each variant

with wildtype TPP1 and assessing whether their effect on telomerase recruitment will be further impaired.

While our manuscript reporting this work was in press, Guo et al. identified an individual (unrelated to the proband in our study) with aplastic anemia harboring the K170Δ mutation [288]. Similar to the family in our study, family members carrying the K170Δ mutation in this second family also have short telomeres. Not surprisingly, Guo et al. also demonstrated that the K170Δ mutation impairs recruitment of telomerase to telomeres [288]. Although this second study did not provide a further link between TPP1 or telomerase dysfunction with disease, combined with our study, it supports our conclusion about the causal relationship between TEL patch mutations and bone marrow failure.

Previously our collaborator, Dr. Sharon Savage, at NCI identified another variant in *ACD* in a different family using a candidate gene strategy, Q205R. Although it is located in the OB-fold domain, structural modeling analysis showed that this variant is not expected to affect the TEL patch structure. Of note, the patient with the Q205R variant was also found to harbor a TER mutation in close vicinity to the RNA templating region; hence, this TER mutation is most likely the cause of disease. Moreover, the Q205R variant does not have a significant effect on the recruitment of telomerase to telomeres (Figure 2.8). Therefore, we hypothesize that Q205R does not contribute to DC in this family. Further characterization of Q205R and the *TER* mutation will provide additional information about the precise molecular defects underlying telomere shortening in this DC patient. We plan to further investigate the effect of Q205R on telomerase processivity and the effect of the TERC mutation on telomerase activity. In addition, the crystal structure of TPP1 with the Q205R variant will provide a more definitive explanation for the structural effect of the mutation on the TEL patch and on the OB domain in general. Based on our data showing that Q205R does not have an effect on the telomerase recruitment function of the TEL patch, we think that we will not see a significant structural effect.

Most of the experiments in our study that involved living cells were performed using transient transfections. One of the possible pitfalls of the transient transfections is

the overexpression of the protein (i.e TPP1), which may mask possible subtle effects caused by the mutations (i.e P491T). Thus, generating stable cell lines expressing the patient mutations (as described previously in Nandakumar et al. 2012) is the next step forward in elucidating the effect of the mutations more extensively [81]. Moreover, the effect of the mutations on cell proliferation and telomere length cannot be evaluated with this method because both of these phenotypes require multiple population doublings to evaluate. Thus, stable cell lines will also be utilized to study how the TPP1 mutations affect cell proliferation and telomere length *in vivo*.

Although DC is characterized by telomere shortening in stem cells due to telomerase deficiency, the exact mechanism of pathogenesis is not known for each mutation. To understand the pathogenesis of the patient mutations and other TEL patch mutations in DC and other bone marrow diseases, it is important to examine their effect directly in the bone marrow, particularly in hematopoietic stem cells (HSCs). It has been shown that conditional deletion *Acd* in mice causes rapid loss of HSCs. In the absence of TPP1, a massive telomere deprotection phenotype was observed in hematopoietic progenitors [286]. Using a similar approach, the effects of the patient mutations and TEL patch mutations in both end-protection and telomere length maintenance can be elucidated via rescue studies in mice. Since the sequence of the TEL patch is highly conserved between mouse and human, the mouse equivalents of the patient and TEL patch mutations could be expressed in mouse HSCs. Using conditional deletion of endogenous *Acd/Tpp1*, the effect of the mutations could be examined in HSCs. Since mouse telomeres are longer, the role of TEL patch mutations in telomere length homeostasis could be studied under high replicative stress to see the possible telomere shortening effect more rapidly.

To understand the mechanisms of diseases, particularly stem cell deficiency related diseases, using induced pluripotent stem (iPS) cells derived from patients is another relevant strategy. It is known that TERT is reactivated, hence telomerase activity is reconstituted in the process of reprogramming [289, 290]. This strategy may be sufficient to rescue the phenotype in some DC types; however, it was shown not to be successful in the rescue of DC patients with *TCAB1* mutations because the defect is

in telomerase trafficking rather than telomerase level and activity [214, 291]. It would still be interesting to see the extent of the recruitment defect and possible related cell proliferation defect in iPS cells from our proband carrying both K170Δ and P491T, the heterozygous carriers of K170Δ (the father and the older sister), and the heterozygous carrier of P491T (the mother) in this family.

A recent study showed the value of using genomic-editing technologies to engineer TEL patch mutations in hESC [82]. However, mutated hESCs undergo senescence; thus, they cannot be used to elucidate the role of the TEL patch in the context of complex tissues and organs. Although cell-based studies can provide valuable information about the pathogenesis of the patient and TEL patch mutations in TPP1, *in vivo* models will still be tremendously more useful to understand the effect of these mutations in different organs and tissues. Therefore, in order to further investigate how the patient and TEL patch mutations affect organ development and tissue homeostasis, we are in the process of engineering mice with targeted mutations using CRISPR/Cas9. We will investigate the effect of these mutations on mouse development, viability and longevity. In particular, we plan to focus on tissues with high cell turn-over rate including hair (hair loss or pre-mature greying), skin (change in the thickness of epidermis) and bone marrow (HSC depletion). Another advantage of this strategy is that we can generate a compound heterozygous mouse to recapitulate the two mutations (K170Δ and P491T) in the proband (from NCI-275 family) and examine whether the mouse phenotype correlates with the proband's severe HH manifestations.

In the future, there could be a variety of clinical applications of this study. One of the more practical applications would be to use the *ACD* gene as a diagnostic tool to screen for DC. DC patients with no known mutations in 9 DC genes could be screened for *ACD* mutations. Moreover, because cancer cells have to maintain their telomere length to avoid senescence/mitotic crisis/apoptosis and telomerase is overexpressed in >90% of cancers to ensure telomere length maintenance, targeting telomerase recruitment and processivity through the TEL patch will potentially lead to the discovery of novel anti-cancer therapeutics. Nakashima et al. showed that a telomerase inhibitor (BIBR1532) inhibits proliferation of HeLa cells harboring TEL patch mutations by

inducing apoptosis [265]. This observation supports the notion that targeting the TPP1-telomerase interaction through TEL patch residues with small molecule–based therapies will be a useful anticancer therapy approach in telomerase-positive cancer cells, especially when it is combined with anti-telomerase therapy. Identification of additional causal mutations in DC and other bone marrow failure diseases is also very important because in the future, these causative mutations could potentially be corrected with one of the several gene-editing methods, such as CRISPR/Cas9 technology, in bone marrow cells from patients *ex vivo*. Cells with the corrected gene could be transplanted back into the same patient using stem cell transplantation.

As mentioned before, stem cells depend on telomerase to maintain their telomere length in order to sustain their self-renewal capacity. Accordingly, understanding the interaction between the TEL patch of TPP1 and telomerase in the context of stem cells is extremely valuable because it is the key interaction for recruitment of telomerase to the telomere for extension of telomeres. In this study, we showed that in a DC patient with extremely short telomeres, the recruitment and processivity of telomerase are compromised due a mutation likely affecting the structural conformation of the TEL patch. This study provides novel insights into the cause-effect relationship between TEL patch mutations in TPP1 and stem cell dysfunction related to telomere shortening in DC. Further studies on TEL patch mutations and other patient mutations will provide additional information regarding how these mutations affect specific tissues and organs, and thus, the importance of the role of the TEL patch for stem cell function in different tissue/organs.

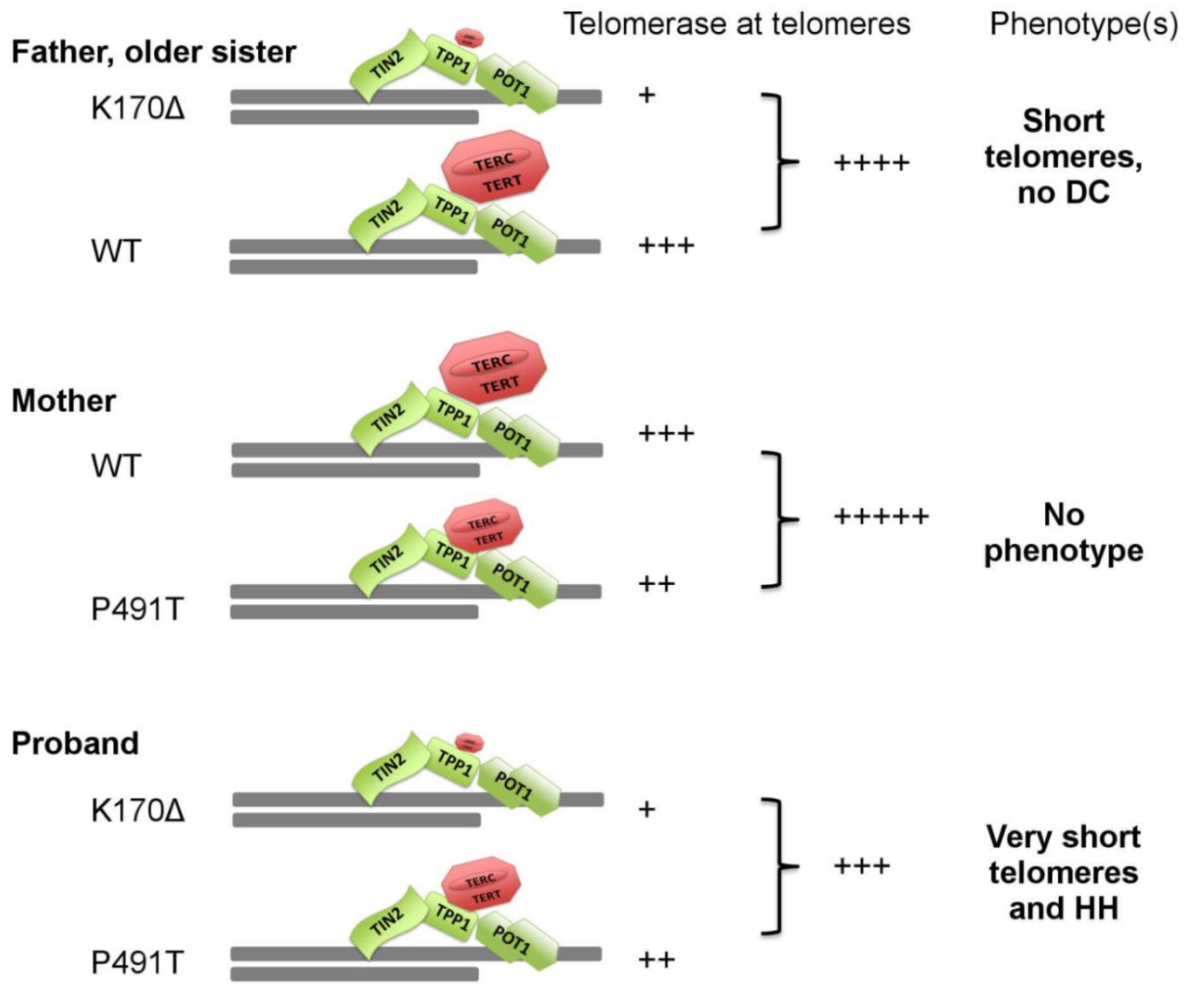

Figure 3.1: Potential mechanism underlying the genotype-phenotype relationship in family NCI-275. Telomerase recruitment is modestly reduced in the presence of one wild type allele and one TPP1-P491T allele, somewhat reduced with one wild type allele and one TPP1-K170Δ allele, and significantly reduced with one TPP1-P491T allele and one TPP1-K170Δ allele.

REFERENCES

1. Savage, S.A., *Human telomeres and telomere biology disorders.* Prog Mol Biol Transl Sci, 2014. **125**: p. 41-66.
2. Savage, S.A. and B.P. Alter, *Dyskeratosis congenita.* Hematol Oncol Clin North Am, 2009. **23**(2): p. 215-31.
3. Hukezalie, K.R. and J.M. Wong, *Structure-function relationship and biogenesis regulation of the human telomerase holoenzyme.* FEBS J, 2013. **280**(14): p. 3194-204.
4. Makarov, V.L., Y. Hirose, and J.P. Langmore, *Long G tails at both ends of human chromosomes suggest a C strand degradation mechanism for telomere shortening.* Cell, 1997. **88**(5): p. 657-66.
5. Moyzis, R.K., et al., *A highly conserved repetitive DNA sequence, (TTAGGG)n, present at the telomeres of human chromosomes.* Proc Natl Acad Sci U S A, 1988. **85**(18): p. 6622-6.
6. Meyne, J., R.L. Ratliff, and R.K. Moyzis, *Conservation of the human telomere sequence (TTAGGG)n among vertebrates.* Proc Natl Acad Sci U S A, 1989. **86**(18): p. 7049-53.
7. Kipling, D. and H.J. Cooke, *Hypervariable ultra-long telomeres in mice.* Nature, 1990. **347**(6291): p. 400-2.
8. Starling, J.A., et al., *Extensive telomere repeat arrays in mouse are hypervariable.* Nucleic Acids Res, 1990. **18**(23): p. 6881-8.
9. de Lange, T., et al., *Structure and variability of human chromosome ends.* Mol Cell Biol, 1990. **10**(2): p. 518-27.
10. Griffith, J.D., et al., *Mammalian telomeres end in a large duplex loop.* Cell, 1999. **97**(4): p. 503-14.
11. Doksani, Y., et al., *Super-resolution fluorescence imaging of telomeres reveals TRF2-dependent T-loop formation.* Cell, 2013. **155**(2): p. 345-56.

12. de Lange, T., *T-loops and the origin of telomeres.* Nat Rev Mol Cell Biol, 2004. **5**(4): p. 323-329.
13. Lipps, H.J. and D. Rhodes, *G-quadruplex structures: in vivo evidence and function.* Trends Cell Biol, 2009. **19**(8): p. 414-22.
14. de Lange, T., *How telomeres solve the end-protection problem.* Science, 2009. **326**(5955): p. 948-52.
15. de Lange, T., *Shelterin: the protein complex that shapes and safeguards human telomeres.* Genes Dev, 2005. **19**(18): p. 2100-10.
16. Zhong, Z., et al., *A mammalian factor that binds telomeric TTAGGG repeats in vitro.* Mol Cell Biol, 1992. **12**(11): p. 4834-43.
17. Chong, L., et al., *A human telomeric protein.* Science, 1995. **270**(5242): p. 1663-7.
18. Broccoli, D., et al., *Human telomeres contain two distinct Myb-related proteins, TRF1 and TRF2.* Nat Genet, 1997. **17**(2): p. 231-5.
19. Sbodio, J.I. and N.W. Chi, *Identification of a tankyrase-binding motif shared by IRAP, TAB182, and human TRF1 but not mouse TRF1. NuMA contains this RXXPDG motif and is a novel tankyrase partner.* J Biol Chem, 2002. **277**(35): p. 31887-92.
20. Smith, S. and T. de Lange, *Tankyrase promotes telomere elongation in human cells.* Curr Biol, 2000. **10**(20): p. 1299-302.
21. Hsiao, S.J., et al., *Tankyrase 2 poly(ADP-ribose) polymerase domain-deleted mice exhibit growth defects but have normal telomere length and capping.* Mol Cell Biol, 2006. **26**(6): p. 2044-54.
22. Grune, T., et al., *Crystal structure and functional analysis of a nucleosome recognition module of the remodeling factor ISWI.* Mol Cell, 2003. **12**(2): p. 449-60.
23. Boyer, L.A., R.R. Latek, and C.L. Peterson, *The SANT domain: a unique histone-tail-binding module?* Nat Rev Mol Cell Biol, 2004. **5**(2): p. 158-163.
24. Bianchi, A., et al., *TRF1 is a dimer and bends telomeric DNA.* EMBO J, 1997. **16**(7): p. 1785-94.

25. Chen, Y., et al., *A shared docking motif in TRF1 and TRF2 used for differential recruitment of telomeric proteins.* Science, 2008. **319**(5866): p. 1092-6.
26. Kim, H., et al., *TRF2 functions as a protein hub and regulates telomere maintenance by recognizing specific peptide motifs.* Nat Struct Mol Biol, 2009. **16**(4): p. 372-9.
27. Bianchi, A., et al., *TRF1 binds a bipartite telomeric site with extreme spatial flexibility.* EMBO J, 1999. **18**(20): p. 5735-44.
28. Ancelin, K., et al., *Targeting assay to study the cis functions of human telomeric proteins: evidence for inhibition of telomerase by TRF1 and for activation of telomere degradation by TRF2.* Mol Cell Biol, 2002. **22**(10): p. 3474-87.
29. Smogorzewska, A., et al., *Control of human telomere length by TRF1 and TRF2.* Mol Cell Biol, 2000. **20**(5): p. 1659-68.
30. van Steensel, B. and T. de Lange, *Control of telomere length by the human telomeric protein TRF1.* Nature, 1997. **385**(6618): p. 740-3.
31. Karlseder, J., et al., *Targeted deletion reveals an essential function for the telomere length regulator Trf1.* Mol Cell Biol, 2003. **23**(18): p. 6533-41.
32. Iwano, T., et al., *Importance of TRF1 for functional telomere structure.* J Biol Chem, 2004. **279**(2): p. 1442-8.
33. Martinez, P., et al., *Increased telomere fragility and fusions resulting from TRF1 deficiency lead to degenerative pathologies and increased cancer in mice.* Genes Dev, 2009. **23**(17): p. 2060-75.
34. Sfeir, A., et al., *Mammalian telomeres resemble fragile sites and require TRF1 for efficient replication.* Cell, 2009. **138**(1): p. 90-103.
35. Bilaud, T., et al., *Telomeric localization of TRF2, a novel human telobox protein.* Nat Genet, 1997. **17**(2): p. 236-9.
36. Fairall, L., et al., *Structure of the TRFH dimerization domain of the human telomeric proteins TRF1 and TRF2.* Mol Cell, 2001. **8**(2): p. 351-61.
37. Stansel, R.M., T. de Lange, and J.D. Griffith, *T-loop assembly in vitro involves binding of TRF2 near the 3' telomeric overhang.* EMBO J, 2001. **20**(19): p. 5532-40.

38. Li, B., S. Oestreich, and T. de Lange, *Identification of human Rap1: implications for telomere evolution.* Cell, 2000. **101**(5): p. 471-83.
39. Celli, G.B. and T. de Lange, *DNA processing is not required for ATM-mediated telomere damage response after TRF2 deletion.* Nat Cell Biol, 2005. **7**(7): p. 712-8.
40. Ye, J.Z., et al., *TIN2 binds TRF1 and TRF2 simultaneously and stabilizes the TRF2 complex on telomeres.* J Biol Chem, 2004. **279**(45): p. 47264-71.
41. Kim, S.H., et al., *TIN2 mediates functions of TRF2 at human telomeres.* J Biol Chem, 2004. **279**(42): p. 43799-804.
42. Liu, D., et al., *PTOP interacts with POT1 and regulates its localization to telomeres.* Nat Cell Biol, 2004. **6**(7): p. 673-80.
43. van Steensel, B., A. Smogorzewska, and T. de Lange, *TRF2 protects human telomeres from end-to-end fusions.* Cell, 1998. **92**(3): p. 401-13.
44. Karlseder, J., et al., *p53- and ATM-dependent apoptosis induced by telomeres lacking TRF2.* Science, 1999. **283**(5406): p. 1321-5.
45. Takai, H., A. Smogorzewska, and T. de Lange, *DNA damage foci at dysfunctional telomeres.* Curr Biol, 2003. **13**(17): p. 1549-56.
46. Karlseder, J., et al., *The telomeric protein TRF2 binds the ATM kinase and can inhibit the ATM-dependent DNA damage response.* PLoS Biol, 2004. **2**(8): p. E240.
47. Takai, K.K., et al., *In vivo stoichiometry of shelterin components.* J Biol Chem, 2010. **285**(2): p. 1457-67.
48. Zhu, X.D., et al., *Cell-cycle-regulated association of RAD50/MRE11/NBS1 with TRF2 and human telomeres.* Nat Genet, 2000. **25**(3): p. 347-52.
49. Martinez, P. and M.A. Blasco, *Telomeric and extra-telomeric roles for telomerase and the telomere-binding proteins.* Nat Rev Cancer, 2011. **11**(3): p. 161-76.
50. Yang, D., et al., *Human telomeric proteins occupy selective interstitial sites.* Cell Res, 2011. **21**(7): p. 1013-27.
51. Li, B. and T. de Lange, *Rap1 affects the length and heterogeneity of human telomeres.* Mol Biol Cell, 2003. **14**(12): p. 5060-8.

52. Sfeir, A., et al., *Loss of Rap1 induces telomere recombination in the absence of NHEJ or a DNA damage signal.* Science, 2010. **327**(5973): p. 1657-61.
53. Kim, S.H., P. Kaminker, and J. Campisi, *TIN2, a new regulator of telomere length in human cells.* Nat Genet, 1999. **23**(4): p. 405-12.
54. Frescas, D. and T. de Lange, *Binding of TPP1 protein to TIN2 protein is required for POT1a,b protein-mediated telomere protection.* J Biol Chem, 2014. **289**(35): p. 24180-7.
55. Ye, J.Z. and T. de Lange, *TIN2 is a tankyrase 1 PARP modulator in the TRF1 telomere length control complex.* Nat Genet, 2004. **36**(6): p. 618-23.
56. Chiang, Y.J., et al., *Telomere-associated protein TIN2 is essential for early embryonic development through a telomerase-independent pathway.* Mol Cell Biol, 2004. **24**(15): p. 6631-4.
57. Takai, K.K., et al., *Telomere protection by TPP1/POT1 requires tethering to TIN2.* Mol Cell, 2011. **44**(4): p. 647-59.
58. Savage, S.A., et al., *TINF2, a component of the shelterin telomere protection complex, is mutated in dyskeratosis congenita.* Am J Hum Genet, 2008. **82**(2): p. 501-9.
59. Yang, D., et al., *TIN2 protein dyskeratosis congenita missense mutants are defective in association with telomerase.* J Biol Chem, 2011. **286**(26): p. 23022-30.
60. Frescas, D. and T. de Lange, *A TIN2 dyskeratosis congenita mutation causes telomerase-independent telomere shortening in mice.* Genes Dev, 2014. **28**(2): p. 153-66.
61. Baumann, P. and T.R. Cech, *Pot1, the putative telomere end-binding protein in fission yeast and humans.* Science, 2001. **292**(5519): p. 1171-5.
62. Lei, M., et al., *DNA self-recognition in the structure of Pot1 bound to telomeric single-stranded DNA.* Nature, 2003. **426**(6963): p. 198-203.
63. Lei, M., E.R. Podell, and T.R. Cech, *Structure of human POT1 bound to telomeric single-stranded DNA provides a model for chromosome end-protection.* Nat Struct Mol Biol, 2004. **11**(12): p. 1223-9.

64. Kibe, T., et al., *Telomere protection by TPP1 is mediated by POT1a and POT1b.* Mol Cell Biol, 2010. **30**(4): p. 1059-66.
65. Hockemeyer, D., et al., *Telomere protection by mammalian Pot1 requires interaction with Tpp1.* Nat Struct Mol Biol, 2007. **14**(8): p. 754-61.
66. Loayza, D., et al., *DNA binding features of human POT1: a nonamer 5'-TAGGGTTAG-3' minimal binding site, sequence specificity, and internal binding to multimeric sites.* J Biol Chem, 2004. **279**(13): p. 13241-8.
67. Xin, H., et al., *TPP1 is a homologue of ciliate TEBP-beta and interacts with POT1 to recruit telomerase.* Nature, 2007. **445**(7127): p. 559-62.
68. Loayza, D. and T. De Lange, *POT1 as a terminal transducer of TRF1 telomere length control.* Nature, 2003. **423**(6943): p. 1013-8.
69. Wang, F., et al., *The POT1-TPP1 telomere complex is a telomerase processivity factor.* Nature, 2007. **445**(7127): p. 506-10.
70. Latrick, C.M. and T.R. Cech, *POT1-TPP1 enhances telomerase processivity by slowing primer dissociation and aiding translocation.* EMBO J, 2010. **29**(5): p. 924-33.
71. Hockemeyer, D., et al., *Recent expansion of the telomeric complex in rodents: Two distinct POT1 proteins protect mouse telomeres.* Cell, 2006. **126**(1): p. 63-77.
72. Wu, L., et al., *Pot1 deficiency initiates DNA damage checkpoint activation and aberrant homologous recombination at telomeres.* Cell, 2006. **126**(1): p. 49-62.
73. He, H., et al., *POT1b protects telomeres from end-to-end chromosomal fusions and aberrant homologous recombination.* EMBO J, 2006. **25**(21): p. 5180-90.
74. Palm, W., et al., *Functional dissection of human and mouse POT1 proteins.* Mol Cell Biol, 2009. **29**(2): p. 471-82.
75. Houghtaling, B.R., et al., *A dynamic molecular link between the telomere length regulator TRF1 and the chromosome end protector TRF2.* Curr Biol, 2004. **14**(18): p. 1621-31.
76. Ye, J.Z., et al., *POT1-interacting protein PIP1: a telomere length regulator that recruits POT1 to the TIN2/TRF1 complex.* Genes Dev, 2004. **18**(14): p. 1649-54.

77. Liu, D., et al., *Telosome, a mammalian telomere-associated complex formed by multiple telomeric proteins.* J Biol Chem, 2004. **279**(49): p. 51338-42.
78. Abreu, E., et al., *TIN2-tethered TPP1 recruits human telomerase to telomeres in vivo.* Mol Cell Biol, 2010. **30**(12): p. 2971-82.
79. Zhong, F.L., et al., *TPP1 OB-fold domain controls telomere maintenance by recruiting telomerase to chromosome ends.* Cell, 2012. **150**(3): p. 481-94.
80. Zaug, A.J., et al., *Functional interaction between telomere protein TPP1 and telomerase.* Genes Dev, 2010. **24**(6): p. 613-22.
81. Nandakumar, J., et al., *The TEL patch of telomere protein TPP1 mediates telomerase recruitment and processivity.* Nature, 2012. **492**(7428): p. 285-9.
82. Sexton, A.N., et al., *Genetic and molecular identification of three human TPP1 functions in telomerase action: recruitment, activation, and homeostasis set point regulation.* Genes Dev, 2014. **28**(17): p. 1885-99.
83. O'Connor, M.S., et al., *A critical role for TPP1 and TIN2 interaction in high-order telomeric complex assembly.* Proc Natl Acad Sci U S A, 2006. **103**(32): p. 11874-9.
84. Keegan, C.E., et al., *Urogenital and caudal dysgenesis in adrenocortical dysplasia (acd) mice is caused by a splicing mutation in a novel telomeric regulator.* Hum Mol Genet, 2005. **14**(1): p. 113-23.
85. Else, T., et al., *Tpp1/Acd maintains genomic stability through a complex role in telomere protection.* Chromosome Res, 2007. **15**(8): p. 1001-13.
86. Vlangos, C.N., et al., *Caudal regression in adrenocortical dysplasia (acd) mice is caused by telomere dysfunction with subsequent p53-dependent apoptosis.* Dev Biol, 2009. **334**(2): p. 418-28.
87. Greider, C.W. and E.H. Blackburn, *Identification of a specific telomere terminal transferase activity in Tetrahymena extracts.* Cell, 1985. **43**(2 Pt 1): p. 405-13.
88. Greider, C.W. and E.H. Blackburn, *A telomeric sequence in the RNA of Tetrahymena telomerase required for telomere repeat synthesis.* Nature, 1989. **337**(6205): p. 331-7.
89. Nugent, C.I. and V. Lundblad, *The telomerase reverse transcriptase: components and regulation.* Genes Dev, 1998. **12**(8): p. 1073-85.

90. Feng, J., et al., *The RNA component of human telomerase.* Science, 1995. **269**(5228): p. 1236-41.
91. Blackburn, E.H. and K. Collins, *Telomerase: an RNP enzyme synthesizes DNA.* Cold Spring Harb Perspect Biol, 2011. **3**(5).
92. Mitchell, J.R. and K. Collins, *Human telomerase activation requires two independent interactions between telomerase RNA and telomerase reverse transcriptase.* Mol Cell, 2000. **6**(2): p. 361-71.
93. Chen, J.L., K.K. Opperman, and C.W. Greider, *A critical stem-loop structure in the CR4-CR5 domain of mammalian telomerase RNA.* Nucleic Acids Res, 2002. **30**(2): p. 592-7.
94. Chen, J.L. and C.W. Greider, *Determinants in mammalian telomerase RNA that mediate enzyme processivity and cross-species incompatibility.* EMBO J, 2003. **22**(2): p. 304-14.
95. Theimer, C.A., C.A. Blois, and J. Feigon, *Structure of the human telomerase RNA pseudoknot reveals conserved tertiary interactions essential for function.* Mol Cell, 2005. **17**(5): p. 671-82.
96. Kim, N.K., et al., *Solution structure and dynamics of the wild-type pseudoknot of human telomerase RNA.* J Mol Biol, 2008. **384**(5): p. 1249-61.
97. Tzfati, Y., et al., *Template boundary in a yeast telomerase specified by RNA structure.* Science, 2000. **288**(5467): p. 863-7.
98. Chen, J.L. and C.W. Greider, *Template boundary definition in mammalian telomerase.* Genes Dev, 2003. **17**(22): p. 2747-52.
99. Autexier, C. and C.W. Greider, *Boundary elements of the Tetrahymena telomerase RNA template and alignment domains.* Genes Dev, 1995. **9**(18): p. 2227-39.
100. Chen, J.L., M.A. Blasco, and C.W. Greider, *Secondary structure of vertebrate telomerase RNA.* Cell, 2000. **100**(5): p. 503-14.
101. Leeper, T.C. and G. Varani, *The structure of an enzyme-activating fragment of human telomerase RNA.* RNA, 2005. **11**(4): p. 394-403.

102. Tesmer, V.M., et al., *Two inactive fragments of the integral RNA cooperate to assemble active telomerase with the human protein catalytic subunit (hTERT) in vitro.* Mol Cell Biol, 1999. **19**(9): p. 6207-16.
103. Bley, C.J., et al., *RNA-protein binding interface in the telomerase ribonucleoprotein.* Proc Natl Acad Sci U S A, 2011. **108**(51): p. 20333-8.
104. Huang, J., et al., *Structural basis for protein-RNA recognition in telomerase.* Nat Struct Mol Biol, 2014. **21**(6): p. 507-12.
105. Ganot, P., M. Caizergues-Ferrer, and T. Kiss, *The family of box ACA small nucleolar RNAs is defined by an evolutionarily conserved secondary structure and ubiquitous sequence elements essential for RNA accumulation.* Genes Dev, 1997. **11**(7): p. 941-56.
106. Mitchell, J.R., J. Cheng, and K. Collins, *A box H/ACA small nucleolar RNA-like domain at the human telomerase RNA 3' end.* Mol Cell Biol, 1999. **19**(1): p. 567-76.
107. Fu, D. and K. Collins, *Distinct biogenesis pathways for human telomerase RNA and H/ACA small nucleolar RNAs.* Mol Cell, 2003. **11**(5): p. 1361-72.
108. Collins, K., *Physiological assembly and activity of human telomerase complexes.* Mech Ageing Dev, 2008. **129**(1-2): p. 91-8.
109. Egan, E.D. and K. Collins, *Specificity and stoichiometry of subunit interactions in the human telomerase holoenzyme assembled in vivo.* Mol Cell Biol, 2010. **30**(11): p. 2775-86.
110. Theimer, C.A., et al., *Structural and functional characterization of human telomerase RNA processing and cajal body localization signals.* Mol Cell, 2007. **27**(6): p. 869-81.
111. Stern, J.L., et al., *Telomerase recruitment requires both TCAB1 and Cajal bodies independently.* Mol Cell Biol, 2012. **32**(13): p. 2384-95.
112. Jady, B.E., E. Bertrand, and T. Kiss, *Human telomerase RNA and box H/ACA scaRNAs share a common Cajal body-specific localization signal.* J Cell Biol, 2004. **164**(5): p. 647-52.

113. Venteicher, A.S., et al., *A human telomerase holoenzyme protein required for Cajal body localization and telomere synthesis.* Science, 2009. **323**(5914): p. 644-8.
114. Tycowski, K.T., et al., *A conserved WD40 protein binds the Cajal body localization signal of scaRNP particles.* Mol Cell, 2009. **34**(1): p. 47-57.
115. Egan, E.D. and K. Collins, *An enhanced H/ACA RNP assembly mechanism for human telomerase RNA.* Mol Cell Biol, 2012. **32**(13): p. 2428-39.
116. Monecke, T., et al., *Crystal structure of the RRM domain of poly(A)-specific ribonuclease reveals a novel m(7)G-cap-binding mode.* J Mol Biol, 2008. **382**(4): p. 827-34.
117. Sexton, A.N. and K. Collins, *The 5' guanosine tracts of human telomerase RNA are recognized by the G-quadruplex binding domain of the RNA helicase DHX36 and function to increase RNA accumulation.* Mol Cell Biol, 2011. **31**(4): p. 736-43.
118. Lingner, J. and T.R. Cech, *Purification of telomerase from Euplotes aediculatus: requirement of a primer 3' overhang.* Proceedings of the National Academy of Sciences, 1996. **93**(20): p. 10712-10717.
119. Lingner, J., et al., *Reverse transcriptase motifs in the catalytic subunit of telomerase.* Science, 1997. **276**(5312): p. 561-7.
120. Gillis, A.J., A.P. Schuller, and E. Skordalakes, *Structure of the Tribolium castaneum telomerase catalytic subunit TERT.* Nature, 2008. **455**(7213): p. 633-7.
121. Friedman, K.L. and T.R. Cech, *Essential functions of amino-terminal domains in the yeast telomerase catalytic subunit revealed by selection for viable mutants.* Genes Dev, 1999. **13**(21): p. 2863-74.
122. Friedman, K.L., et al., *N-terminal domain of yeast telomerase reverse transcriptase: recruitment of Est3p to the telomerase complex.* Mol Biol Cell, 2003. **14**(1): p. 1-13.
123. Armbruster, B.N., et al., *Putative telomere-recruiting domain in the catalytic subunit of human telomerase.* Mol Cell Biol, 2003. **23**(9): p. 3237-46.

124. Armbruster, B.N., et al., *Rescue of an hTERT mutant defective in telomere elongation by fusion with hPot1.* Mol Cell Biol, 2004. **24**(8): p. 3552-61.
125. Schmidt, J.C., A.B. Dalby, and T.R. Cech, *Identification of human TERT elements necessary for telomerase recruitment to telomeres.* Elife, 2014. **3**.
126. Lai, C.K., J.R. Mitchell, and K. Collins, *RNA binding domain of telomerase reverse transcriptase.* Mol Cell Biol, 2001. **21**(4): p. 990-1000.
127. Bryan, T.M., K.J. Goodrich, and T.R. Cech, *Telomerase RNA bound by protein motifs specific to telomerase reverse transcriptase.* Mol Cell, 2000. **6**(2): p. 493-9.
128. Counter, C.M., et al., *The catalytic subunit of yeast telomerase.* Proc Natl Acad Sci U S A, 1997. **94**(17): p. 9202-7.
129. Haering, C.H., et al., *Analysis of telomerase catalytic subunit mutants in vivo and in vitro in Schizosaccharomycespombe.* Proc Natl Acad Sci U S A, 2000. **97**(12): p. 6367-72.
130. Nakayama, J. and F. Ishikawa, *[Structure and regulation mechanisms of telomerase].* Nihon Rinsho, 1998. **56**(5): p. 1102-7.
131. Wyatt, H.D., D.A. Lobb, and T.L. Beattie, *Characterization of physical and functional anchor site interactions in human telomerase.* Mol Cell Biol, 2007. **27**(8): p. 3226-40.
132. Peng, Y., I.S. Mian, and N.F. Lue, *Analysis of telomerase processivity: mechanistic similarity to HIV-1 reverse transcriptase and role in telomere maintenance.* Mol Cell, 2001. **7**(6): p. 1201-11.
133. Lue, N.F., Y.C. Lin, and I.S. Mian, *A conserved telomerase motif within the catalytic domain of telomerase reverse transcriptase is specifically required for repeat addition processivity.* Mol Cell Biol, 2003. **23**(23): p. 8440-9.
134. Mitchell, M., et al., *Structural basis for telomerase catalytic subunit TERT binding to RNA template and telomeric DNA.* Nat Struct Mol Biol, 2010. **17**(4): p. 513-8.
135. Hossain, S., S. Singh, and N.F. Lue, *Functional analysis of the C-terminal extension of telomerase reverse transcriptase. A putative "thumb" domain.* J Biol Chem, 2002. **277**(39): p. 36174-80.

136. Huard, S., T.J. Moriarty, and C. Autexier, *The C terminus of the human telomerase reverse transcriptase is a determinant of enzyme processivity.* Nucleic Acids Res, 2003. **31**(14): p. 4059-70.
137. Banik, S.S., et al., *C-terminal regions of the human telomerase catalytic subunit essential for in vivo enzyme activity.* Mol Cell Biol, 2002. **22**(17): p. 6234-46.
138. Seimiya, H., et al., *Involvement of 14-3-3 proteins in nuclear localization of telomerase.* Embo j, 2000. **19**(11): p. 2652-61.
139. Counter, C.M., et al., *Dissociation among in vitro telomerase activity, telomere maintenance, and cellular immortalization.* Proc Natl Acad Sci U S A, 1998. **95**(25): p. 14723-8.
140. Sexton, A.N., D.T. Youmans, and K. Collins, *Specificity requirements for human telomere protein interaction with telomerase holoenzyme.* J Biol Chem, 2012. **287**(41): p. 34455-64.
141. Rando, T.A., *Stem cells, ageing and the quest for immortality.* Nature, 2006. **441**(7097): p. 1080-6.
142. Rossi, D.J., C.H. Jamieson, and I.L. Weissman, *Stems cells and the pathways to aging and cancer.* Cell, 2008. **132**(4): p. 681-96.
143. Yang, C., et al., *A key role for telomerase reverse transcriptase unit in modulating human embryonic stem cell proliferation, cell cycle dynamics, and in vitro differentiation.* Stem Cells, 2008. **26**(4): p. 850-63.
144. Armstrong, L., et al., *Overexpression of telomerase confers growth advantage, stress resistance, and enhanced differentiation of ESCs toward the hematopoietic lineage.* Stem Cells, 2005. **23**(4): p. 516-29.
145. Wong, C.W., et al., *Kruppel-like transcription factor 4 contributes to maintenance of telomerase activity in stem cells.* Stem Cells, 2010. **28**(9): p. 1510-7.
146. Wright, D.L., et al., *Characterization of telomerase activity in the human oocyte and preimplantation embryo.* Mol Hum Reprod, 2001. **7**(10): p. 947-55.
147. Dolci, S., et al., *Stem cell factor activates telomerase in mouse mitotic spermatogonia and in primordial germ cells.* J Cell Sci, 2002. **115**(Pt 8): p. 1643-9.

148. Yamamoto, Y., et al., *Postmeiotic modifications of spermatogenic cells are accompanied by inhibition of telomerase activity.* Urol Res, 1999. **27**(5): p. 336-45.
149. Wright, W.E., et al., *Telomerase activity in human germline and embryonic tissues and cells.* Dev Genet, 1996. **18**(2): p. 173-9.
150. Choudhary, B., A.A. Karande, and S.C. Raghavan, *Telomere and telomerase in stem cells: relevance in ageing and disease.* Front Biosci (Schol Ed), 2012. **4**: p. 16-30.
151. Weissman, I.L., *Translating stem and progenitor cell biology to the clinic: barriers and opportunities.* Science, 2000. **287**(5457): p. 1442-6.
152. Artegiani, B. and F. Calegari, *Age-related cognitive decline: can neural stem cells help us?* Aging (Albany NY), 2012. **4**(3): p. 176-86.
153. Hiyama, E. and K. Hiyama, *Telomere and telomerase in stem cells.* Br J Cancer, 2007. **96**(7): p. 1020-4.
154. Vaziri, H., et al., *Evidence for a mitotic clock in human hematopoietic stem cells: loss of telomeric DNA with age.* Proc Natl Acad Sci U S A, 1994. **91**(21): p. 9857-60.
155. Kuhn, H.G., H. Dickinson-Anson, and F.H. Gage, *Neurogenesis in the dentate gyrus of the adult rat: age-related decrease of neuronal progenitor proliferation.* J Neurosci, 1996. **16**(6): p. 2027-33.
156. Maslov, A.Y., et al., *Neural stem cell detection, characterization, and age-related changes in the subventricular zone of mice.* J Neurosci, 2004. **24**(7): p. 1726-33.
157. Molofsky, A.V., et al., *Increasing p16INK4a expression decreases forebrain progenitors and neurogenesis during ageing.* Nature, 2006. **443**(7110): p. 448-52.
158. Conboy, I.M., et al., *Notch-mediated restoration of regenerative potential to aged muscle.* Science, 2003. **302**(5650): p. 1575-7.
159. Conboy, I.M. and T.A. Rando, *Aging, stem cells and tissue regeneration: lessons from muscle.* Cell Cycle, 2005. **4**(3): p. 407-10.

160. Nishimura, E.K., S.R. Granter, and D.E. Fisher, *Mechanisms of hair graying: incomplete melanocyte stem cell maintenance in the niche.* Science, 2005. **307**(5710): p. 720-4.
161. Blasco, M.A., et al., *Mouse models for the study of telomerase.* Ciba Found Symp, 1997. **211**: p. 160-70; discussion 170-6.
162. Blasco, M.A., *Mice with bad ends: mouse models for the study of telomeres and telomerase in cancer and aging.* EMBO J, 2005. **24**(6): p. 1095-103.
163. Lee, H.W., et al., *Essential role of mouse telomerase in highly proliferative organs.* Nature, 1998. **392**(6676): p. 569-74.
164. Samper, E., et al., *Long-term repopulating ability of telomerase-deficient murine hematopoietic stem cells.* Blood, 2002. **99**(8): p. 2767-75.
165. Tomas-Loba, A., et al., *Telomerase reverse transcriptase delays aging in cancer-resistant mice.* Cell, 2008. **135**(4): p. 609-22.
166. Jaskelioff, M., et al., *Telomerase reactivation reverses tissue degeneration in aged telomerase-deficient mice.* Nature, 2011. **469**(7328): p. 102-6.
167. Sahin, E., et al., *Telomere dysfunction induces metabolic and mitochondrial compromise.* Nature, 2011. **470**(7334): p. 359-65.
168. Pucci, F., L. Gardano, and L. Harrington, *Short telomeres in ESCs lead to unstable differentiation.* Cell Stem Cell, 2013. **12**(4): p. 479-86.
169. Alter, B.P., et al., *Cancer in dyskeratosis congenita.* Blood, 2009. **113**(26): p. 6549-57.
170. Ballew, B.J. and S.A. Savage, *Updates on the biology and management of dyskeratosis congenita and related telomere biology disorders.* Expert Rev Hematol, 2013. **6**(3): p. 327-37.
171. Rashid, R., et al., *Crystal structure of a Cbf5-Nop10-Gar1 complex and implications in RNA-guided pseudouridylation and dyskeratosis congenita.* Mol Cell, 2006. **21**(2): p. 249-60.
172. Li, L. and K. Ye, *Crystal structure of an H/ACA box ribonucleoprotein particle.* Nature, 2006. **443**(7109): p. 302-7.
173. Hamma, T., et al., *The Cbf5-Nop10 complex is a molecular bracket that organizes box H/ACA RNPs.* Nat Struct Mol Biol, 2005. **12**(12): p. 1101-7.

174. Wong, J.M., et al., *Telomerase RNA deficiency in peripheral blood mononuclear cells in X-linked dyskeratosis congenita.* Hum Genet, 2004. **115**(5): p. 448-55.
175. Wong, J.M. and K. Collins, *Telomerase RNA level limits telomere maintenance in X-linked dyskeratosis congenita.* Genes Dev, 2006. **20**(20): p. 2848-58.
176. Mochizuki, Y., et al., *Mouse dyskerin mutations affect accumulation of telomerase RNA and small nucleolar RNA, telomerase activity, and ribosomal RNA processing.* Proc Natl Acad Sci U S A, 2004. **101**(29): p. 10756-61.
177. Gu, B.W., M. Bessler, and P.J. Mason, *A pathogenic dyskerin mutation impairs proliferation and activates a DNA damage response independent of telomere length in mice.* Proc Natl Acad Sci U S A, 2008. **105**(29): p. 10173-8.
178. Ruggero, D., et al., *Dyskeratosis congenita and cancer in mice deficient in ribosomal RNA modification.* Science, 2003. **299**(5604): p. 259-62.
179. Mitchell, J.R., E. Wood, and K. Collins, *A telomerase component is defective in the human disease dyskeratosis congenita.* Nature, 1999. **402**(6761): p. 551-5.
180. Hoyeraal, H.M., J. Lamvik, and P.J. Moe, *Congenital hypoplastic thrombocytopenia and cerebral malformations in two brothers.* Acta Paediatr Scand, 1970. **59**(2): p. 185-91.
181. Hreidarsson, S., et al., *A syndrome of progressive pancytopenia with microcephaly, cerebellar hypoplasia and growth failure.* Acta Paediatr Scand, 1988. **77**(5): p. 773-5.
182. Knight, S.W., et al., *Unexplained aplastic anaemia, immunodeficiency, and cerebellar hypoplasia (Hoyeraal-Hreidarsson syndrome) due to mutations in the dyskeratosis congenita gene, DKC1.* Br J Haematol, 1999. **107**(2): p. 335-9.
183. Walne, A.J., et al., *Genetic heterogeneity in autosomal recessive dyskeratosis congenita with one subtype due to mutations in the telomerase-associated protein NOP10.* Hum Mol Genet, 2007. **16**(13): p. 1619-29.
184. Vulliamy, T., et al., *Mutations in the telomerase component NHP2 cause the premature ageing syndrome dyskeratosis congenita.* Proc Natl Acad Sci U S A, 2008. **105**(23): p. 8073-8.
185. Vulliamy, T., et al., *The RNA component of telomerase is mutated in autosomal dominant dyskeratosis congenita.* Nature, 2001. **413**(6854): p. 432-5.

186. Vulliamy, T.J., et al., *Mutations in dyskeratosis congenita: their impact on telomere length and the diversity of clinical presentation.* Blood, 2006. **107**(7): p. 2680-5.
187. Bessler, M., D.B. Wilson, and P.J. Mason, *Dyskeratosis congenita and telomerase.* Curr Opin Pediatr, 2004. **16**(1): p. 23-8.
188. Vulliamy, T., et al., *Disease anticipation is associated with progressive telomere shortening in families with dyskeratosis congenita due to mutations in TERC.* Nat Genet, 2004. **36**(5): p. 447-9.
189. Errington, T.M., et al., *Disease-associated human telomerase RNA variants show loss of function for telomere synthesis without dominant-negative interference.* Mol Cell Biol, 2008. **28**(20): p. 6510-20.
190. Ly, H., et al., *Identification and functional characterization of 2 variant alleles of the telomerase RNA template gene (TERC) in a patient with dyskeratosis congenita.* Blood, 2005. **106**(4): p. 1246-52.
191. Marrone, A., et al., *Heterozygous telomerase RNA mutations found in dyskeratosis congenita and aplastic anemia reduce telomerase activity via haploinsufficiency.* Blood, 2004. **104**(13): p. 3936-42.
192. Robart, A.R. and K. Collins, *Investigation of human telomerase holoenzyme assembly, activity, and processivity using disease-linked subunit variants.* J Biol Chem, 2010. **285**(7): p. 4375-86.
193. Marrone, A., et al., *Functional characterization of novel telomerase RNA (TERC) mutations in patients with diverse clinical and pathological presentations.* Haematologica, 2007. **92**(8): p. 1013-20.
194. Comolli, L.R., et al., *A molecular switch underlies a human telomerase disease.* Proc Natl Acad Sci U S A, 2002. **99**(26): p. 16998-7003.
195. Marrone, A., et al., *Telomerase reverse-transcriptase homozygous mutations in autosomal recessive dyskeratosis congenita and Hoyeraal-Hreidarsson syndrome.* Blood, 2007. **110**(13): p. 4198-205.
196. Hathcock, K.S., et al., *Haploinsufficiency of mTR results in defects in telomere elongation.* Proc Natl Acad Sci U S A, 2002. **99**(6): p. 3591-6.

197. Hao, L.Y., et al., *Short telomeres, even in the presence of telomerase, limit tissue renewal capacity.* Cell, 2005. **123**(6): p. 1121-31.
198. Mason, P.J. and M. Bessler, *The genetics of dyskeratosis congenita.* Cancer Genet, 2011. **204**(12): p. 635-45.
199. Armanios, M., et al., *Haploinsufficiency of telomerase reverse transcriptase leads to anticipation in autosomal dominant dyskeratosis congenita.* Proc Natl Acad Sci U S A, 2005. **102**(44): p. 15960-4.
200. Vulliamy, T.J., et al., *Mutations in the reverse transcriptase component of telomerase (TERT) in patients with bone marrow failure.* Blood Cells Mol Dis, 2005. **34**(3): p. 257-63.
201. Yamaguchi, H., et al., *Mutations in TERT, the gene for telomerase reverse transcriptase, in aplastic anemia.* N Engl J Med, 2005. **352**(14): p. 1413-24.
202. Xin, Z.T., et al., *Functional characterization of natural telomerase mutations found in patients with hematologic disorders.* Blood, 2007. **109**(2): p. 524-32.
203. Du, H.Y., et al., *Complex inheritance pattern of dyskeratosis congenita in two families with 2 different mutations in the telomerase reverse transcriptase gene.* Blood, 2008. **111**(3): p. 1128-30.
204. Riyaz, A., et al., *Revesz syndrome.* Indian J Pediatr, 2007. **74**(9): p. 862-3.
205. Walne, A.J., et al., *TINF2 mutations result in very short telomeres: analysis of a large cohort of patients with dyskeratosis congenita and related bone marrow failure syndromes.* Blood, 2008. **112**(9): p. 3594-600.
206. Sasa, G.S., et al., *Three novel truncating TINF2 mutations causing severe dyskeratosis congenita in early childhood.* Clin Genet, 2012. **81**(5): p. 470-8.
207. Du, H.Y., et al., *TINF2 mutations in children with severe aplastic anemia.* Pediatr Blood Cancer, 2009. **52**(5): p. 687.
208. Canudas, S., et al., *A role for heterochromatin protein 1gamma at human telomeres.* Genes Dev, 2011. **25**(17): p. 1807-19.
209. Houghtaling, B.R., S. Canudas, and S. Smith, *A role for sister telomere cohesion in telomere elongation by telomerase.* Cell Cycle, 2012. **11**(1): p. 19-25.
210. Liu, L., et al., *Telomere lengthening early in development.* Nat Cell Biol, 2007. **9**(12): p. 1436-41.

211. Zalzman, M., et al., *Zscan4 regulates telomere elongation and genomic stability in ES cells.* Nature, 2010. **464**(7290): p. 858-63.
212. Mahmoudi, S., et al., *Wrap53, a natural p53 antisense transcript required for p53 induction upon DNA damage.* Mol Cell, 2009. **33**(4): p. 462-71.
213. Jady, B.E., et al., *Cell cycle-dependent recruitment of telomerase RNA and Cajal bodies to human telomeres.* Mol Biol Cell, 2006. **17**(2): p. 944-54.
214. Zhong, F., et al., *Disruption of telomerase trafficking by TCAB1 mutation causes dyskeratosis congenita.* Genes Dev, 2011. **25**(1): p. 11-6.
215. Miyake, Y., et al., *RPA-like mammalian Ctc1-Stn1-Ten1 complex binds to single-stranded DNA and protects telomeres independently of the Pot1 pathway.* Mol Cell, 2009. **36**(2): p. 193-206.
216. Surovtseva, Y.V., et al., *Conserved telomere maintenance component 1 interacts with STN1 and maintains chromosome ends in higher eukaryotes.* Mol Cell, 2009. **36**(2): p. 207-18.
217. Chen, L.Y., S. Redon, and J. Lingner, *The human CST complex is a terminator of telomerase activity.* Nature, 2012. **488**(7412): p. 540-4.
218. Zhao, Y., et al., *Telomere extension occurs at most chromosome ends and is uncoupled from fill-in in human cancer cells.* Cell, 2009. **138**(3): p. 463-75.
219. Price, C.M., et al., *Evolution of CST function in telomere maintenance.* Cell Cycle, 2010. **9**(16): p. 3157-65.
220. Casteel, D.E., et al., *A DNA polymerase-{alpha}{middle dot}primase cofactor with homology to replication protein A-32 regulates DNA replication in mammalian cells.* J Biol Chem, 2009. **284**(9): p. 5807-18.
221. Gu, P., et al., *CTC1 deletion results in defective telomere replication, leading to catastrophic telomere loss and stem cell exhaustion.* EMBO J, 2012. **31**(10): p. 2309-21.
222. Anderson, B.H., et al., *Mutations in CTC1, encoding conserved telomere maintenance component 1, cause Coats plus.* Nat Genet, 2012. **44**(3): p. 338-42.
223. Polvi, A., et al., *Mutations in CTC1, encoding the CTS telomere maintenance complex component 1, cause cerebroretinal microangiopathy with calcifications and cysts.* Am J Hum Genet, 2012. **90**(3): p. 540-9.

224. Crow, Y.J., et al., *Coats' plus: a progressive familial syndrome of bilateral Coats' disease, characteristic cerebral calcification, leukoencephalopathy, slow pre- and post-natal linear growth and defects of bone marrow and integument.* Neuropediatrics, 2004. **35**(1): p. 10-9.
225. Keller, R.B., et al., *CTC1 Mutations in a patient with dyskeratosis congenita.* Pediatr Blood Cancer, 2012. **59**(2): p. 311-4.
226. Walne, A.J., et al., *Mutations in the telomere capping complex in bone marrow failure and related syndromes.* Haematologica, 2013. **98**(3): p. 334-8.
227. Chen, L.Y., J. Majerska, and J. Lingner, *Molecular basis of telomere syndrome caused by CTC1 mutations.* Genes Dev, 2013. **27**(19): p. 2099-108.
228. Uringa, E.J., et al., *RTEL1 contributes to DNA replication and repair and telomere maintenance.* Mol Biol Cell, 2012. **23**(14): p. 2782-92.
229. Vannier, J.B., et al., *RTEL1 dismantles T loops and counteracts telomeric G4-DNA to maintain telomere integrity.* Cell, 2012. **149**(4): p. 795-806.
230. Ballew, B.J., et al., *A recessive founder mutation in regulator of telomere elongation helicase 1, RTEL1, underlies severe immunodeficiency and features of Hoyeraal Hreidarsson syndrome.* PLoS Genet, 2013. **9**(8): p. e1003695.
231. Vannier, J.B., et al., *RTEL1 is a replisome-associated helicase that promotes telomere and genome-wide replication.* Science, 2013. **342**(6155): p. 239-42.
232. Walne, A.J., et al., *Constitutional mutations in RTEL1 cause severe dyskeratosis congenita.* Am J Hum Genet, 2013. **92**(3): p. 448-53.
233. Le Guen, T., et al., *Human RTEL1 deficiency causes Hoyeraal-Hreidarsson syndrome with short telomeres and genome instability.* Hum Mol Genet, 2013. **22**(16): p. 3239-49.
234. Kellenberger, E., et al., *Solution structure of the C-terminal domain of TFIIH P44 subunit reveals a novel type of C4C4 ring domain involved in protein-protein interactions.* J Biol Chem, 2005. **280**(21): p. 20785-92.
235. Yamaguchi, H., et al., *Mutations of the human telomerase RNA gene (TERC) in aplastic anemia and myelodysplastic syndrome.* Blood, 2003. **102**(3): p. 916-8.

236. Calado, R.T., et al., *Short telomeres result in chromosomal instability in hematopoietic cells and precede malignant evolution in human aplastic anemia.* Leukemia, 2012. **26**(4): p. 700-7.
237. Armanios, M., *Telomerase and idiopathic pulmonary fibrosis.* Mutat Res, 2012. **730**(1-2): p. 52-8.
238. Cronkhite, J.T., et al., *Telomere shortening in familial and sporadic pulmonary fibrosis.* Am J Respir Crit Care Med, 2008. **178**(7): p. 729-37.
239. Armanios, M.Y., et al., *Telomerase mutations in families with idiopathic pulmonary fibrosis.* N Engl J Med, 2007. **356**(13): p. 1317-26.
240. Parry, E.M., et al., *Syndrome complex of bone marrow failure and pulmonary fibrosis predicts germline defects in telomerase.* Blood, 2011. **117**(21): p. 5607-11.
241. Hayflick, L. and P.S. Moorhead, *The serial cultivation of human diploid cell strains.* Exp Cell Res, 1961. **25**: p. 585-621.
242. Kim, N.W., et al., *Specific association of human telomerase activity with immortal cells and cancer.* Science, 1994. **266**(5193): p. 2011-5.
243. Stewart, S.A., et al., *Telomerase contributes to tumorigenesis by a telomere length-independent mechanism.* Proc Natl Acad Sci U S A, 2002. **99**(20): p. 12606-11.
244. Smith, L.L., H.A. Coller, and J.M. Roberts, *Telomerase modulates expression of growth-controlling genes and enhances cell proliferation.* Nat Cell Biol, 2003. **5**(5): p. 474-9.
245. Zhu, J., Y. Zhao, and S. Wang, *Chromatin and epigenetic regulation of the telomerase reverse transcriptase gene.* Protein Cell, 2010. **1**(1): p. 22-32.
246. Armanios, M. and C.W. Greider, *Telomerase and cancer stem cells.* Cold Spring Harb Symp Quant Biol, 2005. **70**: p. 205-8.
247. Horn, S., et al., *TERT promoter mutations in familial and sporadic melanoma.* Science, 2013. **339**(6122): p. 959-61.
248. Huang, F.W., et al., *Highly recurrent TERT promoter mutations in human melanoma.* Science, 2013. **339**(6122): p. 957-9.

249. Ding, Z., et al., *Telomerase reactivation following telomere dysfunction yields murine prostate tumors with bone metastases.* Cell, 2012. **148**(5): p. 896-907.
250. Hu, J., et al., *Antitelomerase therapy provokes ALT and mitochondrial adaptive mechanisms in cancer.* Cell, 2012. **148**(4): p. 651-63.
251. Brunsvig, P.F., et al., *Telomerase peptide vaccination in NSCLC: a phase II trial in stage III patients vaccinated after chemoradiotherapy and an 8-year update on a phase I/II trial.* Clin Cancer Res, 2011. **17**(21): p. 6847-57.
252. Greten, T.F., et al., *Low-dose cyclophosphamide treatment impairs regulatory T cells and unmasks AFP-specific CD4+ T-cell responses in patients with advanced HCC.* J Immunother, 2010. **33**(2): p. 211-8.
253. Schlapbach, C., et al., *Telomerase-specific GV1001 peptide vaccination fails to induce objective tumor response in patients with cutaneous T cell lymphoma.* J Dermatol Sci, 2011. **62**(2): p. 75-83.
254. Herbert, B.S., et al., *Lipid modification of GRN163, an N3'-->P5' thio-phosphoramidate oligonucleotide, enhances the potency of telomerase inhibition.* Oncogene, 2005. **24**(33): p. 5262-8.
255. Dikmen, Z.G., et al., *In vivo inhibition of lung cancer by GRN163L: a novel human telomerase inhibitor.* Cancer Res, 2005. **65**(17): p. 7866-73.
256. Hochreiter, A.E., et al., *Telomerase template antagonist GRN163L disrupts telomere maintenance, tumor growth, and metastasis of breast cancer.* Clin Cancer Res, 2006. **12**(10): p. 3184-92.
257. Dokal, I., *Dyskeratosis congenita.* Hematology Am Soc Hematol Educ Program, 2011. **2011**: p. 480-6.
258. Alter, B.P., et al., *Malignancies and survival patterns in the National Cancer Institute inherited bone marrow failure syndromes cohort study.* Br J Haematol, 2010. **150**(2): p. 179-88.
259. Alter, B.P., et al., *Telomere length is associated with disease severity and declines with age in dyskeratosis congenita.* Haematologica, 2012. **97**(3): p. 353-9.
260. Nelson, N.D. and A.A. Bertuch, *Dyskeratosis congenita as a disorder of telomere maintenance.* Mutat Res, 2012. **730**(1-2): p. 43-51.

261. Ballew, B.J., et al., *Germline mutations of regulator of telomere elongation helicase 1, RTEL1, in Dyskeratosis congenita.* Hum Genet, 2013. **132**(4): p. 473-80.
262. Jyonouchi, S., et al., *Dyskeratosis congenita: a combined immunodeficiency with broad clinical spectrum--a single-center pediatric experience.* Pediatr Allergy Immunol, 2011. **22**(3): p. 313-9.
263. Savage, S.A. and A.A. Bertuch, *The genetics and clinical manifestations of telomere biology disorders.* Genet Med, 2010. **12**(12): p. 753-64.
264. Palm, W. and T. de Lange, *How shelterin protects mammalian telomeres.* Annu Rev Genet, 2008. **42**: p. 301-34.
265. Nakashima, M., et al., *Inhibition of telomerase recruitment and cancer cell death.* J Biol Chem, 2013. **288**(46): p. 33171-80.
266. Baerlocher, G.M., et al., *Flow cytometry and FISH to measure the average length of telomeres (flow FISH).* Nat Protoc, 2006. **1**(5): p. 2365-76.
267. Bolger, A.M., M. Lohse, and B. Usadel, *Trimmomatic: a flexible trimmer for Illumina sequence data.* Bioinformatics, 2014. **30**(15): p. 2114-20.
268. DePristo, M.A., et al., *A framework for variation discovery and genotyping using next-generation DNA sequencing data.* Nat Genet, 2011. **43**(5): p. 491-8.
269. Glusman, G., et al., *Kaviar: an accessible system for testing SNV novelty.* Bioinformatics, 2011. **27**(22): p. 3216-7.
270. Sherry, S.T., et al., *dbSNP: the NCBI database of genetic variation.* Nucleic Acids Res, 2001. **29**(1): p. 308-11.
271. Abecasis, G.R., et al., *A map of human genome variation from population-scale sequencing.* Nature, 2010. **467**(7319): p. 1061-73.
272. Adzhubei, I.A., et al., *A method and server for predicting damaging missense mutations.* Nat Methods, 2010. **7**(4): p. 248-9.
273. Kumar, P., S. Henikoff, and P.C. Ng, *Predicting the effects of coding non-synonymous variants on protein function using the SIFT algorithm.* Nat Protoc, 2009. **4**(7): p. 1073-81.
274. Choi, Y., et al., *Predicting the functional effect of amino acid substitutions and indels.* PLoS One, 2012. **7**(10): p. e46688.

275. Reva, B., Y. Antipin, and C. Sander, *Predicting the functional impact of protein mutations: application to cancer genomics.* Nucleic Acids Res, 2011. **39**(17): p. e118.
276. Schwarz, J.M., et al., *MutationTaster evaluates disease-causing potential of sequence alterations.* Nat Methods, 2010. **7**(8): p. 575-6.
277. Shihab, H.A., et al., *Predicting the functional, molecular, and phenotypic consequences of amino acid substitutions using hidden Markov models.* Hum Mutat, 2013. **34**(1): p. 57-65.
278. Kircher, M., et al., *A general framework for estimating the relative pathogenicity of human genetic variants.* Nat Genet, 2014. **46**(3): p. 310-5.
279. Papadopoulos, J.S. and R. Agarwala, *COBALT: constraint-based alignment tool for multiple protein sequences.* Bioinformatics, 2007. **23**(9): p. 1073-9.
280. Waterhouse, A.M., et al., *Jalview Version 2--a multiple sequence alignment editor and analysis workbench.* Bioinformatics, 2009. **25**(9): p. 1189-91.
281. Abreu, E., R.M. Terns, and M.P. Terns, *Visualization of human telomerase localization by fluorescence microscopy techniques.* Methods Mol Biol, 2011. **735**: p. 125-37.
282. Bisht, K.K., et al., *GDP-mannose-4,6-dehydratase is a cytosolic partner of tankyrase 1 that inhibits its poly(ADP-ribose) polymerase activity.* Mol Cell Biol, 2012. **32**(15): p. 3044-53.
283. Arnold, K., et al., *The SWISS-MODEL workspace: a web-based environment for protein structure homology modelling.* Bioinformatics, 2006. **22**(2): p. 195-201.
284. Brunger, A.T., *Version 1.2 of the Crystallography and NMR system.* Nat Protoc, 2007. **2**(11): p. 2728-33.
285. Broer, L., et al., *Meta-analysis of telomere length in 19,713 subjects reveals high heritability, stronger maternal inheritance and a paternal age effect.* Eur J Hum Genet, 2013. **21**(10): p. 1163-8.
286. Jones, M., et al., *Hematopoietic stem cells are acutely sensitive to Acd shelterin gene inactivation.* J Clin Invest, 2014. **124**(1): p. 353-66.

287. Tejera, A.M., et al., *TPP1 is required for TERT recruitment, telomere elongation during nuclear reprogramming, and normal skin development in mice.* Dev Cell, 2010. **18**(5): p. 775-89.
288. Guo, Y., et al., *Inherited bone marrow failure associated with germline mutation of ACD, the gene encoding telomere protein TPP1.* Blood, 2014.
289. Agarwal, S., et al., *Telomere elongation in induced pluripotent stem cells from dyskeratosis congenita patients.* Nature, 2010. **464**(7286): p. 292-6.
290. Takahashi, K., et al., *Induction of pluripotent stem cells from adult human fibroblasts by defined factors.* Cell, 2007. **131**(5): p. 861-72.
291. Batista, L.F., et al., *Telomere shortening and loss of self-renewal in dyskeratosis congenita induced pluripotent stem cells.* Nature, 2011. **474**(7351): p. 399-402.